

การเตรียม การศึกษาลักษณะเฉพาะ และการขั้บยั้งเอนไซม์ไซโตโครมพี 450 ของมนุษย์
โดยนาโนพาร์ทิเคิลของทองคำและเงิน

นางสาวพัทธนันท์ หงส์ปีดิเจริญ

ศูนย์วิทยทรัพยากร
จุฬาลงกรณ์มหาวิทยาลัย

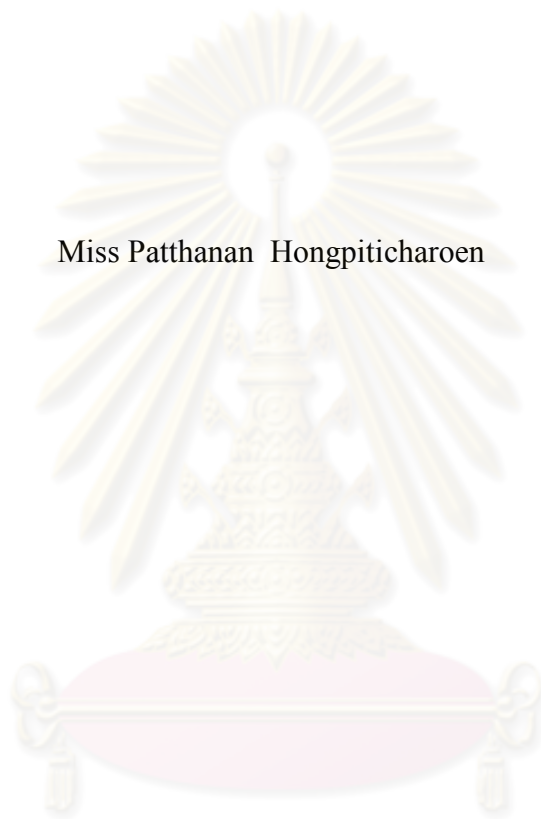
วิทยานิพนธ์นี้เป็นส่วนหนึ่งของการศึกษาตามหลักสูตรปริญญาวิทยาศาสตรมหาบัณฑิต
สาขาวิชาเทคโนโลยีเภสัชกรรม ภาควิชาวิทยาการเภสัชกรรมและเภสัชอุตสาหกรรม
คณะเภสัชศาสตร์ จุฬาลงกรณ์มหาวิทยาลัย

ปีการศึกษา 2552

ลิขสิทธิ์ของจุฬาลงกรณ์มหาวิทยาลัย

PREPARATION, CHARACTERIZATION AND INHIBITION ON HUMAN
CYTOCHROME P450 OF GOLD AND SILVER NANOPARTICLES

Miss Patthanan Hongpiticharoen



A Thesis Submitted in Partial Fulfillment of the Requirements
for the Degree of Master of Science
in Pharmacy Program in Pharmaceutical Technology

Department of Pharmaceutics and Manufacturing Pharmacy

Faculty of Pharmaceutical Sciences

Chulalongkorn University

Academic Year 2009

Copyright of Chulalongkorn University

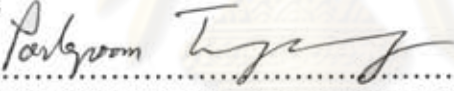
Thesis Title PREPARATION, CHARACTERIZATION AND
INHIBITION ON CYTOCHROME P450 OF GOLD AND
SILVER NANOPARTICLES
By Miss Patthanan Hongpiticharoen
Field of Study Pharmaceutical Technology
Thesis Advisor Assistant Professor Warangkana Warisnoicharoen, Ph.D.
Thesis Co-Advisor Associate Professor Pol. Lt. Col. Somsong Lawanprasert, Ph.D.

Accepted by the Faculty of Pharmaceutical Sciences, Chulalongkorn University
in Partial Fulfillment of the Requirements for the Master's Degree



.....
(Associate Professor Pornpen Pramyothin, Ph.D.)

Dean of the Faculty of
Pharmaceutical Sciences

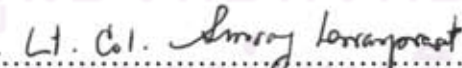
THESIS COMMITTEE


.....
(Associate Professor Parkpoom Tengannuay, Ph.D.)

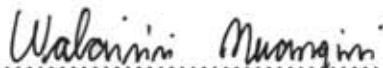
Chairman


.....
(Assistant Professor Warangkana Warisnoicharoen, Ph.D.)


Thesis Advisor


.....
(Associate Professor Pol. Lt. Col. Somsong Lawanprasert, Ph.D.)

Thesis Co-Advisor


.....
(Assistant Professor Pol. Lt. Walaisiri Muangsiri, Ph.D.)

Examiner


.....
(Associate Professor Laddawal Phivthong-ngam, Ph.D.)

Examiner

พัทธานันท์ หงส์ปิติเจริญ : การเตรียม การศึกษาลักษณะเฉพาะ และการยับยั้งเอนไซม์ไซโตโครมที 450 ของมนุษย์ โดยนาโนพาร์ทิเคิลของทองคำและเงิน. (PREPARATION, CHARACTERIZATION AND INHIBITION ON CYTOCHROME P450 OF GOLD AND SILVER NANOPARTICLES) อ. ที่ปริกษา
 วิทยานิพนธ์หลัก : ศศ.คร. วรางคณา วาริสน้อยเจริญ, อ.ที่ปริกษาวิทยานิพนธ์ร่วม : รศ.ดร.พ.ศ.หญิง สมทรง
 ลาวัลย์ประเสริฐ, 125 หน้า.

ปัจจุบันนาโนพาร์ทิเคิลของทองคำและเงินถูกนำมาใช้ในทางการแพทย์มากขึ้น เช่น การนำส่งยา การรักษาโรค และการวินิจฉัยโรค การสังเคราะห์นาโนพาร์ทิเคิลของทองคำและเงินใช้วิธีการดักจับ ในการทดลองนี้มีการใช้สารทำให้เสถียรสามประเภท คือ ซิเตรท โพลีเอทิลีนอิมิน และโพลีไวนิลไพโรลิโดน ขนาดเฉลี่ยของเส้นผ่านศูนย์กลางของอนุภาคของนาโนพาร์ทิเคิลของทองคำที่เตรียมโดยใช้ซิเตรท โพลีเอทิลีนอิมิน และโพลีไวนิลไพโรลิโดนเป็นสารทำให้เสถียรเท่ากับ 8.36 ± 1.94 , 2.67 ± 1.04 และ 5.05 ± 1.51 นาโนเมตร ตามลำดับ ขนาดประจุของนาโนพาร์ทิเคิลของทองคำที่ใช้ซิเตรท โพลีเอทิลีนอิมิน และโพลีไวนิลไพโรลิโดนเป็นสารทำให้เสถียรวัดได้ดังนี้ -34.1 ± 1.3 , 28.7 ± 2.2 และ -3.3 ± 0.7 มิลลิโวลต์ ตามลำดับ ส่วนขนาดอนุภาค และประจุของนาโนพาร์ทิเคิลของเงินมีค่าเท่ากับ 12.42 ± 2.48 นาโนเมตร และ -43.6 ± 0.7 มิลลิโวลต์ตามลำดับ ผลในการยับยั้งเอนไซม์ไซโตโครมที 450 ของมนุษย์ อันได้แก่ CYP1A2 CYP2C9 CYP2C19 และ CYP3A4 ของนาโนพาร์ทิเคิลของทองคำและเงิน ถูกทดสอบโดยการวัดค่าการเรืองแสงฟลูออเรสเซน และทำการทดลองโดยใช้ 96-well plates จากการทดลองพบว่านาโนพาร์ทิเคิลทองคำโดยใช้ซิเตรทเป็นสารทำให้เสถียรสามารถยับยั้งเอนไซม์ไซโตโครมที 450 ได้น้อยที่สุด เมื่อเทียบกับนาโนพาร์ทิเคิลของทองคำที่ใช้โพลีเอทิลีนอิมิน และโพลีไวนิลไพโรลิโดนเป็นสารทำให้เสถียร และนาโนพาร์ทิเคิลของเงิน นาโนพาร์ทิเคิลทองคำที่เตรียมโดยใช้สารที่มีประจุบวก (โพลีเอทิลีนอิมิน) เป็นสารทำให้เสถียรมีประสิทธิภาพในการยับยั้งเอนไซม์ไซโตโครมที 450 มากที่สุด โดยสามารถยับยั้ง CYP1A2, CYP2C9, CYP2C19 และ CYP3A4 ที่ IC_{50} เท่ากับ 64.34 ± 0.05 , 4.47 ± 0.03 , 4.84 ± 0.01 และ 16.89 ± 0.02 ไมโครโมลาร์ ตามลำดับ ซึ่งผลของการยับยั้งเอนไซม์อาจขึ้นกับขนาดและประจุของนาโนพาร์ทิเคิล ข้อมูลการทดลองที่ได้แสดงให้เห็นว่านาโนพาร์ทิเคิลของทองคำโดยใช้ซิเตรท และโพลีไวนิลไพโรลิโดนเป็นสารทำให้เสถียรมีโอกาสดักจับอันตรกิริยาของยาน้อยที่สุด อย่างไรก็ตามกลไกในการยับยั้งของเอนไซม์ไซโตโครมที 450 และผลการศึกษาในกายควรมีการศึกษาเพิ่มเติมต่อไป

ภาควิชา วิทยาการเกษตรกรรมและเกษตรอุตสาหกรรม
 สาขาวิชา เทคโนโลยีเกษตรกรรม
 ปีการศึกษา 2552

ลายมือชื่อนิสิต... พัทธานันท์ หงส์ปิติเจริญ
 ลายมือชื่ออ.ที่ปริกษาวิทยานิพนธ์หลัก...
 ลายมือชื่ออ.ที่ปริกษาวิทยานิพนธ์ร่วม...
 ลาวัลย์ประเสริฐ

5076858133 : MAJOR PHARMACEUTICAL TECHNOLOGY

KEYWORDS : CYTOCHROME P450 / DRUG INTERACTION / GOLD NANOPARTICLES / SILVER NANOPARTICLES / CYP INHIBITION / CYP1A2 / CYP2C9 / CYP2C19 / CYP3A4

PATTHANAN HONGPITICHAROEN: PREPARATION, CHARACTERIZATION AND INHIBITION ON CYTOCHROME P450 OF GOLD AND SILVER NANOPARTICLES. THESIS ADVISOR: ASSIST. PROF. WARANGKANA WARISNOICHAROEN, Ph.D., THESIS CO-ADVISOR: ASSOC. PROF. POL. LT. COL. SOMSONG LAWANPRASERT, Ph.D., 125 pp.

Gold nanoparticles (AuNPs) and silver nanoparticles (AgNPs) have been recently used for clinical applications such as drug delivery, therapy and diagnostics. AuNPs and AgNPs were synthesized by using the chemical reduction method. In this study, the different stabilizers, citrate, polyethyleneimine (PEI) and polyvinylpyrrolidone (PVP), were used for gold nanoparticle synthesis. The average particle diameters of freshly prepared citrate, PEI and PVP stabilized AuNPs were 8.36 ± 1.94 , 2.67 ± 1.04 and 5.05 ± 1.51 nm, respectively. The zeta potential of citrate, PEI and PVP stabilized AuNPs were -34.1 ± 1.3 , 28.7 ± 2.2 and -3.3 ± 0.7 mV, in orderly. The size and zeta potential of AgNPs were 12.42 ± 2.48 nm and -43.6 ± 0.7 mV, respectively. The inhibitory effect of AuNPs and AgNPs was observed on human cytochrome P450 (CYP) isozymes, CYP1A2, CYP2C9, CYP2C19 and CYP3A4. The CYP inhibition was measured fluorometrically in 96-well plates. Citrate stabilized AuNPs had least inhibitory effect on all CYP isozymes compared to PEI and PVP stabilized AuNPs and AgNPs. AuNPs with positively charged stabilizer (PEI) exhibited the greatest inhibition on CYP with IC_{50} of 64.34 ± 0.05 , 4.47 ± 0.03 , 4.84 ± 0.01 and 16.89 ± 0.02 μ M for CYP1A2, CYP2C9, CYP2C19 and CYP3A4, respectively. The potential of CYP inhibition seemed to depend upon the size and charge of the nanoparticles. The data from this study presented that citrate and PVP stabilized AuNPs caused low incidence of drug interaction. The mechanism of CYP inhibition and the effect of *in vivo* are suggested for further study.

Department : Pharmaceutics and Manufacturing Pharmacy

Field of Study : Pharmaceutical Technology

Academic Year: 2009

Student's Signature : *Patthanan Hongpiticharoen*

Advisor's Signature : *Warangkana Warisnoicharoen*

Co-Advisor's Signature : *Pol. Lt. Col. Somsong Lawanprasert*

ACKNOWLEDGEMENTS

I would like to express my sincere gratitude and grateful appreciation to my thesis advisor, Assistant Professor Dr. Warangkana Warisnoicharoen for her valuable advice, guidance and encouragement throughout my graduate study as well as her kindness and supporting. I would like to express my grateful appreciation to my thesis co-advisor, Associate Professor Pol. Lt. Col. Dr. Somsong Lawanprasert for her suggestion, guidance and kindness for the experiment work and presentation of the thesis.

Also, I would like to express my sincere appreciation to my thesis committee for their valuable comment and suggestion. I would like to give the special thanks to Miss Duangjai Panyapojsak for helping me throughout my experiment work.

I would like to thank to the Faculty of Graduate Studies, Chulalongkorn University for supporting scholarship which enabled me to undertake this study.

Thanks are expressed to my colleagues and friends in the Faculty of Pharmaceutical Sciences, Chulalongkorn University for their encouragement, understanding and caring that made me feel like my second home. I am really thankful to my beloved family for supporting educational opportunity, inspiration, loving, caring and understanding. Finally, I would like to extend my thanks and gratitude to everyone whose names are not mentioned here for helping me in everything.

ศูนย์วิทยทรัพยากร
จุฬาลงกรณ์มหาวิทยาลัย

CONTENTS

| | Page |
|--|------|
| ABSTRACT (THAI) | iv |
| ABSTRACT (ENGLISH) | v |
| ACKNOWLEDGEMENTS | vi |
| CONTENTS | vii |
| LIST OF TABLES | xi |
| LIST OF FIGURES | xiv |
| LIST OF ABBREVIATIONS | xix |
| CHAPTER | |
| I INTRODUCTION | 1 |
| 1. Background and significance of the study..... | 1 |
| 2. Objectives of the study..... | 4 |
| II LITERATURE REVIEWS | 5 |
| 1. Nanoparticles..... | 5 |
| 1.1 Gold nanoparticles (AuNPs)..... | 5 |
| 1.2 Silver nanoparticles (AgNPs)..... | 6 |
| 2. AuNPs and AgNPs for pharmaceutical application..... | 7 |
| 3. Xenobiotic biotransformation..... | 10 |
| 3.1 Cytochrome P450 (CYP)..... | 11 |
| 3.2 The main human CYP isozymes..... | 14 |

| CHAPTER | Page |
|--|-------------|
| 4. Drug interaction..... | 19 |
| 4.1 Induction of drug metabolism..... | 19 |
| 4.2 Inhibition of drug metabolism..... | 19 |
| 4.2.1 Reversible inhibition..... | 20 |
| 4.2.2 Quasi-irreversible inhibition <i>via</i> metabolic intermediate complexation..... | 20 |
| 4.2.3 Irreversible inhibition..... | 20 |
| III MATERIALS AND METHODS..... | 21 |
| 1. Materials..... | 21 |
| 1.1 Equipments..... | 21 |
| 1.2 Chemicals..... | 22 |
| 2. Methods..... | 25 |
| 2.1 Preparation of AuNPs and AgNPs..... | 25 |
| 2.1.1 Preparation of AuNPs..... | 25 |
| 2.1.2 Preparation of AgNPs..... | 28 |
| 2.2 Characterization of AuNPs and AgNPs..... | 29 |
| 2.2.1 UV – visible spectroscopy..... | 29 |
| 2.2.2 Size and size distribution..... | 31 |
| 2.2.3 Zeta potential measurement..... | 31 |

| CHAPTER | Page |
|--|-------------|
| 2.3 Human cytochrome P450 inhibition assay for AuNPs and AgNPs..... | 32 |
| 2.3.1 Preparation of Vivid [®] CYP450 screening kit and assay procedure for inhibition test..... | 34 |
| 2.3.2 Verification of CYP inhibition test..... | 39 |
| 2.3.3 CYP inhibition of AuNPs and AgNPs..... | 41 |
| IV RESULTS AND DISCUSSION..... | 44 |
| 1. Preparation of AuNPs and AgNPs..... | 44 |
| 2. Characterization of AuNPs and AgNPs..... | 48 |
| 2.1 UV – visible spectroscopy..... | 48 |
| 2.2 Size and size distribution..... | 61 |
| 2.3 Zeta potential measurement..... | 67 |
| 3. Human cytochrome P450 inhibition of AuNPs and AgNPs..... | 68 |
| 3.1 Verification of CYP inhibition test..... | 68 |
| 3.2 CYP inhibition of citrate stabilized AuNPs..... | 70 |
| 3.3 CYP inhibition of PEI stabilized AuNPs..... | 71 |
| 3.4 CYP inhibition of PVP stabilized AuNPs..... | 74 |
| 3.5 CYP inhibition of AgNPs..... | 77 |
| V CONCLUSION..... | 88 |
| REFERENCES..... | 91 |

CHAPTER

Page

APPENDICES.....100**BIOGRAPHY**.....125

ศูนย์วิทยทรัพยากร
จุฬาลงกรณ์มหาวิทยาลัย

LIST OF TABLES

| Table | Page |
|---|------|
| 1 Total CYP content in various human tissues..... | 12 |
| 2 Cytochrome P450 enzymes and their substrates, inhibitors and inducers..... | 17 |
| 3 The components of Vivid [®] CYP450 screening kit..... | 24 |
| 4 Reconstitution of Vivid [®] substrates..... | 35 |
| 5 Component of master pre-mix per 100 well..... | 35 |
| 6 Pre-mix Vivid [®] substrate and NADP ⁺ per 100 well..... | 36 |
| 7 Concentration of CYP inhibitors per reaction volume (100 μ L)..... | 41 |
| 8 Concentration of AuNPs and AgNPs in reaction volume (100 μ L) for CYP assay..... | 43 |
| 9 The stability of AuNPs and AgNPs with varying concentrations of stabilizers..... | 46 |
| 10 The spectral features of AuNPs and AgNPs with varying concentrations of stabilizers..... | 57 |
| 11 Zeta potential (mean \pm SD, n=3) of citrate, PEI and PVP stabilized AuNPs and AgNPs after preparation and 1 month storage..... | 67 |
| 12 IC ₅₀ and 95% confidence interval of the known inhibitors..... | 70 |
| 13 Percentages of inhibition of AuNPs on CYP isozymes at 406 μ M (n=4)..... | 71 |
| 14 Percentages of inhibition of AgNPs on CYP isozymes at 40 μ M (n=4)..... | 71 |

| Table | Page |
|-------|---|
| 15 | IC ₅₀ values on CYP inhibition of citrate, PEI and PVP stabilized AuNPs and AgNPs (n=4).....80 |
| 16 | Percentage of inhibition of citrate, PEI and PVP solutions (n=2).....81 |
| 17 | The sizes of AuNPs and percentage of CYP inhibition at 406 μ M.....83 |
| 18 | Percentage of inhibition of citrate stabilized AuNPs on CYP1A2 activity (n=4).....101 |
| 19 | Percentage of inhibition of citrate stabilized AuNPs on CYP2C9 activity (n=4).....101 |
| 20 | Percentage of inhibition of citrate stabilized AuNPs on CYP2C19 activity (n=4).....101 |
| 21 | Percentage of inhibition of citrate stabilized AuNPs on CYP3A4 activity (n=4).....102 |
| 22 | Percentage of inhibition of PEI stabilized AuNPs on CYP1A2 activity (n=4)102 |
| 23 | Percentage of inhibition of PEI stabilized AuNPs on CYP2C9 activity (n=4).....102 |
| 24 | Percentage of inhibition of PEI stabilized AuNPs on CYP2C19 activity (n=4)103 |
| 25 | Percentage of inhibition of PEI stabilized AuNPs on CYP3A4 activity (n=4).....103 |

| Table | Page |
|-------|---|
| 26 | Percentage of inhibition of PVP stabilized AuNPs on CYP1A2 activity (n=4)104 |
| 27 | Percentage of inhibition of PVP stabilized AuNPs on CYP2C9 activity (n=4)104 |
| 28 | Percentage of inhibition of PVP stabilized AuNPs on CYP2C19 activity (n=4)105 |
| 29 | Percentage of inhibition of PVP stabilized AuNPs on CYP3A4 activity (n=4)105 |
| 30 | Percentage of inhibition of AgNPs on CYP1A2 activity (n=4).....106 |
| 31 | Percentage of inhibition of AgNPs on CYP2C9 activity (n=4).....106 |
| 32 | Percentage of inhibition of AgNPs on CYP2C19 activity (n=4).....107 |
| 33 | Percentage of inhibition of AgNPs on CYP3A4 activity (n=4).....107 |
| 34 | Inhibitory effect of α -naphthoflavone on CYP1A2 activity (n=2).....108 |
| 35 | Inhibitory effect of sulfaphenazole on CYP2C9 activity (n=2).....109 |
| 36 | Inhibitory effect of miconazole on CYP2C19 activity (n=2).....110 |
| 37 | Inhibitory effect of ketoconazole on CYP3A4 activity (n=2).....111 |

LIST OF FIGURES

| Figure | Page |
|--------|---|
| 1 | Gold nanoparticles used for drug delivery and targeted delivery system.....9 |
| 2 | Detoxification of the liver.....11 |
| 3 | Structure of ferriprotoporphyrin 9 in cytochrome P450.....13 |
| 4 | Typical reaction by CYP enzyme.....14 |
| 5 | Preparation of citrate stabilized AuNPs.....26 |
| 6 | Preparation of PEI stabilized AuNPs.....27 |
| 7 | Preparation of PVP stabilized AuNPs.....28 |
| 8 | Preparation of AgNPs.....29 |
| 9 | Schematic diagram of fluorescent dye assay on CYP activity.....33 |
| 10 | The structures of Vivid [®] BOMCC (7-benzyloxymethyloxy-3 cyanocoumarin) and EOMCC (7-ethyloxymethyloxy-3-cyanocoumarin) substrates.....33 |
| 11 | Schematic diagram of metabolism of blocked dye substrate into fluorescent metabolite.....34 |
| 12 | Schematic diagram of microplate organization for Vivid [®] CYP450 screening kit protocol.....37 |
| 13 | Four steps of enzyme inhibition assay.....38 |

| Figure | Page |
|--------|--|
| 14 | The appearances of nanoparticles prepared according to conditions 1, 2 and 3 of, citrate stabilized AuNPs after preparation (A) and after 1 month storage (B), PEI stabilized AuNPs after preparation (C) and 1 month storage (D), PVP stabilized AuNPs after preparation (E) and 1 month storage (F) and AgNPs after preparation (G) and 1 month storage (H).....47 |
| 15 | The appearances of citrate stabilized AuNPs (A), PEI stabilized AuNPs (B), PVP stabilized AuNPs (C) and AgNPs (D) after 6 month storage.....48 |
| 16 | UV absorption spectra of citrate stabilized AuNPs prepared with condition 1 after preparation and 1 month storage.....49 |
| 17 | UV absorption spectra of citrate stabilized AuNPs prepared with condition 2 after preparation and 1 month storage.....50 |
| 18 | UV absorption spectra of citrate stabilized AuNPs prepared with condition 3 after preparation and 1 month storage.....50 |
| 19 | UV absorption spectra of PEI stabilized AuNPs prepared with condition 1 after preparation and 1 month storage.....51 |
| 20 | UV absorption spectra of PEI stabilized AuNPs prepared with condition 2 after preparation and 1 month storage.....51 |
| 21 | UV absorption spectra of PEI stabilized AuNPs prepared with condition 3 after preparation and 1 month storage.....52 |

| Figure | Page |
|--------|---|
| 22 | UV absorption spectra of PVP stabilized AuNPs prepared with condition 1 after preparation and 1 month storage.....52 |
| 23 | UV absorption spectra of PVP stabilized AuNPs prepared with condition 2 after preparation and 1 month storage.....53 |
| 24 | UV absorption spectra of PVP stabilized AuNPs prepared with condition 3 after preparation and 1 month storage.....53 |
| 25 | UV absorption spectra of AgNPs prepared with condition 1 after Preparation and 1 month storage.....54 |
| 26 | UV absorption spectra of AgNPs prepared with condition 2 after preparation and 1 month storage.....54 |
| 27 | UV absorption spectra of AgNPs prepared with condition 3 after preparation and 1 month storage.....55 |
| 28 | UV absorption spectra of citrate, PEI and PVP stabilized AuNPs after preparation (A) and 1 month storage (B).....58 |
| 29 | UV absorption spectra of AgNPs after preparation (A) and 1 month storage (B).....59 |
| 30 | UV absorption spectra of hydrogen tetrachloroaurate solution.....60 |
| 31 | UV absorption spectra of silver nitrate solution.....60 |
| 32 | TEM images of citrate stabilized AuNPs (A), PEI stabilized AuNPs (B), PVP stabilized AuNPs (C) and AgNPs (D) after preparation.....62 |

| Figure | Page |
|--------|---|
| 33 | TEM images of citrate stabilized AuNPs (A), PEI stabilized AuNPs (B), PVP stabilized AuNPs (C) and AgNPs (D) after 1 month storage.....62 |
| 34 | Size distribution of citrate stabilized AuNPs after preparation.....63 |
| 35 | Size distribution of citrate stabilized AuNPs after 1 month storage.....63 |
| 36 | Size distribution of PEI stabilized AuNPs after preparation.....64 |
| 37 | Size distribution of PEI stabilized AuNPs after 1 month storage.....64 |
| 38 | Size distribution of PVP stabilized AuNPs after preparation.....65 |
| 39 | Size distribution of PVP stabilized AuNPs after 1 month storage.....65 |
| 40 | Size distribution of AgNPs after preparation.....66 |
| 41 | Size distribution of AgNPs after 1 month storage.....66 |
| 42 | Inhibition curve of PEI stabilized AuNPs on CYP1A2.....72 |
| 43 | Inhibition curve of PEI stabilized AuNPs on CYP2C9.....73 |
| 44 | Inhibition curve of PEI stabilized AuNPs on CYP2C19.....73 |
| 45 | Inhibition curve of PEI stabilized AuNPs on CYP3A4.....74 |
| 46 | Inhibition curve of PVP stabilized AuNPs on CYP1A2.....75 |
| 47 | Inhibition curve of PVP stabilized AuNPs on CYP2C9.....75 |
| 48 | Inhibition curve of PVP stabilized AuNPs on CYP2C19.....76 |
| 49 | Inhibition curve of PVP stabilized AuNPs on CYP3A4.....76 |
| 50 | Inhibition curve of AgNPs on CYP1A2.....77 |
| 51 | Inhibition curve of AgNPs on CYP2C9.....78 |

| Figure | Page |
|--------|--|
| 52 | Inhibition curve of AgNPs on CYP2C19.....78 |
| 53 | Inhibition curve of AgNPs on CYP3A4.....79 |
| 54 | Inhibition curve of α -naphthoflavone on CYP1A2.....108 |
| 55 | Inhibition curve of sulfaphenazole on CYP2C9.....109 |
| 56 | Inhibition curve of miconazole on CYP2C19.....110 |
| 57 | Inhibition curve of ketoconazole on CYP3A4.....111 |



ศูนย์วิทยทรัพยากร
จุฬาลงกรณ์มหาวิทยาลัย

LIST OF ABBREVIATIONS

| | |
|---------------|--|
| °C | degree Celsius |
| ϵ | dielectric constant |
| μM | micromolar |
| μL | microlitter |
| η | viscosity |
| π | ratio of a circle's area to square of its radius |
| ζ | zeta potential |
| a | radius of sphere |
| A | absorbance |
| ACN | acetonitrile |
| AgNPs | silver nanoparticles |
| AuNPs | gold nanoparticles |
| BOMCC | 7-benzyloxymethyloxy-3-cyanocoumarin |
| C | concentration of the absorbing species |
| CI | confidence interval |
| cm | centrimeter |
| CYP | cytochrome P450 |
| d_0 | path length of the spectrometer |

| | |
|------------------|---|
| DMSO | dimethylsulfoxide |
| DNA | deoxyribonucleic acid |
| e.g. | example gratia |
| EOMCC | 7-ethyloxymethyloxy-3-cyanocoumarin |
| <i>et al.</i> | <i>et alii</i> (and others) |
| <i>etc.</i> | <i>et cetera</i> (and other similar things) |
| F | Farads |
| FAD | flavin adenine dinucleotide |
| FMN | flavin mononucleotide |
| g | gram |
| G-6-P | glucose-6-phosphate |
| G-6-PD | glucose-6-phosphate dehydrogenase |
| GSH | glutathione reduced form |
| HIV | human immunodeficiency virus |
| IC ₅₀ | median (50%) inhibitory concentration |
| i.e. | <i>id est</i> (that is) |
| L | pathlength through the sample |
| m | meter |
| mg | milligram |
| min | minute |
| mL | milliliter |

| | |
|------------------|--|
| mM | millimolar |
| mmole | millimole |
| mol | mole |
| mV | millivolt |
| M | molar |
| MW | molecular weight |
| N | number density of particles per unit volume |
| nm | nanometer |
| NADP | nicotinamide adenine dinucleotide phosphate |
| NADPH | nicotinamide adenine dinucleotide phosphate (reduced form) |
| Pa | Pascal |
| PEI | polyethyleneimine |
| pH | potential of hydrogen |
| ppm | part per million |
| PVP | polyvinylpyrrolidone |
| Q_{ext} | extinction efficiency |
| RES | reticuloendothelial system |
| RFU | relative fluorescence unit or fluorescent intensity |
| RNA | ribonucleic acid |
| S | second |

| | |
|--------|-----------------------------------|
| SD | standard deviation |
| SPR | surface Plasmon resonance |
| TEM | transmission electron microscopy |
| Tris | Tris (hydroxymethyl) aminomethane |
| U | unit |
| U_E | electrophoretic mobility |
| UV | ultraviolet |
| UV-vis | ultraviolet-visible |



ศูนย์วิทยทรัพยากร
จุฬาลงกรณ์มหาวิทยาลัย

CHAPTER I

INTRODUCTION

1. Background and significance of the study

Nanotechnology is widely used to revolutionize drug delivery, drug manufacturing and medical diagnostic. Recently, metallic nanoparticles such as gold and silver nanoparticles are studied for the medicinal purpose. Gold nanoparticles (AuNPs) have been developed for many applications, including diagnostic, therapy, delivery application and as biomarkers. AuNPs are attracted for delivery of various payloads into their targets. The payloads could be small drug molecules or large biomolecules such as proteins, DNA or RNA (Han *et al.*, 2007). The release of the compounds could be triggered by internal or external stimuli. The examples of internal stimuli are glutathione (GSH) and pH, while the external stimuli are light (Ghosh *et al.*, 2008). Recently, there are many researches in drug delivery system using nanobioconjugates. For example, AuNPs with 2 nm core diameter could be conjugated with paclitaxel, a chemotherapeutic drug. According to the hydrophobic nature of many anticancer drugs, the solubility of anticancer drugs in water is the major problems. Therefore, AuNPs were developed for drug delivery to resolve this problem. In addition, small structure of nano-size can avoid the opsonization by reticuloendothelial system (RES) and present the ability to accumulate in a broader range of tumors (Gibson, Khanal and Zubarev, 2007). Therefore, the advantages for delivery system include the ability to remain in the bloodstream for a considerable time without being eliminated. Conventional surface nonmodified nanoparticles are usually caught in the circulation by RES, such as liver and spleen, depending on their

size and surface characteristics. In addition, size of AuNPs can be varied by the method and chemical used for synthesis. Silver nanoparticles (AgNPs) have shown antimicrobial activity. They can inhibit growth of various microorganisms, resulting in the different fields of applications such as using in medical devices and antimicrobial system. According to the study of Kim *et al.* (2007), yeast and *E.coli* were inhibited at low concentration of AgNPs while the inhibitory effects on *S. aureus* were mild. AgNPs also inhibited the growth of HIV-1 virus *in vitro* (Elechiguerra *et al.*, 2005).

There are several methods for AuNP synthesis. The principle of them is the reaction between Au³⁺ and reducer in the presence of varieties of stabilizers, such as citrate ion, polymers, dendrimers to generate AuNPs (Liu *et al.*, 2006). Nanoparticles tend to fairly unstable in solution due to small size, so stabilizer is used for avoiding the aggregation of the particles. Stabilizer is absorbed at the particle surface to keep the nanoparticles suspended and prevent their agglomeration by providing charge or solubility properties (Wang, Yan and Chen, 2005). Therefore, the charge of stabilizer could affect on the particle stability. In addition, the charge of the particle could have an effect to cell transmission, which involving to CYP inhibition. Hence, citrate, PEI and PVP, which show anionic, cationic and nonionic charges, are attracted to be the stabilizers of AuNPs in this study.

In order to use AuNPs and AgNPs for nanomedicine, understanding of the properties and the biological effect of the nanoparticles is necessary. Some biological studies have shown that the metallic nanoparticles lead to the alteration of the biological effects (Bhattacharya *et al.*, 2008). According to the study of Mukherjee *et al.* (2005), AuNPs could inhibit vascular endothelial growth factor (VEGF), hence

they could be used in cancer therapy. AuNPs also interrupt the function of cell cycle by increasing in the percentage of cells in the G1-phase (Gap phase) and significant decreasing in the percentage of cells in the S-phase (Synthesis phase) (Bhattacharya *et al.*, 2007). In addition, AgNPs could bind to the glycoprotein subunits on the cell surface (Elechiguerra *et al.*, 2005).

Cytochrome P450 (CYP) is an important drug metabolizing enzymes in the liver and some other extrahepatic tissues. It catalyzes the initial step in the biotransformation (known as phase I metabolism) of xenobiotics, including drugs, pollutants and endogenous compounds (Coleman, 2005). Metabolites from phase I metabolism can be non-toxic and excreted or even more toxic (known as reactive meabolites) which are further metabolized by phase II metabolism. Phase II metabolism deals with the conjugative reactions using endogenous co-substrates conjugated with the electrophilic functional group on the phase I metabolites or on the parent compound itself so as to be further readily excreted from the body. Thus it is not necessary for any compounds to undergo both phases I and II metabolism.

Regarding CYP, there are more than fifty CYP isozymes present in humans. Approximately 70% of CYP expressed in adult human liver include CYPs 1A2, 2A6, 2B6, the 2C subfamily (2C8, 2C9, 2C18 and 2C19), 2D6, 2E1 and the 3A subfamily (3A4 and 3A5). Each type of isozymes possesses different functions as following: CYP1A2 metabolizes drugs with structures like aromatic amines such as caffeine, β -naphthylamine (carcinogen) and theophylline, while CYP2C9 metabolizes S-warfarin, phenytoin, etc. CYP2C19 metabolizes significant drugs such as omeprazole, diazepam, antidepressants, antimalarials, etc. CYP3A4 which is the major isozyme in the liver metabolizes a large number of drugs such as most calcium channel blockers,

benzodiazepines, cyclosporine, etc. All these isozymes of CYP can be inhibited by particular xenobiotics as called inhibitors while some isozymes can be induced by particular xenobiotics as called inducers. Therefore, modulation of CYP isozymes by either inhibitors or inducers can influence metabolism of drugs that are metabolized by those CYP isozymes (Goshman, Fish and Roller, 1999; Coleman, 2005).

In an attempt to develop AuNPs and AgNPs for clinical applications, effect of them on CYP is exclusively needed to be clarified in order to address whether these nanoparticles influence drug metabolism. If the metallic nanoparticles inhibit any CYP isozymes, they would possibly cause drug interaction with particular medicines that are metabolized by those CYP isozymes. Thus using AuNPs and AgNPs to deliver the interacting medicines or even administration of the metallic nanoparticles concomitantly with other interacting medicines should be concerned. Therefore, the purpose of this study was to prepare AuNPs and AgNPs and their inhibitory effect investigate the effect of AuNPs and AgNPs on human CYPs which were involved in drug metabolism such as CYPs 1A2, 2C9, 2C19 and 3A4 using recombinant human CYP using an *in vitro* study.

2. Objectives of the study

- 2.1 To synthesize and characterize of gold and silver nanoparticles
- 2.2 To investigate the inhibitory effect of synthesized gold and silver nanoparticles on human cytochrome P450 (CYP1A2, CYP2C9, CYP2C19 and CYP3A4)

CHAPTER II

LITERATURE REVIEWS

1. Nanoparticles

Nanoparticles are normally defined as particles with the size between 1 and 100 nm. They are able to disperse in water (hydrosol) or organic solvents (organosols), depending on the preparation conditions and stabilizing agents surrounding the particles. Nanoparticles are attractive in medical purpose by using atomic scale tailoring of materials. The structure and function of biosystems at the nanoscale lead to numerous researches, resulting in the improvement in biology, biotechnology, medicine and healthcare. Recently, metallic nanoparticles are widely study due to their unique catalytic, electronic, magnetic and optical properties. Metallic nanoparticles with biological aspect have been developed for diagnostic devices, physical therapy applications and drug delivery vehicles (Singh *et al.*, 2008; Zhou *et al.*, 2009).

1.1 Gold nanoparticles (AuNPs)

Gold is the highly functional metal developed in many applications, especially in the field of nanoscience and nanotechnology. AuNPs are most stable metallic nanoparticles. Colloidal gold was used to make ruby glass and for coloring ceramics and these are still continuing. In 1618, colloidal gold was used for treatment in various diseases, such as heart and venereal problems, dysentery, epilepsy and tumor and for diagnosis of syphilis, published by philosopher and medical doctor Francisci Antonii. In 1857, Michael Faraday reported the formation of deep red solutions of colloidal gold by reduction of aqueous solution of chloroaurate (AuCl_4^-) using

phosphorus in carbon disulfide (CS₂) (a two-phase system). In the 20th century, various methods for the preparation of gold colloids were found (Daniel and Astruc, 2004). The conventional method to synthesize AuNPs is the reduction of Au (III) salt (HAuCl₄) by sodium citrate in water. This method was developed by Turkevich and co-workers in 1951, and later refined by Frens in the 1970s. Sodium citrate acts as both of a weak reducer and stabilizer. The color of the reaction mixture changes gradually during synthesis as the following order: pale yellow (AuCl₄⁻), colorless (Au atom), very dark blue, purple and finally ruby red (AuNPs) (Pong *et al.*, 2007). After that, the Brust-Schiffrin method (two-phase synthesis) was introduced in 1994. Au (III) salt (HAuCl₄) is reduced by sodium tetraborohydride (NaBH₄) in the presence of organic stabilizer (e.g. alkanethiols, phosphines, quaternary ammonium salts, surfactants, polymers, etc.) (Nakamoto, Kashiwagi and Yamamoto, 2005). Normally, colloidal solutions of spherical AuNPs are red with the surface plasmon resonance (SPR) band centered at 520 nm. The plasmon resonance phenomenon occurs at metallic surfaces and nanoparticles are reflected by strong absorption of the incident light due to oscillating free electrons on metals. The collective oscillations of free electrons are also known as plasmon. Nevertheless, this phenomenon in nanoparticles can be also called in other terms such as localized surface plasmon resonance or particle plasmon resonance (PPR). SPR band depends weakly on size of the particle and the reflective index of the surrounding media, but strongly on shape alteration and inter-particle distance (Lee and Pérez-Luna, 2005; Baptista *et al.*, 2007).

1.2 Silver nanoparticles (AgNPs)

AgNPs have attracted interest from the chemical industry and medicine due to unique properties such as high thermal conductivity, high resistance of oxidation and

antibacterial activity. AgNPs are widely used in numerous products, containing textiles, personal care products, food storage containers, home appliances, food supplements and medical applications (Navarro *et al.*, 2008). Normally, colloidal solutions of AgNPs are yellow with the surface plasmon resonance (SPR) band near 400 nm. There are several methods for the synthesis of AgNPs such as a chemical reduction method and a radiolytic process. However, the chemical reduction method is widely used, according to the production of nanoparticles without aggregation, high yield and low preparation cost (Song *et al.*, 2009).

2. AuNPs and AgNPs for pharmaceutical application

For therapeutic application, AuNPs themselves can be used for treatment in several diseases such as rheumatoid arthritis and cancer. This is because AuNPs present antiangiogenic effect. Angiogenesis exhibits the formation of new blood vessels, leading to the growth and progression of tumors and the promotion and maintenance of other diseases like neoplasia and rheumatoid arthritis. AuNPs can inhibit vascular endothelial growth factor (VEGF) or vascular permeability factor (VPF) and basic fibroblast growth factor (bFGF), which are two critical cytokines for the induction of angiogenesis (Mukherjee *et al.*, 2005). AuNPs have been developed for use in clinical diagnostics specific detection because of their physical properties, consisting of unique optical properties and high surface areas. The functional ligand on the surface of AuNPs exhibits the selective binding of biomarkers. AuNP-based diagnostics can be divided into three approaches as following: 1) utilization of AuNP color change depending on aggregation; 2) utilization of surface functionalities of the gold core to provide highly selective nanoparticles for diagnosis; 3) utilization of

AuNPs in electrochemical based methods, coupled with metal deposition for signal enhancement (Baptista *et al.*, 2007).

AgNPs themselves have proved to be the most effective antimicrobial efficacy against bacteria, viruses and other eukaryotic microorganisms. For centuries, silver has been used for the treatment of burns and chronic wounds. The antimicrobial activity of silver involves in the amount of silver and the rate of silver released. Silver at metallic state is inert but ionized silver is highly reactive. The ionized silver can bind to tissue proteins and result in structural changes in the bacterial cell wall and nuclear membrane, leading to cell distortion and death. In addition, it binds to bacterial DNA and RNA, causing denaturing and inhibition of bacterial replication. AgNPs present efficient antimicrobial property compared to other silver salts according to their extremely large surface area, contributing to better contact with microorganisms. The nanoparticles release silver ions in the bacterial cells, resulting in the enhancement of bactericidal activity. According to the recent research, AgNPs with the size range of 1-10 nm demonstrate the capacity to interact with HIV-1 virus *via* preferential binding to the gp120 subunit of the viral envelope glycoprotein, as presented *in vitro* (Elechiguerra *et al.*, 2005). AgNPs also show microbial growth inhibition. Yeast and *E. coli* are inhibited at low concentration of AgNPs, while the growth-inhibitory effects on *S. aureus* are mild (Kim *et al.*, 2007). Thus, AgNPs are widely used as consumer and clinical products. However, AgNPs have some risks as the exposure to silver such as argyrosis and argyria, which are toxic to mammalian cells (Rai, Yadav and Gade, 2008; Singh *et al.*, 2008).

Currently, AuNPs can be developed for use as drug delivery as shown in Figure 1. There are various payloads which can be delivered by nanoparticles such

as small drug molecules or large biomolecules, proteins, DNA or RNA. The release of the payloads could be triggered by internal (e.g. glutathione (GSH) or pH) or external (e.g. light) stimuli. The advantages for using AuNPs as carrier in drug delivery include as following: 1) the gold core is essentially inert and non-toxic; 2) the synthesis is less complicated, resulting in forming monodisperse nanoparticles with core sizes ranging from 1 to 150 nm; 3) the surface of AuNPs can be tailored by functional ligand providing effective cellular uptake, controlled payload release and targeting a specific cell (Ghosh *et al.*, 2008; Han *et al.*, 2007). AuNPs are used for drug delivery system by using nanobioconjugates. From the study of Gibson *et al.* (2007), AuNPs could be conjugated with paclitaxel, which is a chemotherapeutic drug. The small particles can avoid the reticuloendothelial system (RES) capture and accumulate in a broader range of tumor.

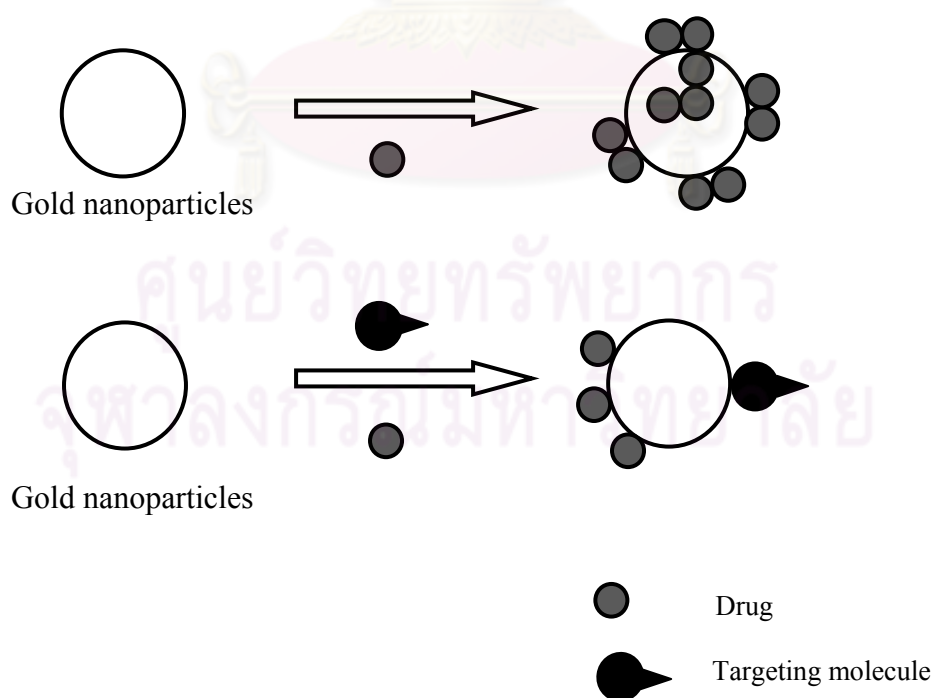


Figure 1 Gold nanoparticles used for drug delivery and targeted delivery system

Because AuNPs and AgNPs could be developed for treatment and drug delivery system, the effect of them on human metabolizing enzymes is necessary in order to determine the incidence of drug interaction during the co-administration with drugs. The findings are useful for drug conjugation with AuNPs or AgNPs as delivery system.

3. Xenobiotic biotransformation

Metabolic process or xenobiotic biotransformation includes the elimination of drugs and other foreign compounds (xenobiotic) from the body by converting lipophilic compounds into more readily excreted polar metabolites. The main biotransforming organ is the liver and the metabolizing enzymes exist in the hepatocytes. Metabolic process is also occurred in other organs (extrahepatic metabolism) e.g. intestine, kidney, lung, brain, skin, etc. Generally, drug metabolizing reaction can be divided into two phases: Phase I reactions involves in chemical alteration of drug structure by oxidation, reduction, hydrolysis, cyclization and decyclization reactions; Phase II reactions relates to conjugation of the drug molecule by glucuronidation, sulfation, acetylation, etc. If the metabolites of phase I reactions are sufficiently polar, they may be ready to excrete from the body or they may be more active or toxic, called toxification or bioactivation. Some of phase I metabolites are not eliminated and undergo to phase II reactions in order to form highly polar compounds. Metabolites from these reactions are more hydrophilic molecules, excreting into urine or bile. In addition, most of them can be less toxic or non-toxic, called detoxification as presented in Figure 2.

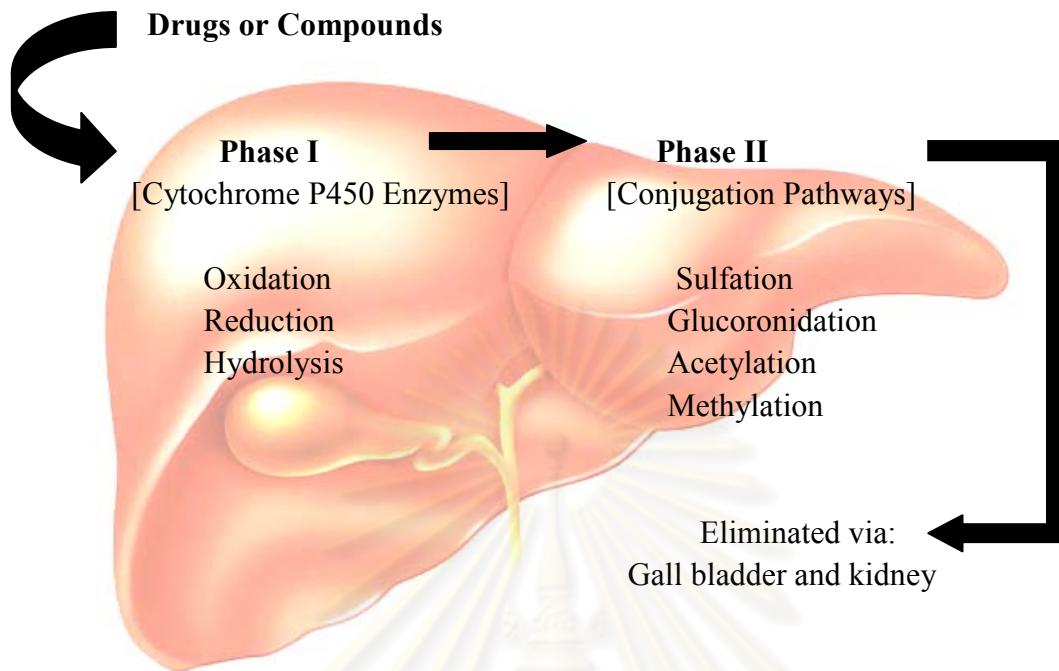


Figure 2 Detoxification of the liver (Shimada *et al.*, 1994)

3.1 Cytochrome P450 (CYP)

CYPs are heme-containing proteins with molecular weight of 45-55 KDa, found in the endoplasmic reticulum and mitochondria. CYPs are synthesized mainly in the liver and lesser in the small intestine, kidney, adrenals and other sites. CYP content, which resides in human tissues, is shown in Table 1.

Table 1 Total CYP content in various human tissues (Pelkonen *et al.*, 2008)

| Tissue | CYP content (nmol/mg microsomal protein) |
|-----------------|---|
| Liver | 0.30 - 0.60 |
| Adrenal | 0.23 - 0.54 |
| Small intestine | 0.03 - 0.21 |
| Brain | 0.10 |
| Kidney | 0.03 |
| Lung | 0.01 |
| Testis | 0.01 |

The name of CYP450 enzymes is identified because they are bound to membranes within a cell (cyto) and contain a heme pigment (chrome and P), expressed an absorption spectrum peak at 450 nm when exposed to carbon monoxide (Lynch and Price, 2007). CYPs are classified by their amino acid sequence homology. If 40% or greater amino acid structure of enzymes is identified, they are included in the same family. In the same family, enzymes with greater than 55% sequence identity are included in the same subfamily. The abbreviation of CYP contains a number indicating the gene family, a letter signifying the subfamily and the last number denoting the enzyme such as 1A2, 2C9, 2C19, 3A4. The CYP3A4 family is the most important enzyme because it constitutes approximately 30% of all microsomal species in human livers and has the widest substrate specificity of all CYPs. There are many factors that may influence CYP activity such as age, gender, genetic and environmental factors. These may lead to variability on CYP expression between individuals, known as genetic polymorphism. Environmental factors (e.g. drugs, diet and lifestyle) also affect metabolic variability. For example, CYP1A2

activity may be increased by smoking and consumption of cruciferous vegetables (Glue and Clement, 1997).

CYP structure includes hydrophobic pocket and heme moiety. Hydrophobic pocket is the site where the substrate is bound. It contains many amino acid residues that can bind a molecule. Heme structure (ferriprotoporphoryn 9; F-9) is the highly specialized lattice structure, supporting a CYP iron molecule (Fe^{2+}) which is the core of the enzyme as shown in Figure 3. The iron is used to catalyze the oxidation of the substrate, requiring a supply of electrons which is carried initially by NADPH (Coleman, 2005).

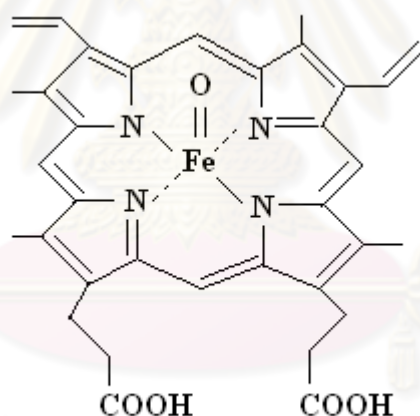


Figure 3 Structure of ferriprotoporphoryn 9 in cytochrome P450

From the CYP typical reaction (Figure 4), CYPs initially form complex with substrate (RH). Then NADPH-dependent cytochrome P450 reductase supply one electron to CYP-substrate molecule. Molecule of oxygen, an electron and two hydrogen ions combine with the reduced cytochrome P450-substrate complex,

providing the product (oxidized substrate; ROH), reoxidation of CYP, NADP⁺ and water (Gibson and Skett, 1996).



Figure 4 Typical reaction by CYP enzyme

NADPH cytochrome P450 reductase is essential to carry the electrons to CYP. It is resided next to the CYP in the endoplasmic reticulum membrane. NADPH reductases are found in most tissue, especially in liver. They are flavin-containing enzyme or flavoprotein, which includes two components, flavin adenine dinucleotide (FAD) and flavin mononucleotide (FMN). NADPH is produced by the consumption of glucose by the pentose phosphate pathway in the cytoplasm. NADPH reductase is acted as fuel pump by using NADPH to supply two electrons to CYP, which can receive only one electron. The mechanism starts with FAD is reduced by NADPH, and then released as NADP⁺. Next, FAD carries two electrons as FADH₂, which passes to FMN to form FMNH₂. Finally, two electrons are passed to CYP. The ratio of NADPH cytochrome P450 reductase to CYP is 1:5 (Coleman, 2005).

3.2 The main human CYP isozymes

There are three main families of CYPs, which are relevant to xenobiotic transformation, including family 1, 2 and 3. CYP3A4 is responsible for the metabolism of the largest number of drugs followed by CYP2D6, the CYP2C family, CYP1A2 and CYP2E1, respectively (Table 2). In addition, the CYP3A family

presents in the largest amounts in the liver followed by the CYP2C family, CYP1A2, CYP2E1 and CYP2D6, respectively. CYP2D6 presents less than 2 percentage of the total content of CYPs in the liver; however, it is responsible for the metabolism of the large amount of drugs especially antidepressant (Coleman, 2005; Shimada *et al.*, 1994).

CYP1A2 expresses from a gene on chromosome 15 in humans and it is linked with estrogen metabolism. Drug substrates consist of caffeine, propranolol and theophylline. CYP1A2 inducer includes polycyclic aromatic hydrocarbons (PAH) in cigarette smoke, leading to the decrease of theophylline level in smokers. Drug inhibitors contain cimetidine, fluvoxamine, erythromycin, clarithromycin, especially in slow acetylators and oral contraceptives. The increase of CYP1A2 leads to the incidence of breast (Hong *et al.*, 2004), colorectal (Kiss *et al.*, 2007) and lung cancers (Seow *et al.*, 2001).

CYP2C9 exhibits the function related to its structure with small, acidic and lipophilic molecules. Its substrates include tolbutamide, warfarin and diclofenac. Drugs that inhibit CYP2C9 constitute of sulphafenazole, fluoxetine and isoniazid. Drug inducers consist of rifampicin and phenobarbital (Goshman *et al.*, 1999).

CYP2C19 presents genetic polymorphism. Approximately 3-5% of Caucasians and 20% of Asians and African-Americans are poor metabolizers. CYP2C19 metabolizes amitriptyline, omeprazole and phenytoin. It is inducible by carbamazepine and norethindrone. Its inhibitors are cimetidine, fluoxetine and ketoconazole (Goshman *et al.*, 1999; Hasler *et al.*, 1999).

CYP2D6 metabolizes more than 80 drugs, including haloperidol, chlorpromazine, propranolol, codeine. All antidepressants except fluvoxamine,

nefazodone, citalopram and bupropion either inhibit CYP2D6 or are metabolized by CYP2D6. Its potent inhibitors contain quinidine, paroxetine, fluoxetine and norfluoxetine. In contrast, this enzyme is non-inducible (Goshman *et al.*, 1999; Hasler *et al.*, 1999).

CYP2E1 metabolizes acetaminophen, ethanol, chlorzoxazone and halothane. Its strong inducers are ethanol and acetone. CYP2E1 inhibitor contains disulfiram (Goshman *et al.*, 1999).

CYP3A4 is responsible for the metabolism of more than 150 drugs, including most calcium channel blockers, benzodiazepines, cyclosporine and tacrolimus. CYP3A4 does not exhibit genetic polymorphism; however, there are large interindividual variations in isozyme levels. These lead to complicated prediction of drug interactions. Besides, about 70% of CYP3A4 appears in the gut to metabolize substrates before reaching to the liver. This results in the decrease of bioavailability. Potent inhibitors of CYP3A4 include macrolides and imidazole antibiotics and grapefruit juice. Drug inducers consist of glucocorticoids, phenytoin and rifampin (Coleman, 2005; Goshman *et al.*, 1999).

ศูนย์วิทยทรัพยากร
จุฬาลงกรณ์มหาวิทยาลัย

Table 2 Cytochrome P450 enzymes and their substrates, inhibitors and inducers (Goshman *et al.*, 1999)

| Isozyme | Substrates | Inhibitors | Inducers |
|----------------|--|--|--|
| CYP1A2 | Clozapine Cyclobenzaprine Fluvoxamine Imipramine Mexiletine Propranolol Theophylline | Cimetidine Ciprofloxacin Clarithromycin Enoxacin Erythromycin Fluvoxamine Ofloxacin Ticlopidine | Polycyclic aromatic hydrocarbons (Cigarette Smoke) Tetrachlorodibenzo-dioxin (TCDD) |
| CYP2C9 | Diclofenac Flurbiprofen Ibuprofen Losartan Naproxen Phenytoin Piroxicam Sulfamethoxazole Tolbutamide Warfarin | Amiodarone Fluconazole Fluoxetine Isoniazid Paroxetine Ticlopidine | Phenobarbital Rifampin |
| CYP2C19 | Amitriptyline Clomipramine Cyclophosphamide Diazepam Imipramine Lansoprazole Nelfinavir Omeprazole Phenytoin | Cimetidine Fluoxetine Fluvoxamine Ketoconazole Lansoprazole Omeprazole Paroxetine Ticlopidine | Carbamazepine Norethindrone |

Table 2 (cont') Cytochrome P450 enzymes and their substrates, inhibitors and inducers (Goshman *et al.*, 1999)

| Isozyme | Substrates | Inhibitors | Inducers |
|----------------|--|--|--|
| CYP2D6 | Amitriptyline Codeine Desipramine Dextromethorphan Imipramine Metoprolol Nortriptyline Oxycodone Paroxetine Propranolol Risperidone Timolol | Amiodarone Fluoxetine Haloperidol Indinavir Paroxetine Quinidine Ritonavir Sertraline | Rifampin |
| CYP2E1 | Acetaminophen Chlorzoxazone Ethanol Enflurane Isoflurane | Disulfiram | Ethanol Isoniazid |
| CYP3A | Alprazolam Astemizole Buspirone Carbamazepine Cisapride Cyclosporine Protease inhibitors Lovastatin Midazolam Simvastatin | Amiodarone Cimetidine Clarithromycin Erythromycin Grapefruit juice Itraconazole Ketoconazole | Carbamazepine Glucocorticoids Phenytoin Rifampin Ritonavir |

4. Drug interaction

Drug interaction is the result of an alteration of CYP metabolism. Drugs interact with CYP in several ways. Drugs may be metabolized by only one isozyme (e.g., metoprolol by CYP2D6) or by multiple isozymes (e.g., warfarin by CYP1A2, CYP2D6 and CYP3A4). Drugs that result in CYP metabolic drug interactions involve in either inhibitors or inducers, which interrupt enzyme function. Enzyme induction leads to acceleration of enzyme synthesis, causing faster drug metabolism and subtherapeutic drug concentration. Enzyme inhibition results in accumulation of drug. If the drug has a narrow therapeutic window, serious toxicity may occur in a short time (Lynch and Price, 2007; Goshman *et al.*, 1999).

4.1 Induction of drug metabolism

Enzyme induction is the process that the enzyme is synthesized in response to a specific inducer molecule, resulting in the translation of the gene of the enzyme by a chemical signal (Coleman, 2005). Enzyme induction can result in accelerated enzyme synthesis, faster drug metabolism and subtherapeutic drug concentrations. This effect mostly occurs gradually over day, rather than hours.

4.2 Inhibition of drug metabolism

Inhibition of drug metabolism is more essentially serious than enzyme induction because the clinical situation of the patient can change in a short time after consuming the inhibitor, resulting in irreversible damage (e.g. stroke, heart attack, etc.). Mechanisms of inhibition can be occurred in several ways. Existed enzyme may be destroyed or lost the catalytic capacity, which induced by inhibitors. Moreover, inhibitors may reduce enzyme development. The mechanism of CYP inhibition can be divided into 3 types: reversible, quasi-irreversible, and irreversible

inhibitions. Type of inhibition depends on many factors such as drug concentration and the characteristics of CYP isozyme (Coleman, 2005; Lin and Lu, 1998).

4.2.1 Reversible inhibition

This type of inhibition is the most common mechanism of CYP inhibition. The effect of this inhibition type will be transient and reversible after releasing of the inhibitor. Also, CYP can be function as the normal situation after the elimination of the inhibitor. It occurs as a result of the binding of CYP and its inhibitor at the hydrophobic substrate binding site (Lin and Lu, 1998).

4.2.2 Quasi-irreversible inhibition via metabolic intermediate complexation

This inhibition causes a reactive metabolite, called metabolite-intermediate (MI) complex which is formed after binding tightly or inhibited to the CYP heme. It leads to the inactivation of CYP function. This inhibition can be reversible for *in vitro* drug metabolism by adding highly lipophilic compounds for dislocating MI from CYP. However, MI is stable for *in vivo*, resulting in the irreversible CYP, so new enzyme need to synthesize to restore activity (Hasler *et al.*, 1999; Lin and Lu, 1998).

4.2.3 Irreversible inhibition

This inhibition causes the irreversible inhibition of substrate and enzyme binding. It results in a reactive intermediate, which can destroy CYP, leading to the irreversible inactivation of CYP when it releases from CYP. The intermediate is classified as mechanism-based inactivators or suicide substrate. It can bind with either heme or apoprotein or both of them of CYP structure (Lin and Lu, 1998).

CHAPTER III

MATERIALS AND METHODS

1. Materials

1.1 Equipments

1. De-ionized water (DI water) system (ELGASStat Option 3B)
(ELGA, England)
2. Fluorescence, absorbance and luminescence reader Victor³ V
model (PerkinElmer, USA)

Light source : Tungsten-halogen lamp
($\lambda = 340-850$ nm)

Detection unit : Photomultiplier tube

Fluorometry : Fluorescein

Optical emission filter : 450/10 nm

Optical excitation filter : 390/20 nm
3. Micropipettes SL-20 (2-20 μ L), SL-200 (20-200 μ L) and SL-1000
(100-1,000 μ L) (Rainin Instrument, USA)
4. Micropipettes tips (Gibson, France)
5. Multichannel pipettes (12 channels) 20 and 100 μ L (Rainin
Instrument, USA)
6. Multichannel tips RT-L250 (250 μ L), TR-222-C (200 μ L) (Rainin
Instrument, USA)
7. Reagent reservoir (Rainin Instrument, USA)
8. Refrigerated centrifuge (Hitachi, Japan)

9. Spectrophotometer (Evolution 300, USA)

| | | |
|--------------|---|--|
| Light source | : | Xenon lamp ($\lambda = 190-1100$ nm) |
| Bandwidths | : | 0.5, 1.0, 1.5, 2.0, 4.0 nm |
| Detector | : | Silicon photodiode |

10. Timer (Citizen, Japan)

11. Transmission Electron Microscopy (JEM-2100) (Jeol, Japan)

| | | |
|----------------------|---|---|
| Magnification | : | 50 – 1,500,000 X |
| Accelerating voltage | : | 80, 100, 120, 160, 200 kV |
| Resolution (HR) | : | Point to point 0.23 nm Lattice 0.14 nm |

12. Ultra-purifier water system (Maxima UF, England)

13. Vortex mixer (Clay Adams, USA)

14. Zetasizer NanoZS (Malvern, UK)

| | | |
|------------------|---|--|
| Laser | : | 4 mW He-Ne (633 nm) |
| Laser attenuator | : | Automatic (transmission 100% to 0.0003%) |
| Detector | : | Avalanche photodiode (O.E. > 50% at 633 nm) |

15. Ultracentrifugal filter 3 kDa (Millipore, USA)

16. 96-well black plates (PerkinElmer, USA)

1.2 Chemicals

1. Acetonitrile anhydrous (ACN) (C_2H_3N , MW = 41.05) (Labscan Asia, Thailand)

2. α -naphthoflavone ($C_{19}H_{12}O_2$, MW = 272.3) (Sigma-Aldrich, USA)
3. Dimethylsulfoxide (DMSO) (C_2H_6OS , MW = 78.13) (Sigma-Aldrich, USA)
4. Hydrochloric acid (HCl, MW = 36.45) (Carlo Erba Reagents, Italy)
5. Hydrogen tetrachloroaurate (III) trihydrate ($HAuCl_4 \cdot 3H_2O$, MW = 393.83) (Sigma-Aldrich, USA)
6. Ketoconazole ($C_{26}H_{28}Cl_2N_4O_4$, MW = 531.43) (Siam Pharmaceutical, Lot no. 06092115664, Thailand)
7. Miconazole ($C_{18}H_{14}Cl_4N_2O$, MW = 479.1) (Government Pharmaceutical Organization, Thailand)
8. Nitric acid (HNO_3 , MW = 63.01) (Carlo Erba Reagents, Italy)
9. Polyethyleneimine (PEI) ($(CH_2CH_2NH)_n$, MW ~ 750 kDa) (Sigma-Aldrich, USA)
10. Polyvinylpyrrolidone K30 (PVP K30) ($(C_6H_9NO)_n$, MW ~ 45-55 kDa) (BASF, Germany)
11. Silver nitrate ($AgNO_3$, MW = 169.87) (Sigma-Aldrich, USA)
12. Sodium borohydride ($NaBH_4$, MW = 37.83) (Merck, Germany)
13. Sulfaphenazole ($C_{15}H_{14}N_4O_2S$, MW = 314.36) (Sigma-Aldrich, USA)
14. Tris(hydroxymethyl)aminomethane (Tris base) ($C_4H_{11}NO_3$, MW = 121.14) (Sigma-Aldrich, USA)
15. Trisodium citrate dihydrate ($Na_3C_6H_5O_7 \cdot 2H_2O$, MW = 294.07) (Sigma-Aldrich, USA)
16. Ultrapure water (18.2 M Ω) (Elga, UK)

17. Vivid[®] CYP450 blue screening kits (Invitrogen, USA), including five components as shown in Table 3.

Table 3 The components of Vivid[®] CYP450 screening kit

| Components | Composition | Size |
|-------------------------------------|--|----------|
| Reaction buffer | <u>CYP1A2 and CYP3A4:</u> Potassium phosphate buffer (200 mM, pH 8.0) <u>CYP2C9 and CYP2C19:</u> Potassium phosphate buffer (100 mM, pH 8.0) | 50 mL |
| BACULOSOMES [®] Reagent | <u>CYP1A2:</u> CYP1A2 and NADPH-P450 reductase (P450-specific content 0.9-1.1 μ M) <u>CYP3A4:</u> CYP3A4 and NADPH-P450 reductase (P450-specific content 0.9-1.1 μ M) <u>CYP2C9:</u> CYP2C9 and NADPH-P450 reductase (P450-specific content 0.9-1.1 μ M) <u>CYP2C19:</u> CYP2C19 and NADPH-P450 reductase (P450-specific content 0.9-1.1 μ M) | 0.5 mmol |
| Regeneration System | 333 mM glucose-6-phosphate (G-6-P) and 30 U/mL glucose-6-phosphate dehydrogenase (G-6- PD) in 100 mM potassium phosphate buffer (pH 8.0) | 0.5 mL |
| Substrate | <u>CYP1A2 and CYP2C19:</u> EOMCC (7-ethyloxymethyloxy-3-cyanocoumarin) <u>CYP2C9 and CYP3A4:</u> BOMCC (7-benzyloxymethyloxy-3-cyanocoumarin) | 0.1 mg |
| NADP ⁺ | NADP ⁺ solution (10 mM) in potassium phosphate buffer (100 mM, pH 8.0) | 0.5 mL |

2. Methods

2.1 Preparation of AuNPs and AgNPs

2.1.1 Preparation of AuNPs

Fifty milliter of citrate and polyethyleneimine (PEI) stabilized AuNPs 1,015 μM (200 ppm of Au atom) and polyvinylpyrrolidone (PVP) stabilized AuNPs 2,031 μM (400 ppm of Au atom) were prepared according to the method described by Kimling *et al.* (2006). Trisodium citrate dihydrate ($\text{Na}_3\text{C}_6\text{H}_5\text{O}_7 \cdot 2\text{H}_2\text{O}$), polyethyleneimine ($\text{CH}_2\text{CH}_2\text{NH}$)_n, polyvinylpyrrolidone K30 ($\text{C}_6\text{H}_9\text{NO}$)_n and hydrogen tetrachloroaurate (III) trihydrate ($\text{HAuCl}_4 \cdot 3\text{H}_2\text{O}$) were used. All glassware was cleaned in aqua regia consisting 3 parts of HCl and 1 part of HNO_3 , rinsed with ultrapure water and then oven dried prior to use.

2.1.1.1 Preparation of citrate stabilized AuNPs

Citrate stabilized AuNPs were prepared by the classical Turkevich method (Kimling *et al.*, 2006). $\text{Na}_3\text{C}_6\text{H}_5\text{O}_7 \cdot 2\text{H}_2\text{O}$ was used as a reducer and stabilizer. Thirty percent of $\text{HAuCl}_4 \cdot 3\text{H}_2\text{O}$ and ultrapure water were added into the flask. Then the mixture was stirred and heated to 90 °C while the flask was closed. Next, 0.202 M $\text{Na}_3\text{C}_6\text{H}_5\text{O}_7 \cdot 2\text{H}_2\text{O}$ was added and continued stirring for 15 minutes (Figure 5). The molar ratios of citrate solution to gold solution were varied to receive the proper condition and the products were characterized by UV- visible spectroscopy. After obtaining the 50 mL AuNPs, the colloid was kept at room temperature and light protected for 24 hours, and then kept at 3-5°C.

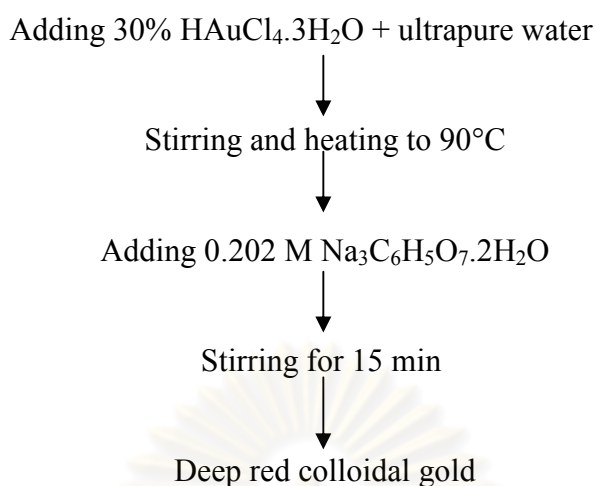


Figure 5 Preparation of citrate stabilized AuNPs

2.1.1.2 Preparation of PEI stabilized AuNPs

PEI stabilized AuNPs were synthesized as described by Turkevich method (Kimling *et al.*, 2006). PEI acted as a reducer and stabilizer. Thirty percent of $\text{HAuCl}_4 \cdot 3\text{H}_2\text{O}$ and ultrapure water were added into the flask. Then the mixture was stirred and heated to 90 °C while the flask was closed. Next, 0.01 M PEI was added and continued stirring for 15 minutes (Figure 6). The molar ratios of PEI solution to gold solution were varied to obtain the optimal condition, detected by UV- visible spectroscopy. AuNPs were kept at room temperature and light protected for 24 hours, and then kept at 3-5°C.

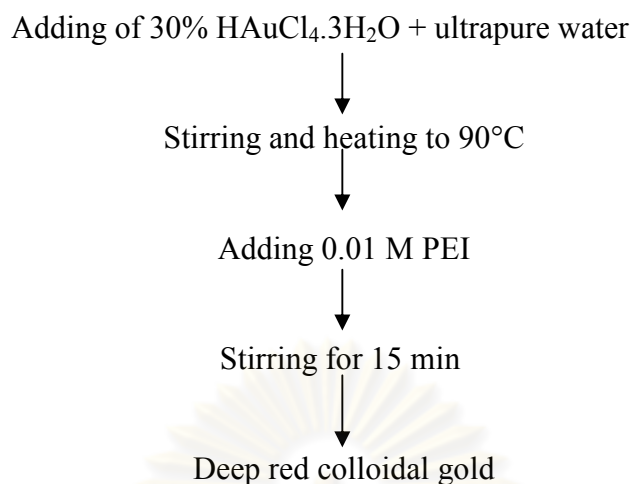


Figure 6 Preparation of PEI stabilized AuNPs

2.1.1.3 Preparation of PVP stabilized AuNPs

Brust-Schiffirin method was adapted to prepare PVP stabilized AuNPs (Brust *et al.*, 1998). PVP K30 was used for stabilization whereas sodium borohydride (NaBH_4) was used as a reducer. Thirty percent of $\text{HAuCl}_4 \cdot 3\text{H}_2\text{O}$ and ultrapure water were added into the flask. The mixture was stirred. Next, 5% PVP K30 was added and 0.035 M NaBH_4 was dropped (1 drop per second). The mixture was stirred for 15 minutes (Figure 7). The various molar ratios of gold and PVP concentration were studied to attain the optimal condition, characterized by UV- visible spectroscopy. The colloid was kept at room temperature and light protected for 24 hours, and then kept at 3-5°C.

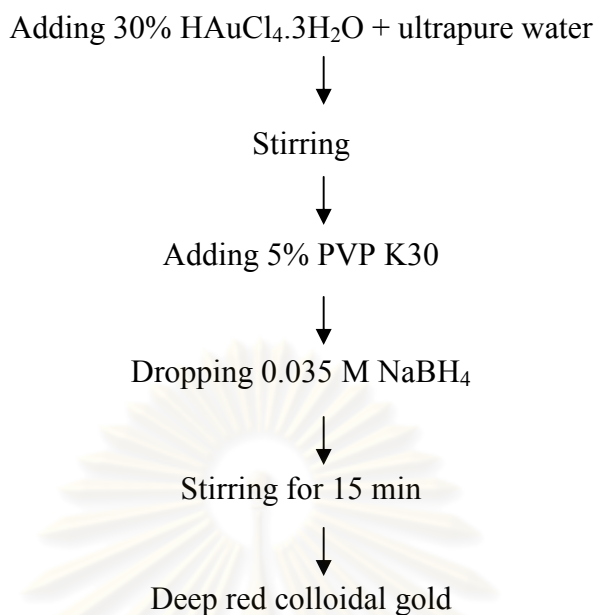


Figure 7 Preparation of PVP stabilized AuNPs

2.1.2 Preparation of AgNPs

A 50-mL of 500 μM (54 ppm) AgNPs was synthesized by adding 1.25 mM NaBH_4 into the flask. Then the mixture was chilled with ice (0°C) and stirred for 30 minutes. Next, 2.5 mM AgNO_3 was dropped about 1 drop per second as shown in Figure 8 (Solomon *et al.*, 2007). The various concentration ratios of sodium borohydride (NaBH_4) to silver solution were observed to gain the suitable condition. AgNPs were kept at room temperature and stored in a closed container, and then kept at $3\text{-}5^\circ\text{C}$.

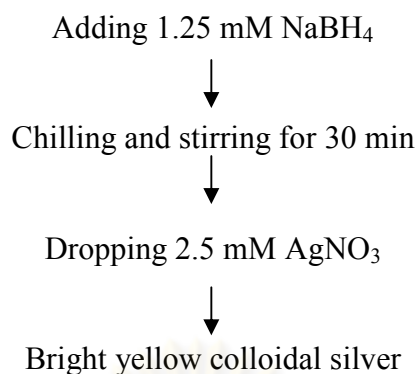


Figure 8 Preparation of AgNPs

2.2 Characterization of AuNPs and AgNPs

AuNPs and AgNPs were characterized after preparation and 1 month storage using UV-visible spectroscopy (Evolution 300, USA) for observing the surface plasmon resonance (SPR). The particle size and size distribution were examined using Transmission Electron Microscopy (TEM) (Jeol, Japan) technique. Additionally, the zeta potential of AuNPs and AgNPs was determined for the surface charge of the nanoparticles by using Zetasizer NanoZS (Malvern, UK).

2.2.1 UV – visible spectroscopy

The optical spectra were obtained with Xenon lamp in single beam. UV quartz cuvette with path length of 10 mm was used for the experiment. The range of the wavelength was observed between 300 to 800 nm. Ultrapure water was used as a reference standard. The absorbance of UV-visible spectra is related to the excitation of a surface plasmon resonance (SPR) (Kimling *et al.*, 2006). The excitation of surface plasmon resonance is due to the collective oscillations of electron at the metallic nanoparticles - dielectric medium interface such as AuNPs or AgNPs and their solvent, which is associated with the electromagnetic field of the coming light.

The color appearance of metallic nanoparticles depends on the surface plasmon band, which occurs from their surface plasmon resonance. The peak extinction (absorbance) wavelength of this band (λ_{\max}) is dependent upon the size, shape, material and dielectric environment of the nanoparticles (Yonzon, Zhang and Van Duyne, 2003). The UV-visible absorbance is also associated with size and the number density of the metallic nanoparticles per unit volume. The calculated value for extinction efficiency (Q_{ext}) can be related to the observed absorbance (A) as presented in the following equation (Haiss *et al.*, 2007):

$$A = \frac{\pi R^2 Q_{\text{ext}} d_0 N}{2.303} \quad (1)$$

with A = absorbance
 R = radius of the spherical particle (nm)
 Q_{ext} = extinction efficiency ($\text{M}^{-1}\text{cm}^{-1}$)
 d_0 = path length of the spectrometer (cm)
 N = number density of particles per unit volume (g/cm^3)

The plasmon absorption is clearly visible and its maximum red-shifts (the increase of λ_{\max}) with increasing particle diameter. This equation also expresses the optical property of AuNPs. The feature of SPR is the dependence of the position and width on the particle size. The spherical AuNPs with 10-40 nm diameter appear as red color, whereas non-spherical AuNPs or the particles above 40 nm diameter appear as blue color (Haiss *et al.*, 2007; Kimling *et al.*, 2006).

2.2.2 Size and size distribution

The particle size and size distribution were studied using Transmission Electron Microscopy (TEM) (Jeol, Japan) technique. The samples were prepared by dropping 10 μL into a carbon-coated 200-mesh copper grid. The grid was air-dried. Then the copper grid with the nanoparticle was examined by TEM measurement. Size distribution was determined by calculation of a number of particle sizes obtained from a TEM image.

2.2.3 Zeta potential measurement

The zeta potential of AuNPs and AgNPs was also measured the surface charge of the nanoparticles by Zetasizer NanoZS (Malvern, UK). Zeta potential is measured by using laser doppler electrophoresis. An electric field is applied to the nanoparticles, resulting in the acceleration of the particles. Light, scattered by moving particles, alters frequency. The interference between the scattered light and original beam provides a modulated signal. Then the frequency analysis leads to electrophoretic mobility (U_E) and the zeta potential is calculated by using the Henry's equation as following (Sjöblom, 2006):

$$U_E = \frac{2 \varepsilon \zeta f(\kappa a)}{3 \eta} \quad (2)$$

ζ = zeta potential (millivolt; mV)

ε = dielectric constant (Farads per meter; F/m)

η = viscosity (Pascal second; Pa s)

$f(\kappa a)$ = Henry's function

Disposable zeta cell was used for the experiment. Ultrapure water was used as a reference standard. The nanoparticles were determined for the zeta potential at the effective shear plane between the movable and non-movable part of the double layer. According to the study, zeta potential was used to detect the charges of AuNPs and AgNPs due to the stabilizers. It also presents the stability effect due to the repulsive electrostatic forces between the particles protecting them against agglomeration and sedimentation in the water suspension (Note, Kosmella and Koetz, 2006).

2.3 Human cytochrome P450 inhibition assay for AuNPs and AgNPs

The CYP inhibition test was processed in 96-well plate using fluorescent Victor³ V plate reader for quantitative detection of light emitting, or light absorbing following the interaction of CYP and AuNPs or AgNPs. The metallic nanoparticles were analyzed in tetraplicated (n=4) for the production of the fluorescent signal in the reactions using Vivid[®] CYP450 blue screening kit, containing Baculosome CYP450, which are prepared from insect cells expressing a particular human CYP isozyme and rabbit NADPH-P450 reductase. Four isozymes, CYP1A2, CYP2C9, CYP2C19 and CYP3A4, were tested in this experiment. Baculosome CYP450 cleaves the blocked dye substrate, which has two potential sites for metabolism. The oxidation at either site releases the highly fluorescent metabolite, which is quantitatively determined as shown in Figure 9 (Invitrogen Corporation, 2008).

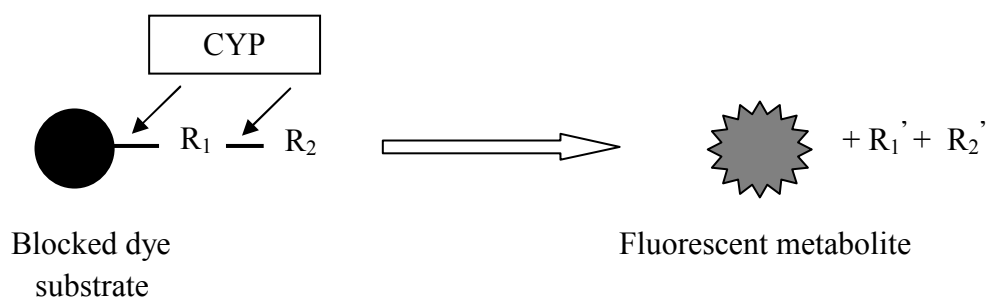


Figure 9 Schematic diagram of fluorescent dye assay on CYP activity

Figure 10 shows the structure of the Vivid[®] substrates which are BOMCC (10 μ M for CYP2C9 or 5 μ M for CYP 3A4) and EOMCC (3 μ M for CYP1A2 or 10 μ M for CYP 2C19). The structures are metabolized by specific CYP into fluorescent metabolite as present in Figure 11. If test compound has ability to inhibit CYP, the formation of fluorescent metabolite is less or absence.

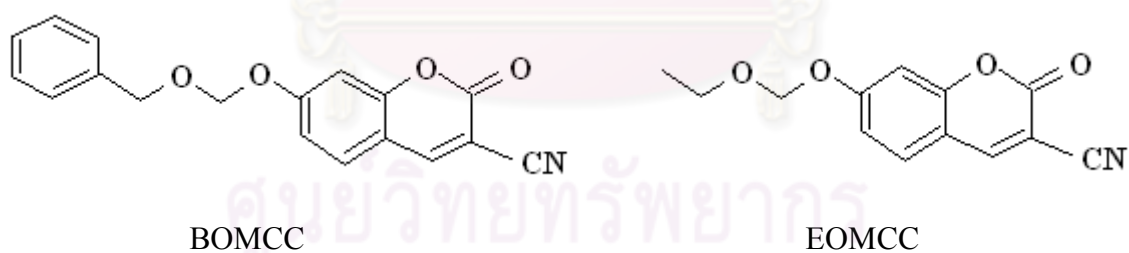


Figure 10 The structures of Vivid[®] BOMCC (7-benzyloxymethoxy-3-cyanocoumarin) and EOMCC (7-ethyloxymethoxy-3-cyanocoumarin) substrates

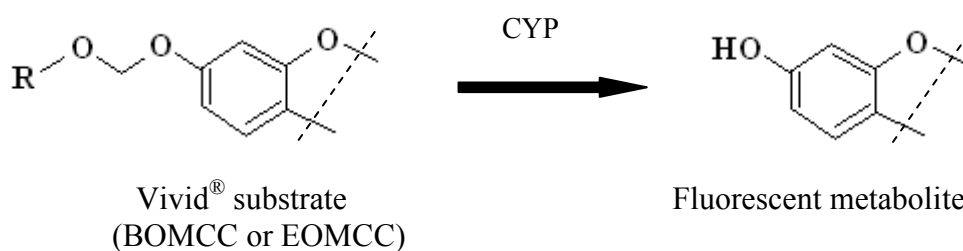


Figure 11 Schematic diagram of metabolism of blocked dye substrate into fluorescent metabolite (Marks and Larson, 2009)

2.3.1 Preparation of Vivid[®] CYP450 screening kit and assay procedure for inhibition test

Vivid[®] CYP450 screening kit consists of reaction buffer (potassium phosphate buffer), Baculosome[®] reagent (CYP and NADPH-reductase), regeneration system (333 mM glucose-6-phosphate and 30 U/mL glucose-6-phosphate dehydrogenase in 100 mM potassium phosphate buffer (pH 8.0)), substrate (EOMCC: ethyloxymethyloxy-3-cyanocoumarin or BOMCC: 7-benzyloxymethyloxy-3-cyanocoumarin) and NADP⁺ as shown in Table 3. The assay protocol was followed according to the manufacturer's instruction (Invitrogen Corporation).

2.3.1.1 Preparation of Vivid[®] CYP450 screening kit for inhibition assay

The preparation of Vivid[®] CYP450 screening kit started with thawing the frozen kit components and then keeping them on ice until use. Vivid[®] substrates of 0.1 mg were reconstituted by using acetonitrile anhydrous in the various amounts as presented in Table 4. The mixture was mixed using vortex mixer. The reconstituted substrate was kept at room temperature; otherwise, it should be kept at -20°C.

Table 4 Reconstitution of Vivid[®] substrates

| Isozyme type | Vivid[®] CYP substrate, mg per container | Anhydrous acetonitrile added (μL) |
|---------------------|--|--|
| 1A2 | EOMCC, 0.1 | 205 |
| 2C9 | BOMCC, 0.1 | 160 |
| 2C19 | EOMCC, 0.1 | 205 |
| 3A4 | BOMCC, 0.1 | 160 |

After that, CYP Baculosomes[®] reagent, regeneration system and buffer were mixed for preparing of master pre-mix. The amount of components per 100 well is shown in Table 5. The master pre-mix solution was mixed by inversion in the container and stored on ice before use.

Table 5 Component of master pre-mix per 100 well

| Isozyme type | Vivid[®] CYP reaction buffer added (μL per 100 well) | Regeneration system added (μL per 100 well) | CYP Baculosome[®] added (μL per 100 well) |
|---------------------|--|--|---|
| 1A2 | 4850 (Buffer I) | 100 | 50 |
| 2C9 | 4800 (Buffer II) | 100 | 100 |
| 2C19 | 4850 (Buffer II) | 100 | 50 |
| 3A4 | 4850 (Buffer I) | 100 | 50 |

Reaction buffer I was 200 mM potassium phosphate buffer

Reaction buffer II was 100 mM potassium phosphate buffer

Next, the mixture of pre-mix reconstitution of Vivid[®] substrate, NADP⁺ and buffer were prepared and the amount of components per well is shown in Table 6.

Table 6 Pre-mix Vivid[®] CYP substrate and NADP⁺ per 100 well

| Isozyme type | Vivid[®] CYP reaction buffer added (μL per 100 well) | Reconstituted substrate added (μL per 100 well) | NADP⁺ added (μL per 100 well) |
|---------------------|--|--|---|
| 1A2 | 885 (Buffer I) | 15 | 100 |
| 2C9 | 850 (Buffer II) | 50 | 100 |
| 2C19 | 850 (Buffer II) | 50 | 100 |
| 3A4 | 850 (Buffer I) | 50 | 100 |

Reaction buffer I was 200 mM potassium phosphate buffer

Reaction buffer II was 100 mM potassium phosphate buffer

2.3.1.2 Preparation of stop solutions

Stop solution was prepared to terminate the reaction between enzymes and substrates. 0.5 M Tris base (pH 10.5) solution was prepared by weighing 15.1425 g of Tris base to a 250-mL volumetric flask and then adjusting the volume with water. pH of the solution was adjusted to 10.5 by using NaOH and HCl. The solution was kept at 4 °C.

2.3.1.3 Assay procedure

The assay condition was established for setting up the microplate (96-well plate) according to Figure 12. The control well included the solvent controls containing the solvent of sample solutions. Background of test compound and solvent control were used for preventing fluorescent error in the system by subtracting background fluorescence during data analysis. The inhibition test were analyzed in tetraplicate (n=4) by using two microplates. Each microplate included duplicate (n=2) of the sample solution.

| | 1 | 2 | 3 | 4 | 5 | 6 | 7 | 8 | 9 | 10 | 11 | 12 |
|---|---|---|---|---|---|---|---|---|-----------------------|----|----|----|
| A | Sample solution in various concentrations | | | | | | | | Solvent control | | | |
| B | Background of inhibitor solution | | | | | | | | Background of solvent | | | |
| C | | | | | | | | | | | | |
| D | | | | | | | | | | | | |
| E | | | | | | | | | | | | |
| F | | | | | | | | | | | | |
| G | | | | | | | | | | | | |
| H | | | | | | | | | | | | |

Figure 12 Schematic diagram of microplate organization for Vivid[®] CYP450 screening kit protocol

First of all, the blank plate was measured for the fluorescence on Victor³ V plate reader using filter with wavelength of 409 and 460 nm for excitation and emission, respectively. The reaction was processed in black, flat-bottomed, 96-well plates with a mixture volume of 100 μ L per well. Forty microliter of sample solutions were added into the sample solution or its background wells while the solvent of each sample solution was added into the solvent control or its background wells. Then 50 μ L of master pre-mix solution was added into the test compound or solvent control wells whereas the reaction buffer was added into the background wells. The incubation time was required for 20 minutes at room temperature to allow sample solutions to interact with CYP. After that, 10 μ L of Pre-mix Vivid[®] CYP substrate and NADP⁺ solution was added to start the reaction. Then the mixing compounds were incubated for 30 minutes (CYP3A4, CYP2C19 and CYP1A2) or 40 minutes (CYP2C9) at room temperature and protected from light. The incubated time

of CYP2C9 was longer than the others because this CYP has less fluorescent sensitivity than other CYPs. Next, 10 μL of the stop solution was added to quench the reaction. The process of enzyme inhibition assay is shown in Figure 13. Finally, the fluorescence was measured to acquire the results for analysis.

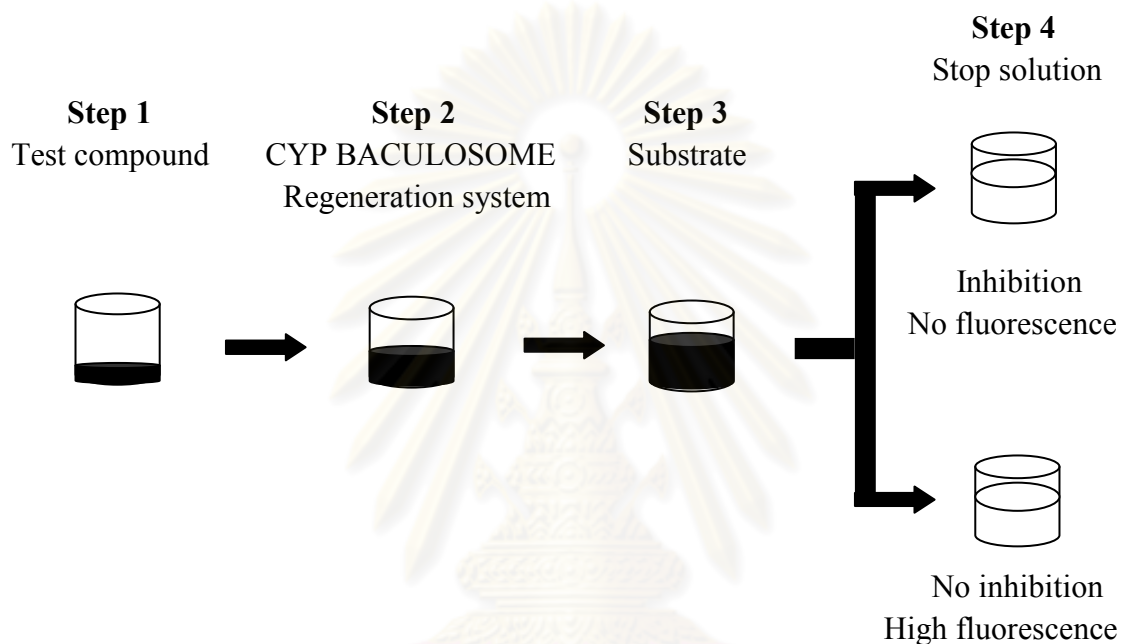


Figure 13 Four steps of enzyme inhibition assay

2.3.1.4 Data analysis

The relative fluorescence unit (RFU) was obtained from the measurement of the fluorescence of the final mixture. The percent inhibition was calculated using this following equation:

$$\% \text{ inhibition} = \left[1 - \frac{(\text{RFU test compound} - \text{RFU background of test compound})}{(\text{RFU solvent control} - \text{RFU background of solvent control})} \times 100 \right] \quad (3)$$

The percentages of inhibition for each test compound concentration were plotted versus log value of each test compound concentration to produce inhibitory curve. The GraphPad Prism 4.03 program (San Diego, CA) was used to generate nonlinear regression curve by using an equation for sigmoidal dose-response (variable hill slope). The concentration with 50% of CYP inhibition (median inhibition concentration, IC_{50}) was determined and the data were presented as mean \pm SD. The goodness of fit of the inhibitory curve (R^2) was also calculated.

2.3.2 Verification of CYP inhibition test

The known standard inhibitors of CYPs were used for validating the assay procedure. P450 inhibitors used in the assay included α -naphthoflavone, sulfaphenazole, miconazole and ketoconazole for CYP1A2, CYP2C9, CYP2C19 and CYP3A4, respectively (Marques-Soares *et al.*, 2003; Monostory, Hazai and Vereczkey, 2004). DMSO of 2.5% was used as drug solvent for CYP1A2, CYP2C9 and CYP2C19 assay, while 2.5% ACN was used as drug solvent for CYP3A4 assay.

2.3.2.1 Preparation of inhibitor solutions

A. Preparation of α -naphthoflavone solutions

α -Naphthoflavone of 10 mM in DMSO was prepared. Then 25 μ L of drug stock solution and 975 μ L of water were mixed to obtain the solution of 250 μ M α -naphthoflavone containing 2.5% DMSO. The concentrations of α -naphthoflavone were varied by serially diluted with 2.5% DMSO for use in the assay.

B. Preparation of sulfaphenazole solutions

Sulfaphenazole was dissolved in DMSO to obtain the drug concentration of 3 mM. After that, 25 μ L of stock solution and 975 μ L of water were

mixed to obtain the final concentration of 75 μM in 2.5% DMSO. The serial concentration of sulfaphenazole was prepared by diluting with 2.5% DMSO.

C. Preparation of miconazole solutions

One hundred micromolar of miconazole in DMSO was prepared. The mixture of 25 μL of stock solution and 975 μL of water were prepared to generate 2.5 μM miconazole in 2.5% DMSO. The concentrations of miconazole were varied by serially diluted with 2.5% DMSO for the inhibition assay.

D. Preparation of ketoconazole solutions

Ketoconazole of 4.585 mM in acetonitrile (ACN) was prepared. The mixture of 25 μL of stock solution and 975 μL of water were prepared to produce 114.63 μM ketoconazole in 2.5% ACN. The concentrations of ketoconazole were serially diluted with 2.5% ACN for enzyme assay.

It was noted that the concentrations of the inhibitor and their solvent used in the reaction were decreased for 2.5 times of their prepared concentrations as shown in Table 7. This is because 40 μL of sample solutions were added into the test well, containing 100 μL of the total reaction volume. Therefore, the solvent for CYP1A2, CYP2C9 and CYP2C19 were 1% DMSO and for CYP3A4 was 1% ACN, in reaction volume. The known inhibitors were tested for CYP inhibition using the previously described procedure and the IC_{50} values of each drug solution were determined.

Table 7 Concentration of CYP inhibitors per reaction volume (100 μ L)

| Concentration of CYP inhibitors (μM) | | | |
|--|-----------------------|-------------------|---------------------|
| CYP1A2 | CYP2C9 | CYP2C19 | CYP3A4 |
| α-Naphthoflavone | Sulfaphenazole | Miconazole | Ketoconazole |
| 0.005 | 0.001 | 0.010 | 0.110 |
| 0.010 | 0.010 | 0.025 | 0.275 |
| 0.025 | 0.050 | 0.050 | 0.550 |
| 0.050 | 0.250 | 0.100 | 2.200 |
| 0.100 | 2.000 | 0.250 | 11.000 |
| 0.250 | 10.000 | 0.500 | 55.000 |
| 0.500 | 30.000 | 1.000 | |
| 1.000 | | | |

2.3.3 CYP inhibition of AuNPs and AgNPs

2.3.3.1 Preparation of test compounds

AuNPs and AgNPs were 2 times repetitively centrifuged (20 minutes, 5000 x g) by using 3 kDa ultracentrifugal filters to get rid of the excess stabilizer. Concentrations of the test compounds were varied ranging between 0.05 and 2,031 μ M by diluting with water which was used as a control. The 40 μ L of sample solutions were added into the test well, containing 100 μ L of the total reaction volume. The final concentrations of AuNPs and AgNPs are shown in Table 8.

2.3.3.2 Assay procedure

The assay condition was performed in microplate (96-well plate) as previously described. The reaction was processed in black, flat-bottomed, 96-well plates with a mixture volume of 100 μ L per well. Forty microliter of AuNPs or AgNPs was added into the test compound or its background well whereas ultrapure water was added into the solvent control or its background well. Then 50 μ L of Master Pre-Mix

solution was added into the test compound or solvent control well while the reaction buffer was added into the background well. The incubation time was required for 20 minutes at room temperature to allow AuNPs and AgNPs to interact with CYP. After that, 10 μL of Pre-mix Vivid[®] CYP substrate and NADP^+ solution was added to start the reaction. The mixing compounds were incubated for 30 minutes (CYP3A4, CYP2C19 and CYP1A2) or 40 minutes (CYP2C9) at room temperature and protected from light. After that, 10 μL of the stop solution was added to quench the reaction. The fluorescence was determined to obtain the results for analysis as described previously.

2.3.3.3 Statistical analysis

The IC_{50} values of nanoparticles on CYP were determined as previously described. The mean differences of the IC_{50} on four CYPs of AuNPs stabilized by each stabilizer and AgNPs were compared by using one-way analysis of variance (ANOVA) and $p < 0.05$ was considered to be significant. Then bonferroni post hoc test was used for determining significant different among IC_{50} values.

ศูนย์วิทยทรัพยากร
จุฬาลงกรณ์มหาวิทยาลัย

Table 8 Concentration of AuNPs and AgNPs in reaction volume (100 μ L) for CYP assay

| Concentration of test compounds for CYP assay | | | | | | | | | | | | | | | | |
|---|-----|------|-----|---------------------------------|-----|------|-----|---------------------------------|-----|------|-----|------------------|-----|------|-----|-----|
| Citrate stabilized AuNPs (μ M) | | | | PEI stabilized AuNPs (μ M) | | | | PVP stabilized AuNPs (μ M) | | | | AgNPs (μ M) | | | | |
| 1A2 | 2C9 | 2C19 | 3A4 | 1A2 | 2C9 | 2C19 | 3A4 | 1A2 | 2C9 | 2C19 | 3A4 | 1A2 | 2C9 | 2C19 | 3A4 | |
| 203 | 203 | 20 | 203 | 2 | 0.2 | 0.2 | 2 | 2 | 0.2 | 2 | 2 | 10 | 10 | 2 | 2 | |
| 406 | 406 | 203 | 406 | 10 | 2 | 2 | 4 | 20 | 2 | 20 | 20 | 20 | 14 | 10 | 10 | |
| | | 406 | 406 | 20 | 4 | 4 | 6 | 203 | 20 | 203 | 203 | 30 | 20 | 14 | 14 | |
| | | 406 | 406 | 30 | 6 | 6 | 10 | 406 | 203 | 406 | 406 | 40 | 26 | 20 | 20 | |
| | | 406 | 406 | 51 | 10 | 10 | 20 | 609 | 406 | 609 | 609 | 60 | 30 | 30 | 30 | |
| | | 406 | 406 | 152 | 20 | 20 | 203 | 812 | 609 | 812 | 812 | 80 | 40 | 40 | 40 | |
| | | 406 | 406 | 254 | 203 | 203 | 406 | | 812 | | | | | | | |
| | | 406 | 406 | 406 | 406 | 406 | 406 | 406 | 406 | 406 | 406 | 406 | 406 | 406 | 406 | 406 |
| | | 406 | 406 | 406 | 406 | 406 | 406 | 406 | 406 | 406 | 406 | 406 | 406 | 406 | 406 | 406 |

CHAPTER IV

RESULTS AND DISCUSSION

1. Preparation of AuNPs and AgNPs

AuNPs and AgNPs could be prepared by the chemical reduction method. Au^{3+} and Ag^+ are reduced to obtain Au^0 and Ag^0 . The stabilizers used for synthesis of AuNPs were citrate (in form of trisodium citrate dihydrate), polyethyleneimine (PEI) and polyvinylpyrrolidone (PVP). The molar ratios of stabilizer (citrate, PEI and PVP) to hydrogen tetrachloroaurate (HAuCl_4) were varied from 0.2 : 1 to 135 : 1. The molar ratio of stabilizer (NaBH_4) to silver was also varied from 9 : 5 to 11 : 5 to receive the most stable condition and the products were characterized by UV- visible spectroscopy (Table 9). It was noted that the concentrations of hydrogen tetrachloroaurate (HAuCl_4) and silver nitrate (AgNO_3) were kept constant at 1.0 mM and 0.5 mM, respectively. The appearances of prepared AuNPs and AgNPs after preparation and after 1 month storage are presented in Figure 14. The color of AuNPs was pink red and of AgNPs appeared yellow. The molar ratios of trisodium citrate to hydrogen tetrachloroaurate were varied from 8 : 1 to 40 : 1 for synthesis of citrate stabilized AuNPs. This is because the molar ratio of trisodium citrate to hydrogen tetrachloroaurate at around 8 : 1 showed the surface plasmon resonance (SPR) of 520 nm and diameter of 17 nm (Kimling *et al.*, 2006). According to the citrate stabilized AuNPs results, it was found that the suitable concentration ratio of trisodium citrate to hydrogen tetrachloroaurate might be 16 : 1 (condition 2). The condition 1 showed the settled particles on the bottom after 1 month storage whereas the condition 3 was unsuccessful for synthesis. The molar ratios of PEI and hydrogen tetrachloroaurate

were varied from 0.2 : 1 to 1.4 : 1 for PEI stabilized AuNPs synthesis. According to the study of Sun *et al.* (2003), the molar ratio of PEI and hydrogen tetrachloroaurate with 0.68 : 1 presented stable AuNPs with SPR of 520 nm and diameter of 12 nm. Therefore, the molar ratio of PEI and hydrogen tetrachloroaurate was at least 0.68 : 1 might produce the stable AuNPs. From the result of PEI stabilized AuNPs, the concentration ratios of PEI to hydrogen tetrachloroaurate of 0.7 : 1 and 1.4 : 1 (conditions 2 and 3) could produce the stable PEI stabilized AuNPs. However, which of 0.7 : 1 was chosen for cytochrome P450 inhibition study due to less amount of stabilizer used. AuNPs prepared using condition 1 presented the alteration of λ_{\max} and the color of suspension from red to purple, indicating the change of the particle size (Kimling *et al.*, 2006). In addition, the molar ratios of polyvinylpyrrolidone (PVP) to hydrogen tetrachloroaurate were varied from 45 : 1 to 135 : 1. According to previous study, the molar ratio of PVP to hydrogen tetrachloroaurate of 45 : 1 provided stable AuNPs with SPR of 521 nm while the lower molar ratio presented the aggregation of the nanoparticles (Pardiñas-Blanco *et al.*, 2007). However, in the present study, the molar ratios of PVP to hydrogen tetrachloroaurate of 90 : 1 and 135 : 1 (condition 2 and 3) were the concentrations that could form stable AuNPs. Nonetheless, that of 90 : 1 was selected for further study owing to less amount of stabilizer used. The AuNPs prepared using condition 1 demonstrated the precipitation after 1 month storage. From the results, PEI presented the most effective stabilizer since the lowest amount was used for AuNP synthesis. This is because PEI is polyelectrolytes, which are capable of combining both steric and electrostatic stabilization (Sun *et al.*, 2003). In addition, PVP (nonionic stabilizer) was used at the largest amount for the synthesis followed by citrate and PEI, which exhibited negatively and positively charged

stabilizers. Citrate provides electrostatic stabilization whereas PVP, which is polymer, presents steric stabilization. According to AgNP synthesis, sodium borohydride (NaBH_4) acts as both a reducer and electrostatic stabilizer. From the study of Solomon *et al.* (2007), the molar ratio of sodium borohydride to silver nitrate at 2 : 1 produced the most stable AuNPs. Therefore, the molar ratio of sodium borohydride to silver nitrate was varied from 9 : 5 to 11 : 5. From AgNP results, the concentration of sodium borohydride should be twice which of silver nitrate (condition 2) to receive the stable nanoparticles. The conditions 1 and 3 were unsuccessful for synthesis. In conclusion, the citrate, PEI and PVP stabilized AuNPs and AgNPs prepared using condition 2 were chosen for use in enzyme inhibition assay. The condition 2 of citrate, PEI and PVP stabilized AuNPs and AgNPs were also shown the stability after 6 month storage as presented in Figure 15.

Table 9 The stability of AuNPs and AgNPs with varying concentrations of stabilizers

| Citrate stabilized AuNPs | | |
|---------------------------------|--|--------------------------------|
| Condition | [trisodium citrate] : [HAuCl₄] | Stability after 1 month |
| 1 | 8 : 1 | unstable |
| 2 | 16 : 1 | stable |
| 3 | 40 : 1 | unstable |
| PEI stabilized AuNPs | | |
| Condition | [PEI] : [HAuCl₄] | Stability after 1 month |
| 1 | 0.2 : 1 | unstable |
| 2 | 0.7 : 1 | stable |
| 3 | 1.4 : 1 | stable |
| PVP stabilized AuNPs | | |
| Condition | [PVP] : [HAuCl₄] | Stability after 1 month |
| 1 | 45 : 1 | unstable |
| 2 | 90 : 1 | stable |
| 3 | 135 : 1 | stable |
| AgNPs | | |
| Condition | [NaBH₄] : [AgNO₃] | Stability after 1 month |
| 1 | 9 : 5 | unstable |
| 2 | 10 : 5 | stable |
| 3 | 11 : 5 | unstable |

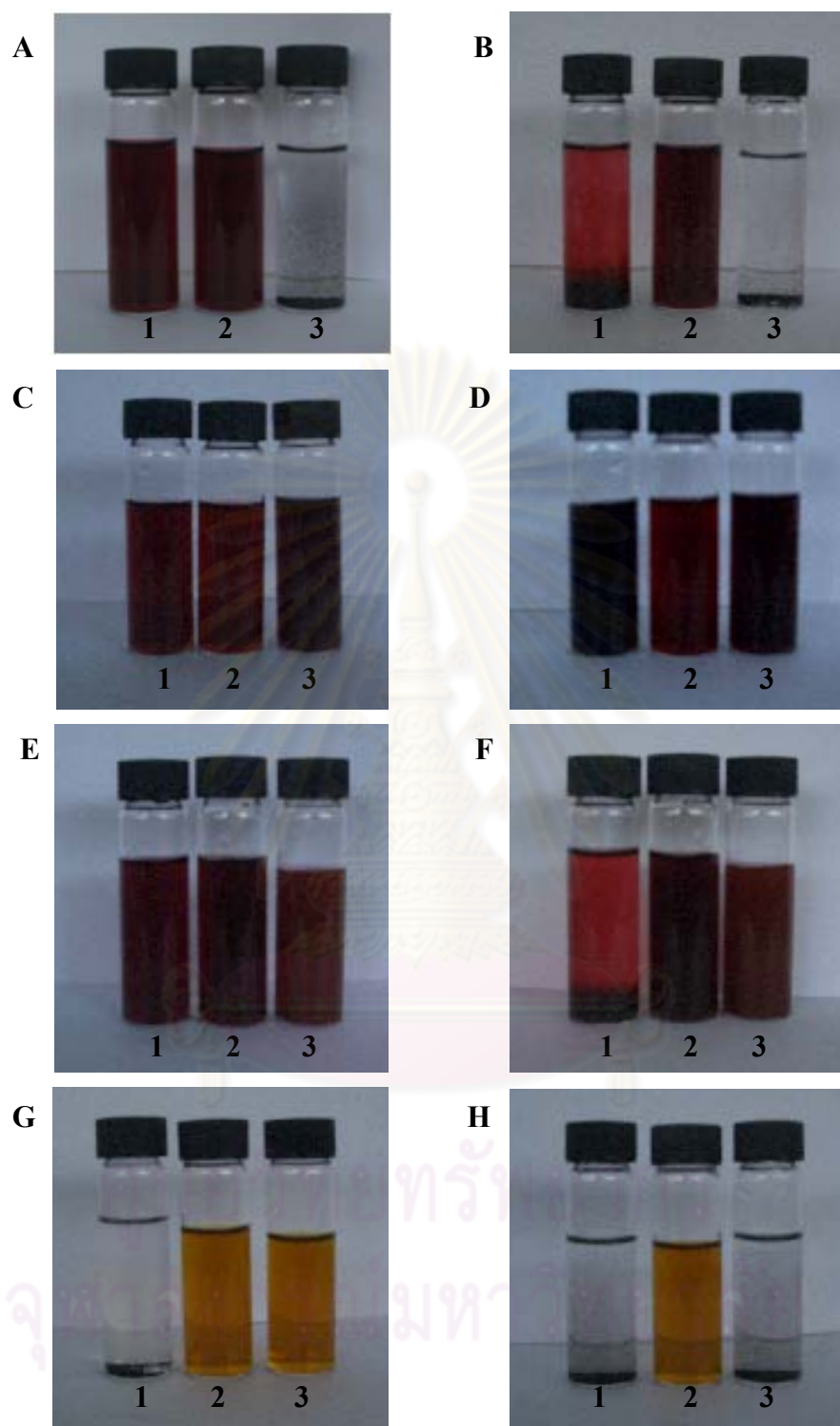


Figure 14 The appearances of nanoparticles prepared according to conditions 1,2 and 3 of, citrate stabilized AuNPs after preparation (A) and after 1 month storage (B), PEI stabilized AuNPs after preparation (C) and 1 month storage (D), PVP stabilized AuNPs after preparation (E) and 1 month storage (F) and AgNPs after preparation (G) and 1 month storage (H)

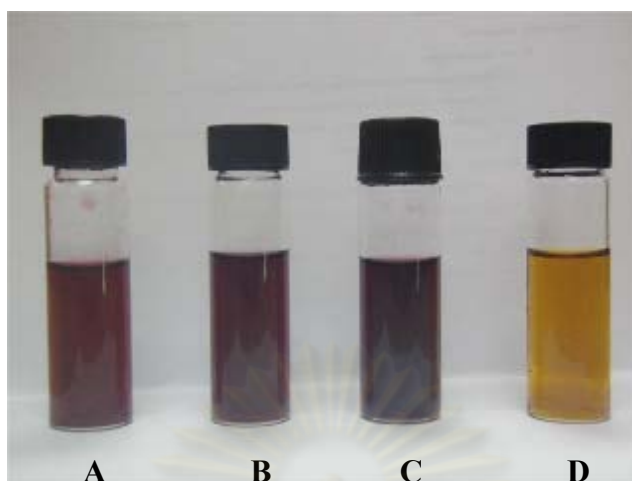


Figure 15 The appearances of citrate stabilized AuNPs (A), PEI stabilized AuNPs (B), PVP stabilized AuNPs (C) and AgNPs (D) after 6 month storage

2. Characterization of AuNPs and AgNPs

2.1 UV – visible spectroscopy

The surface plasmon resonances of AuNPs and AgNPs prepared previously with varied molar ratios of stabilizer and hydrogen tetrachloroaurate (for AuNPs) and silver nitrate (for AgNPs) after preparation and 1 month storage are represented in Figures 16 - 27. The maximal absorption wavelength of AuNPs and AgNPs after preparation and 1 month storage are presented in Table 10. The characteristics of the UV – visible absorption peak were related to particle diameter, degree of aggregation and particle concentration (Haiss *et al.*, 2007; Song *et al.*, 2009). Normally, the peak absorbance wavelength of surface plasmon band (λ_{\max}) of AuNPs and AgNPs were approximately in the range of 520 and 400 nm, respectively (Daniel and Astruc, 2004; Solomon *et al.*, 2007). Thus, the λ_{\max} of AuNPs and AgNPs found in the present study (520 – 525 nm for AuNPs and 420 nm for AgNPs) were in agreement with other studies. The absence of peak was reported for AuNPs with core diameter less than 1 nm, as well as for bulk gold (Daniel and Astruc, 2004). According to Figures

16 and 22, the peak heights of AuNPs reduced after 1 month storage due to the precipitation of AuNPs because of the decrease of AuNP concentration in the upper layer. The unchange of absorption peak of AuNPs and AgNPs after storage could be observed for nanoparticles prepared by using optimum molar ratio of stabilizer to gold and silver solutions as seen in Figures 17, 20, 21, 23, 24 and 26. However, the absorption peak of AgNPs became broader after 1 month storage, possibly indicating some aggregation of the nanoparticles (Song *et al.*, 2009).

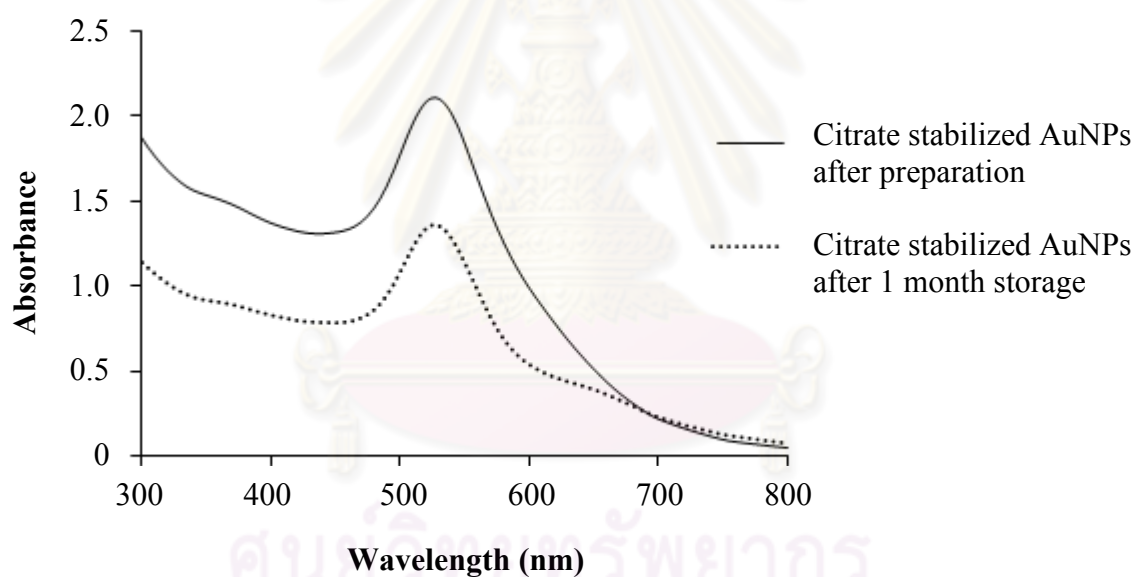


Figure 16 UV absorption spectra of citrate stabilized AuNPs prepared with condition 1 after preparation and 1 month storage

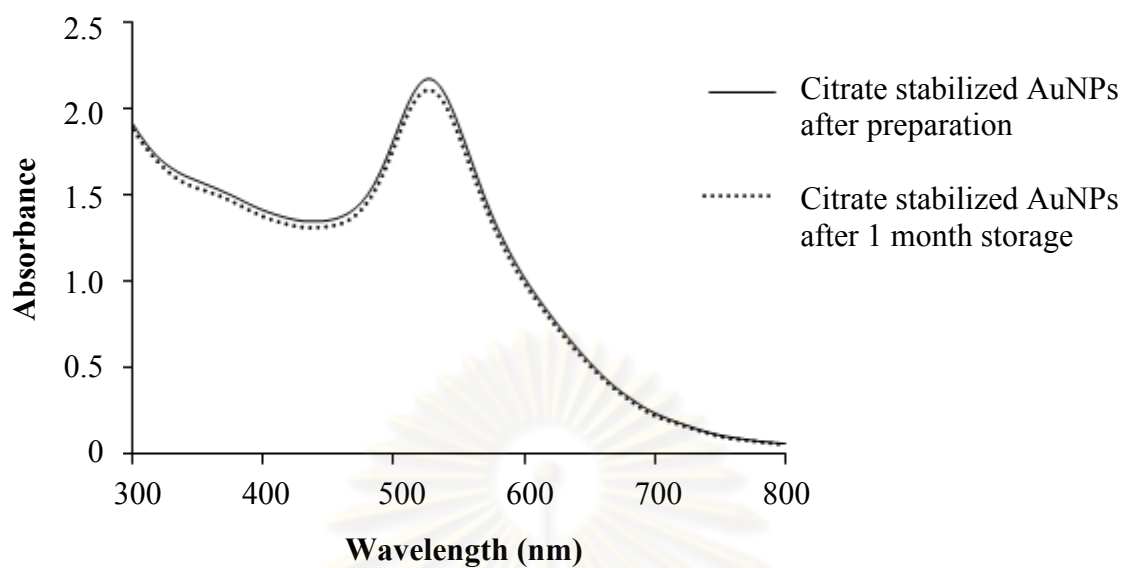


Figure 17 UV absorption spectra of citrate stabilized AuNPs prepared with condition 2 after preparation and 1 month storage

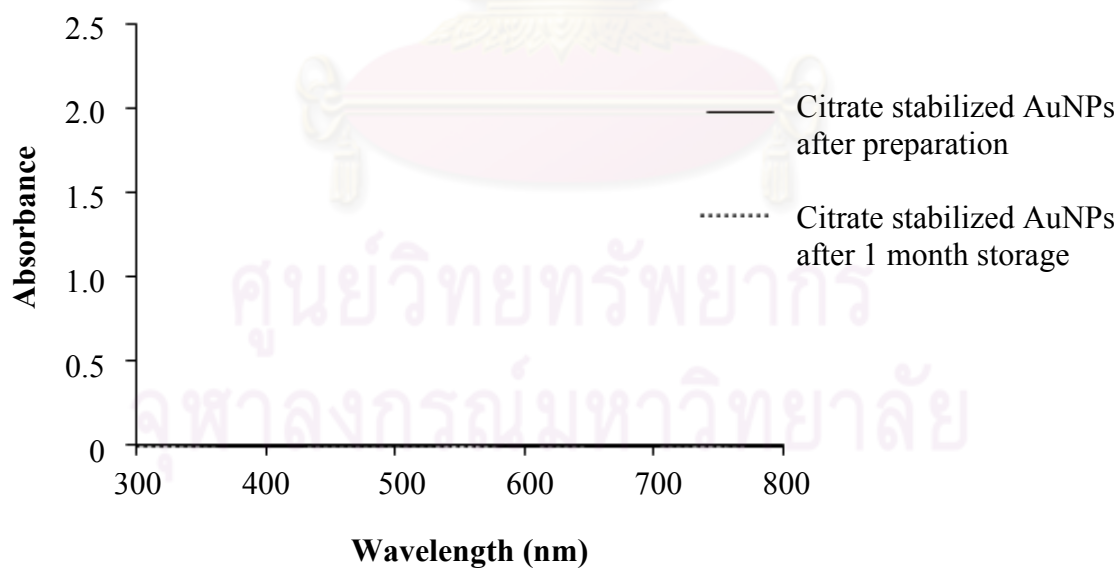


Figure 18 UV absorption spectra of citrate stabilized AuNPs prepared with condition 3 after preparation and 1 month storage

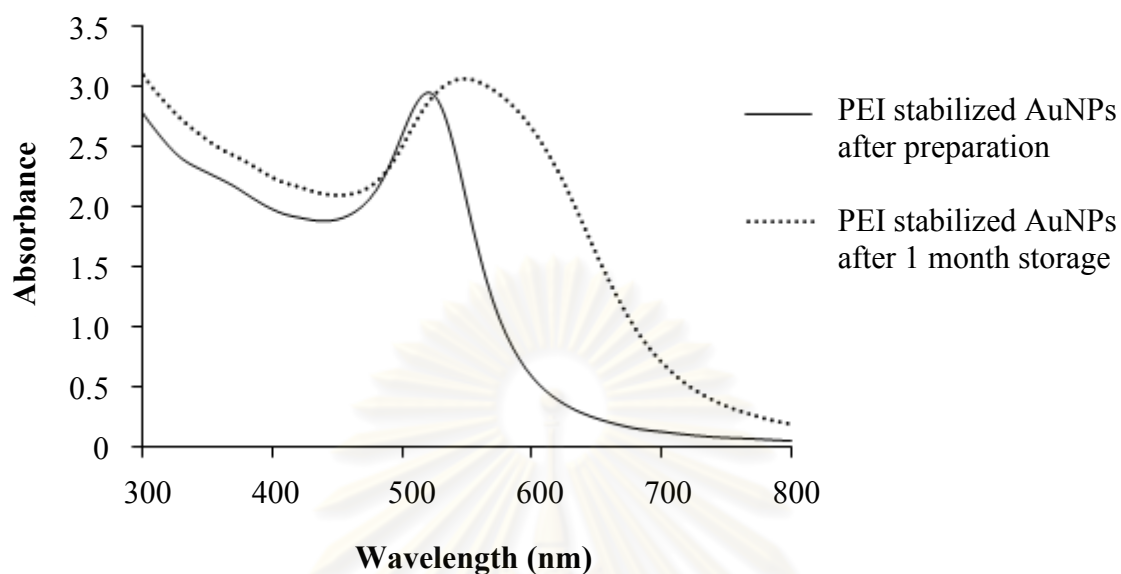


Figure 19 UV absorption spectra of PEI stabilized AuNPs prepared with condition 1 after preparation and 1 month storage

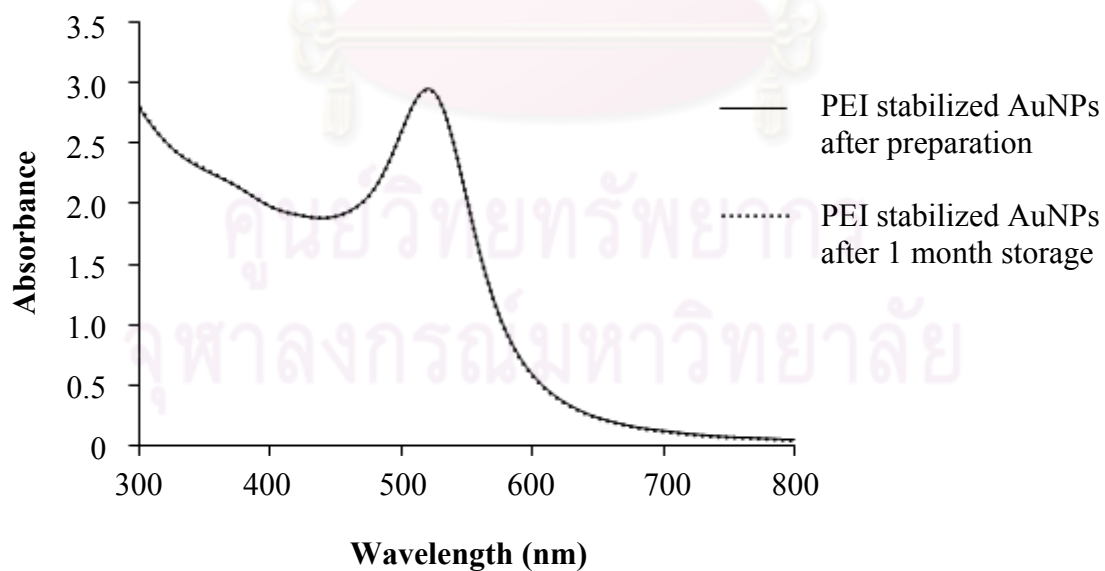


Figure 20 UV absorption spectra of PEI stabilized AuNPs prepared with condition 2 after preparation and 1 month storage

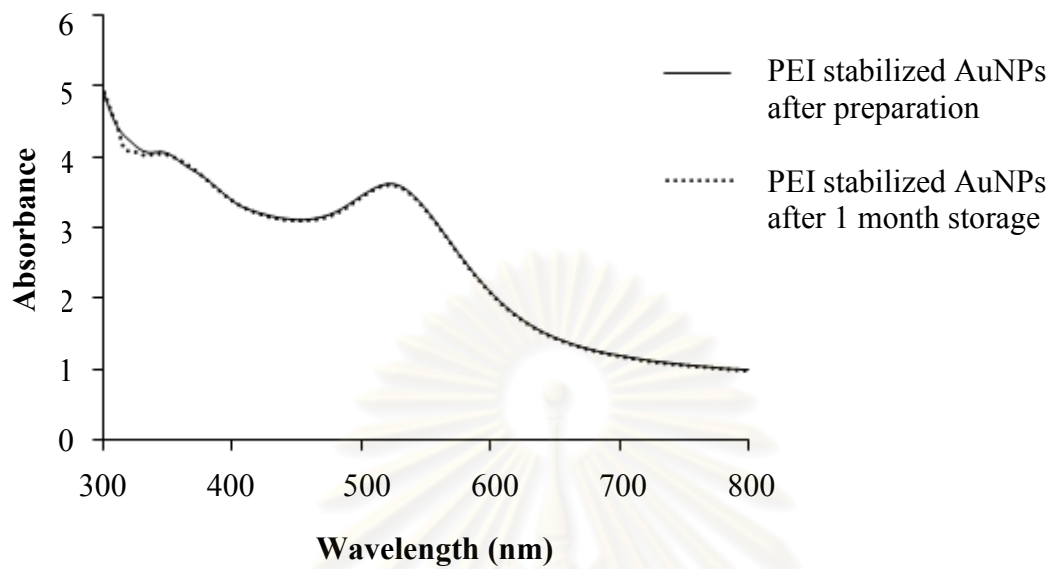


Figure 21 UV absorption spectra of PEI stabilized AuNPs prepared with condition 3 after preparation and 1 month storage

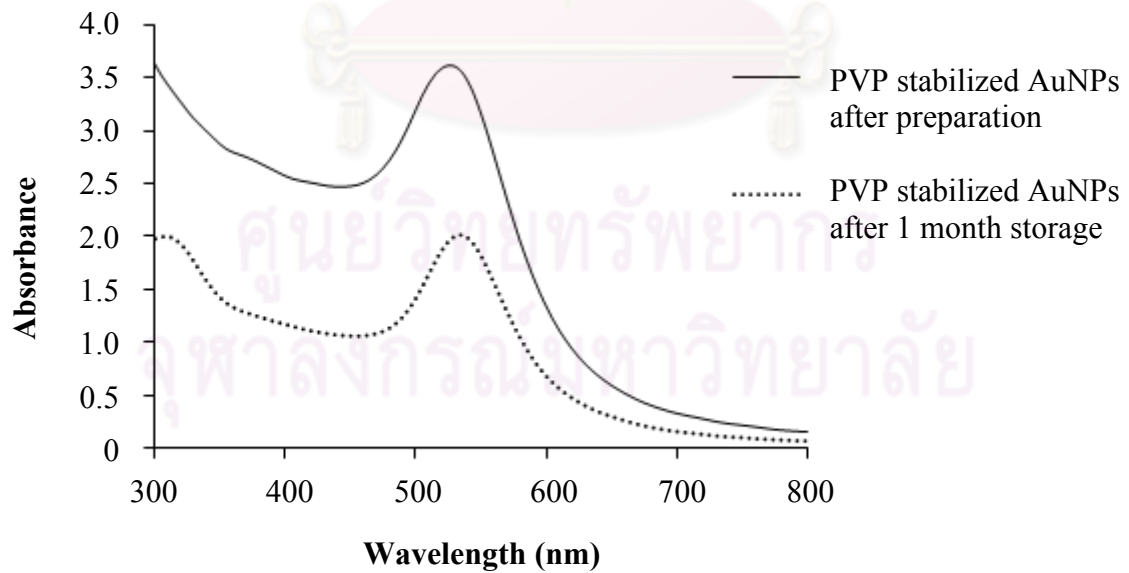


Figure 22 UV absorption spectra of PVP stabilized AuNPs prepared with condition 1 after preparation and 1 month storage

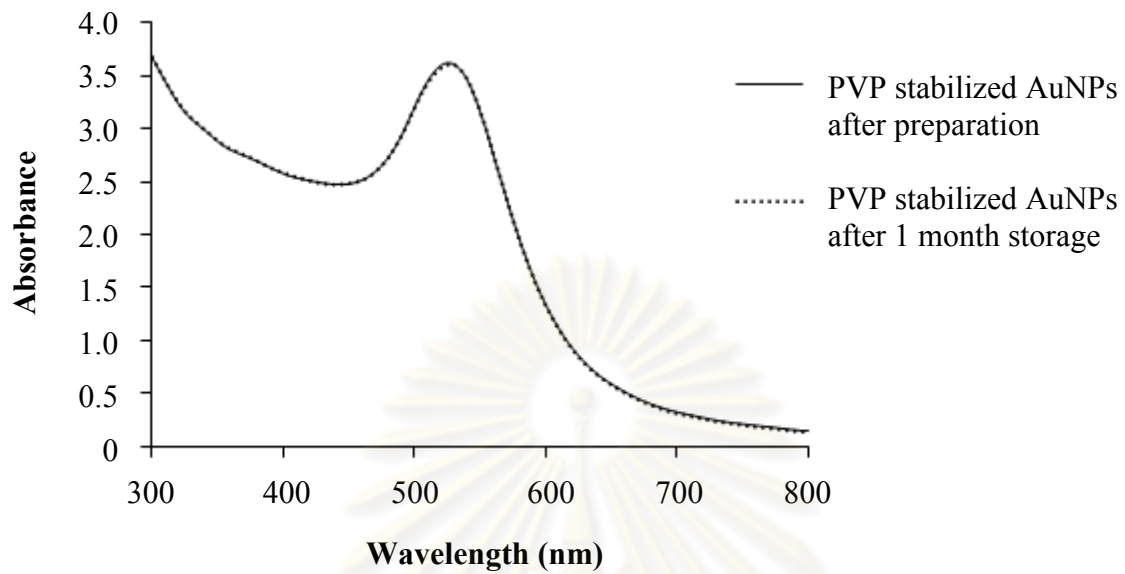


Figure 23 UV absorption spectra of PVP stabilized AuNPs prepared with condition 2 after preparation and 1 month storage

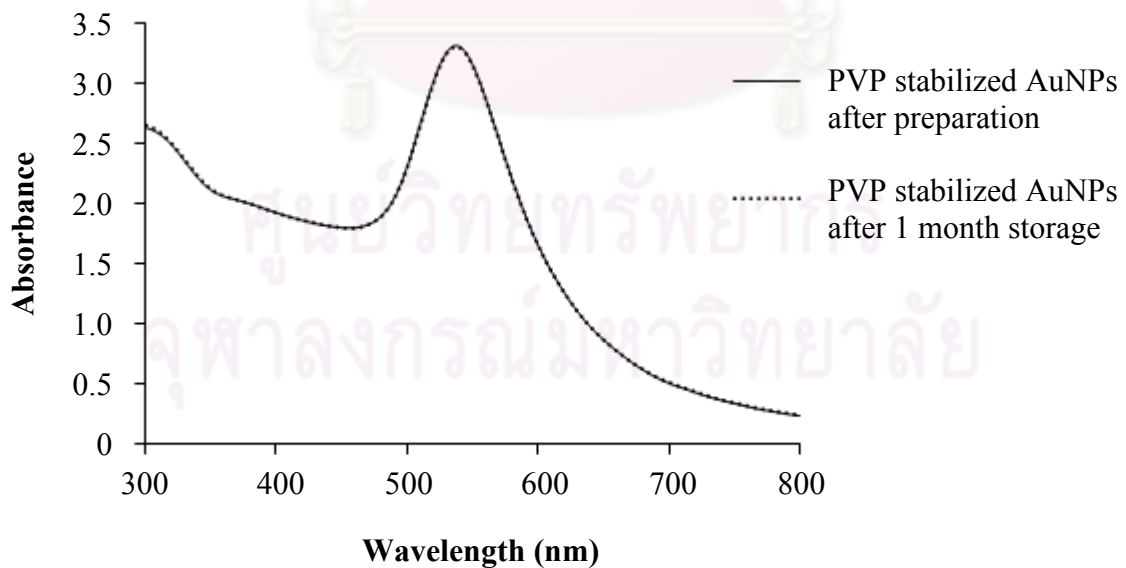


Figure 24 UV absorption spectra of PVP stabilized AuNPs prepared with condition 3 after preparation and 1 month storage

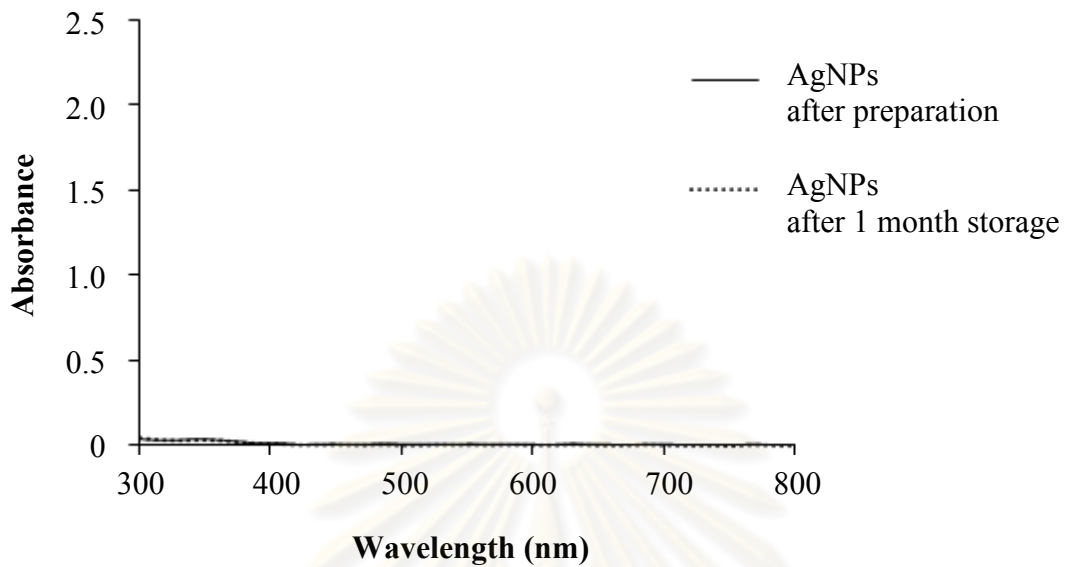


Figure 25 UV absorption spectra of AgNPs prepared with condition 1 after preparation and 1 month storage

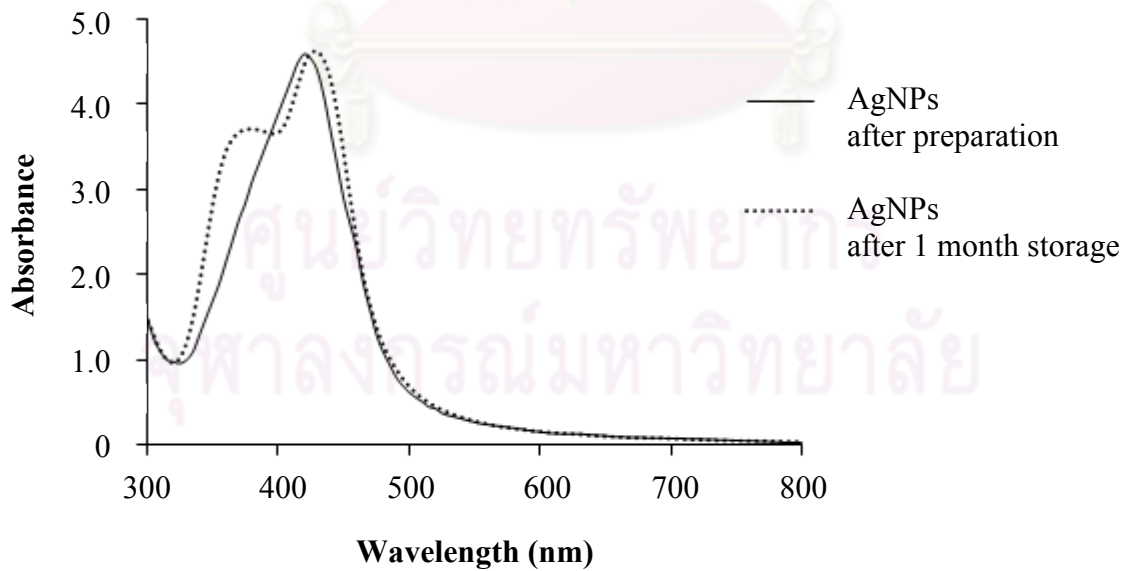


Figure 26 UV absorption spectra of AgNPs prepared with condition 2 after preparation and 1 month storage

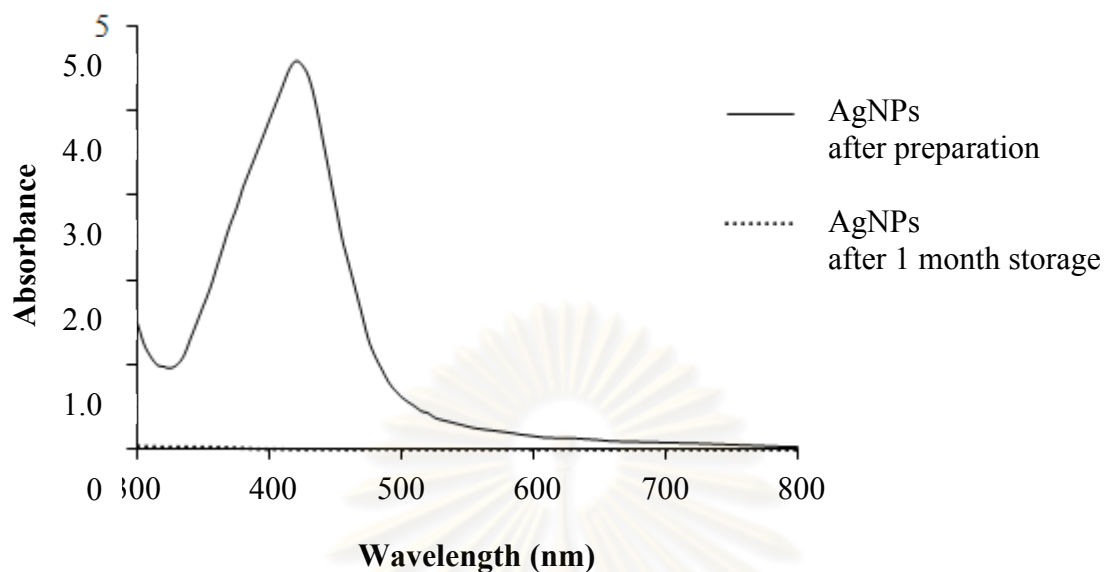


Figure 27 UV absorption spectra of AgNPs prepared with condition 3 after preparation and 1 month storage

AuNPs containing 1015 μM Au atom and AgNPs containing 500 μM Ag atom prepared followed condition 2 were compared for their properties characterized by using UV- visible spectroscopy. Surface plasmon resonance (SPR) of citrate, PEI and PVP stabilized AuNPs after preparation was centered at 525, 520 and 525 nm, respectively (Figure 28A). Citrate, PEI and PVP stabilized AuNPs after 1 month storage presented SPR at 525, 520 and 525 nm, respectively (Figure 28B). It could be seen that particle sizes of AuNPs may not alter and no aggregation occurred after 1 month storage. The peak height of AuNPs with three stabilizers was varied due to the dispersion and diameter of the nanoparticles. PEI stabilized AuNPs presented the narrowest absorption peak, the best degree of dispersion and homogeneous size of the nanoparticles, followed by PVP and citrate stabilized AuNPs (Song *et al.*, 2009).

The SPR of AgNPs after preparation and 1 month storage centered at 420 and 430 nm, respectively (Figure 29 A and B). The shift in wavelength of maximal

absorbance observed might be due to the aggregation of AgNPs occurred after 1 month storage. In fact, the SPR is due to the collective oscillations of electron at the surface of the nanoparticles that is correlated with the electromagnetic field of the coming light. The SPR are dependent on the size and shape of the particle and inter-particle distance (Baptista *et al.*, 2007). The shift of the peak to longer wavelength means the particle size is larger (Daniel and Astruc, 2004; Jensen *et al.*, 2000). In addition, hydrogen tetrachloroaurate and silver nitrate solutions were observed by UV-visible spectroscopy for approving that Au^{3+} and Ag^+ were completely reduced to be Au^0 and Ag^0 after synthesis of nanoparticles by chemical reduction method (Figures 30 and 31). Hydrogen tetrachloroaurate and silver nitrate solutions were exhibited surface plasmon bands at 310 and 305 nm, respectively, which did not appear in synthesized nanoparticles. This can be concluded that hydrogen tetrachloroaurate and silver nitrate were transformed to nanoparticles by chemical reduction method.

Table 10 The spectral features of AuNPs and AgNPs with varying concentrations of stabilizers

| Citrate stabilized AuNPs | | | |
|---------------------------------|--|---|---|
| Condition | [trisodium citrate] : [HAuCl₄] | λ_{\max} (nm) after preparation | λ_{\max} (nm) after 1 month |
| 1 | 8 : 1 | 525 | 525 |
| 2 | 16 : 1 | 525 | 525 |
| 3 | 40 : 1 | ND | ND |
| PEI stabilized AuNPs | | | |
| Condition | [PEI] : [HAuCl₄] | λ_{\max} (nm) after preparation | λ_{\max} (nm) after 1 month |
| 1 | 0.2 : 1 | 520 | 550 |
| 2 | 0.7 : 1 | 520 | 520 |
| 3 | 1.4 : 1 | 520 | 520 |
| PVP stabilized AuNPs | | | |
| Condition | [PVP] : [HAuCl₄] | λ_{\max} (nm) after preparation | λ_{\max} (nm) after 1 month |
| 1 | 45 : 1 | 525 | 535 |
| 2 | 90 : 1 | 525 | 525 |
| 3 | 135 : 1 | 535 | 535 |
| AgNPs | | | |
| Condition | [NaBH₄] : [AgNO₃] | λ_{\max} (nm) after preparation | λ_{\max} (nm) after 1 month |
| 1 | 9 : 5 | ND | ND |
| 2 | 10 : 5 | 420 | 430 |
| 3 | 11 : 5 | 420 | ND |

ND = can not be detected or unstable

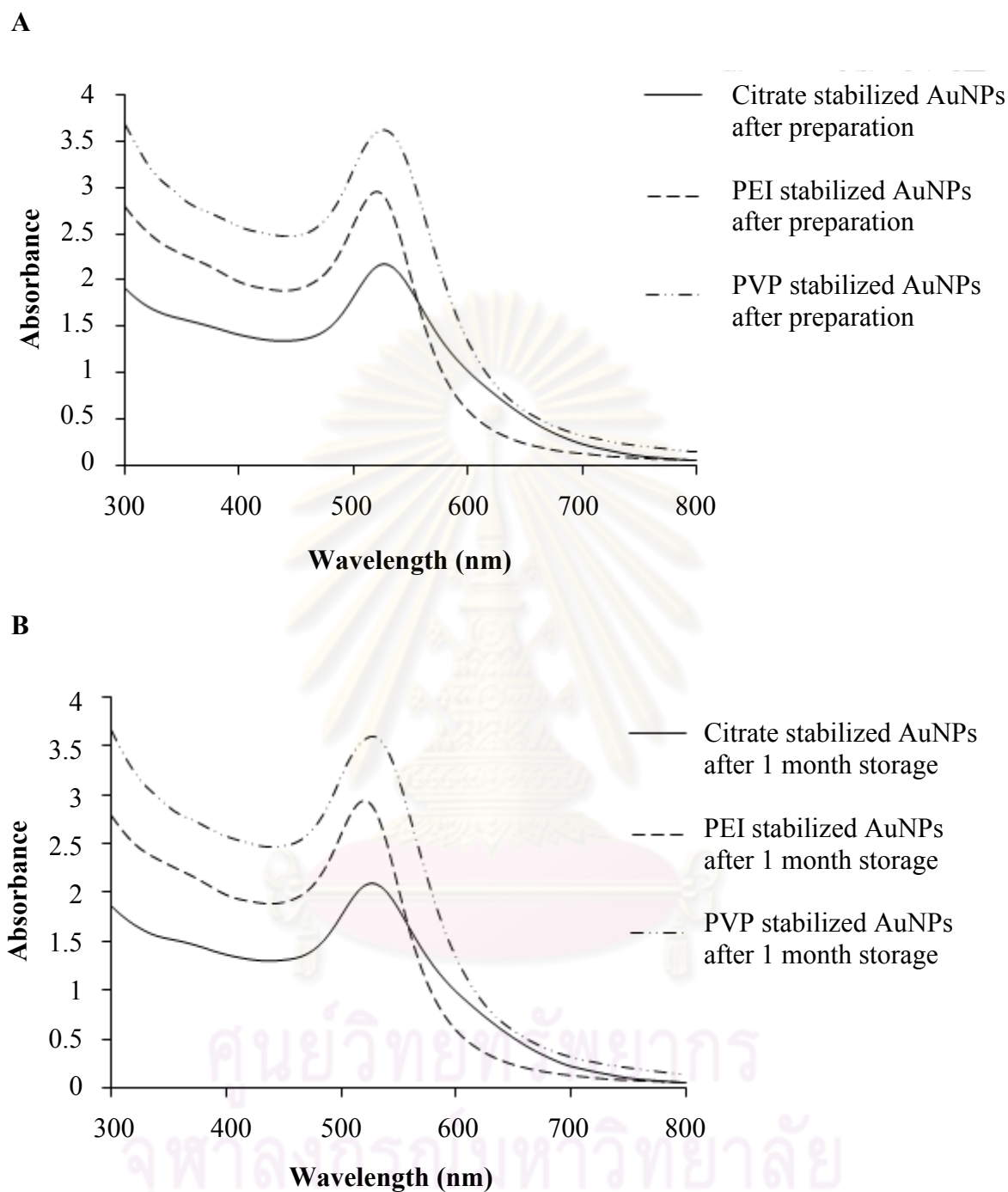


Figure 28 UV absorption spectra of citrate, PEI and PVP stabilized AuNPs after preparation (A) and 1 month storage (B)

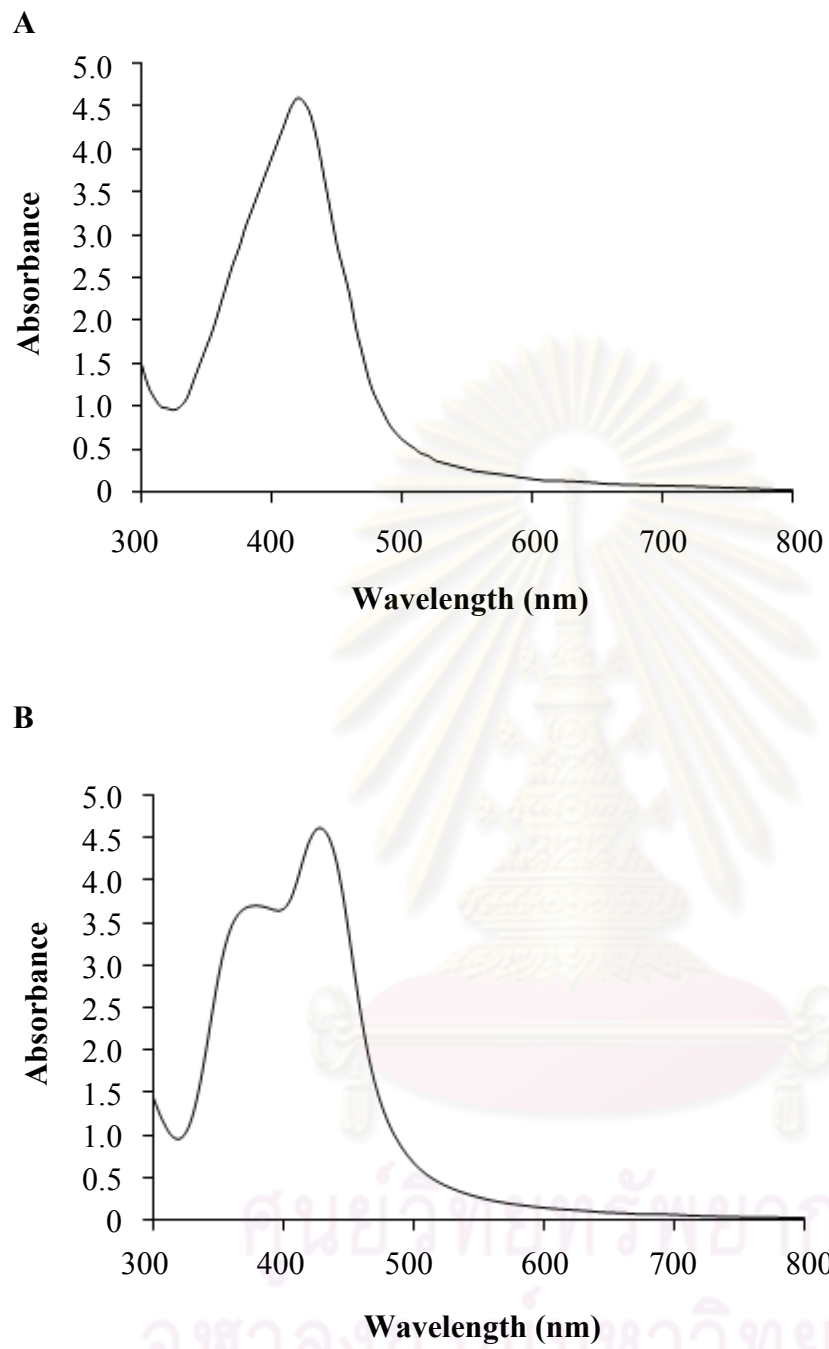


Figure 29 UV absorption spectra of AgNPs after preparation (A) and 1 month storage (B)

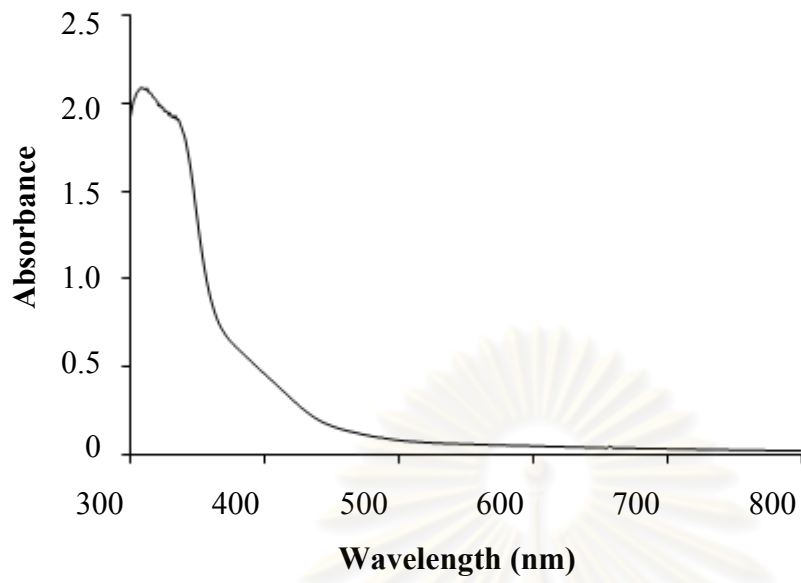


Figure 30 UV absorption spectra of hydrogen tetrachloroaurate solution

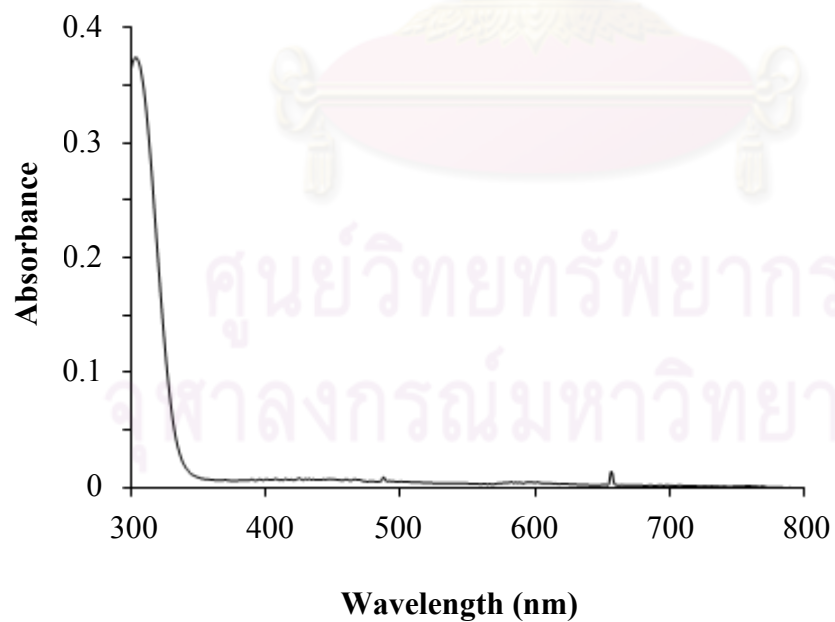


Figure 31 UV absorption spectra of silver nitrate solution

2.2 Size and size distribution

AuNPs and AgNPs were characterized for their size and appearance of the particles by using Transmission Electron Microscopy (TEM) after preparation and 1 month storage. TEM images of spherical shape of AuNPs and AgNPs after preparing and 1 month storage are exhibited in Figures 32 and 33. Size distribution of AuNPs and AgNPs were determined as shown in Figures 34 – 41. The average particle diameters of citrate, PEI and PVP stabilized AuNPs and AgNPs were 8.36 ± 1.94 , 2.67 ± 1.04 , 5.05 ± 1.51 and 12.42 ± 2.48 nm in orderly for freshly prepared systems. From the previous study, the average particle diameters of citrate, PEI and PVP stabilized AuNPs and AgNPs were 13 - 15, 2.3 ± 0.9 , less than 10 and 12.0 ± 3.4 nm, respectively, for freshly synthesized nanoparticles (Pong *et al.*, 2007; Thomas and Klibanov, 2003; Kim, Kim and Lee, 2008; Solomon *et al.*, 2007). The results showed that the average particle sizes of the nanoparticles from previous studies and present study were similar. The average sizes of nanoparticles after 1 month storage were found to be 11.38 ± 3.32 , 5.71 ± 1.65 , 6.48 ± 1.64 and 15.46 ± 4.58 nm for citrate, PEI and PVP AuNPs and AgNPs, respectively. An increase in the particle sizes of the nanoparticles after 1 month storage was considered to agglomeration of the particles and the decreased inter-particle distance.

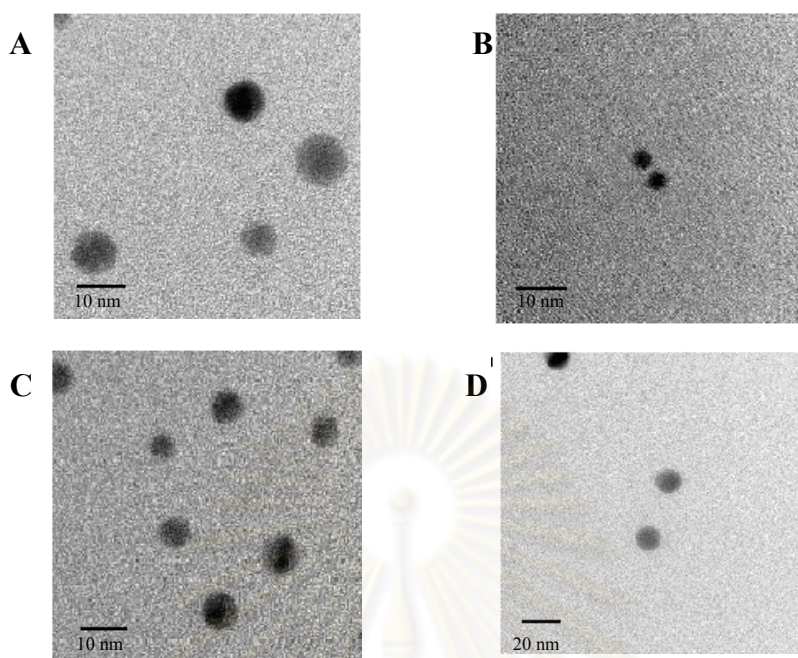


Figure 32 TEM images of citrate stabilized AuNPs (A), PEI stabilized AuNPs (B), PVP stabilized AuNPs (C) and AgNPs (D) after preparation

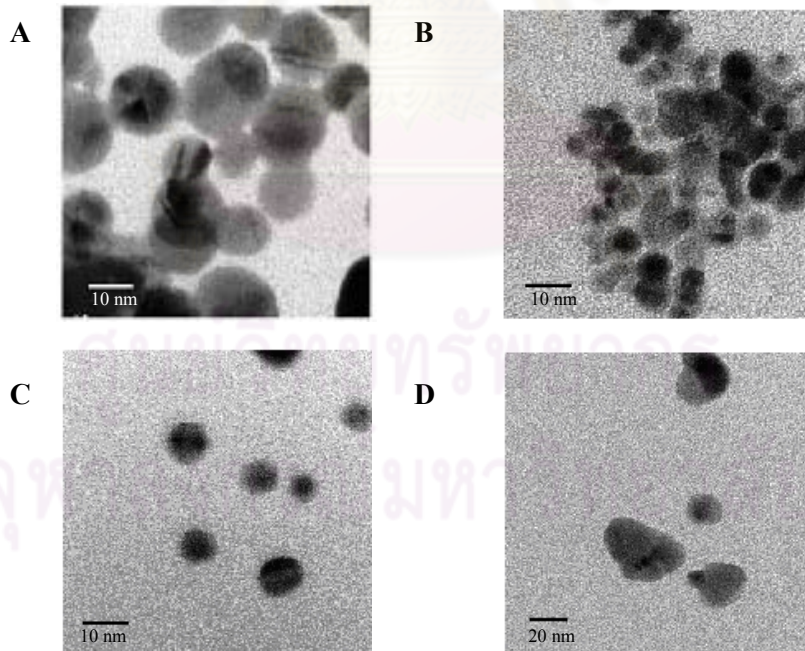


Figure 33 TEM images of citrate stabilized AuNPs (A), PEI stabilized AuNPs (B), PVP stabilized AuNPs (C) and AgNPs (D) after 1 month storage

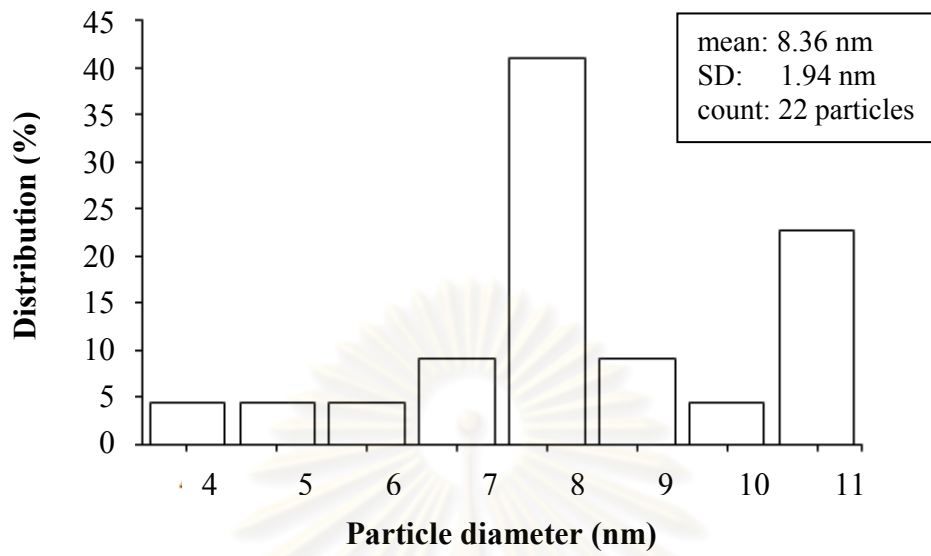


Figure 34 Size distribution of citrate stabilized AuNPs after preparation

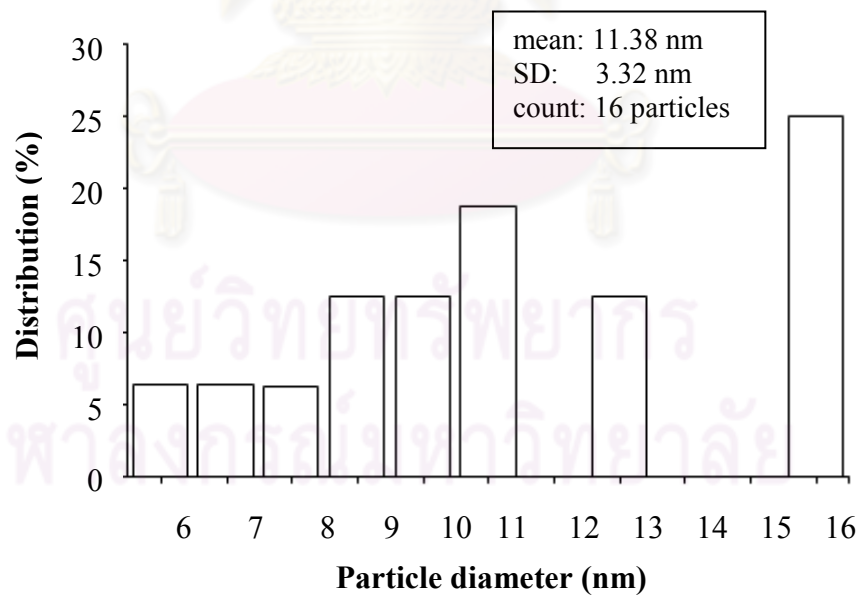


Figure 35 Size distribution of citrate stabilized AuNPs after 1 month storage

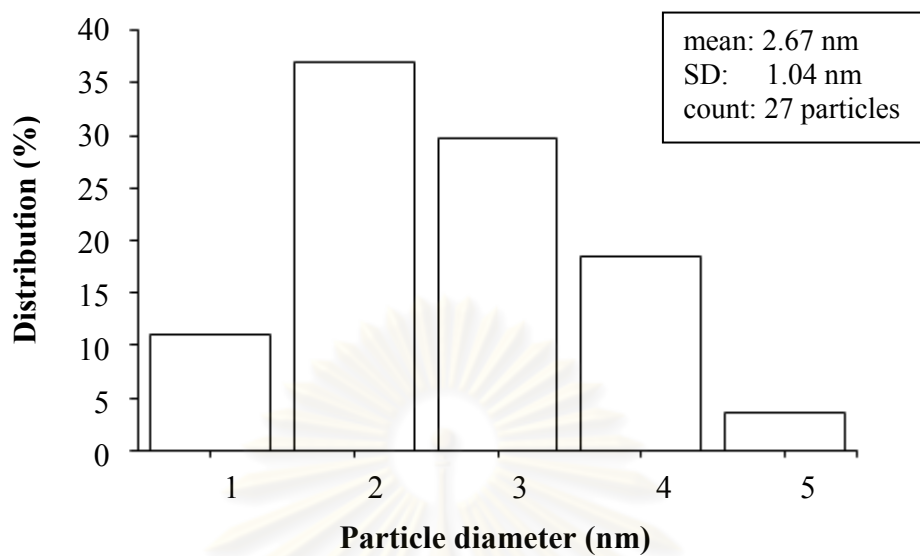


Figure 36 Size distribution of PEI stabilized AuNPs after preparation

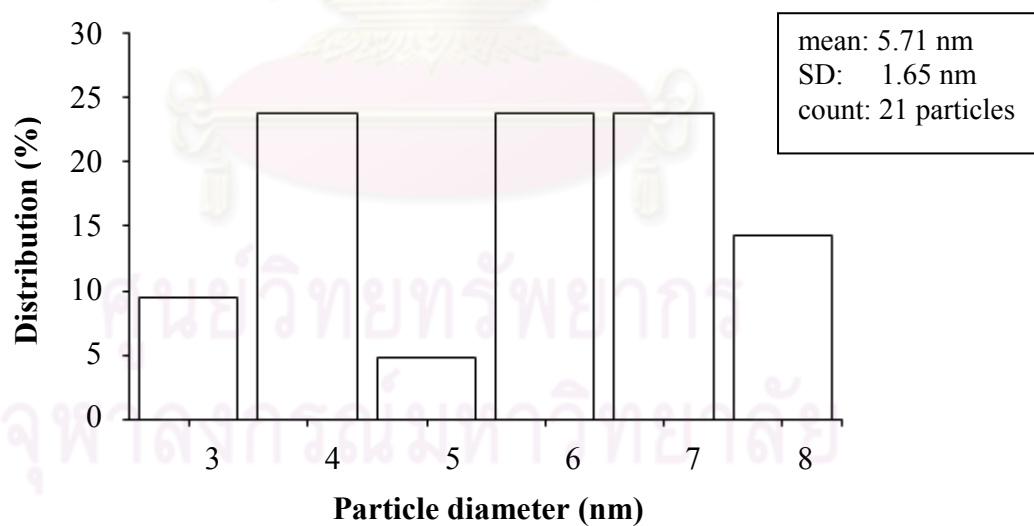


Figure 37 Size distribution of PEI stabilized AuNPs after 1 month storage

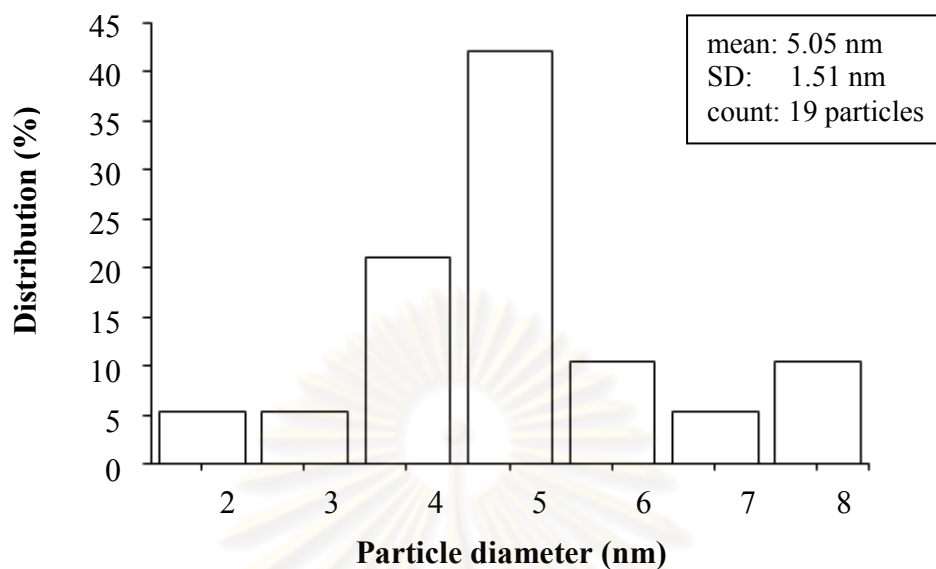


Figure 38 Size distribution of PVP stabilized AuNPs after preparation

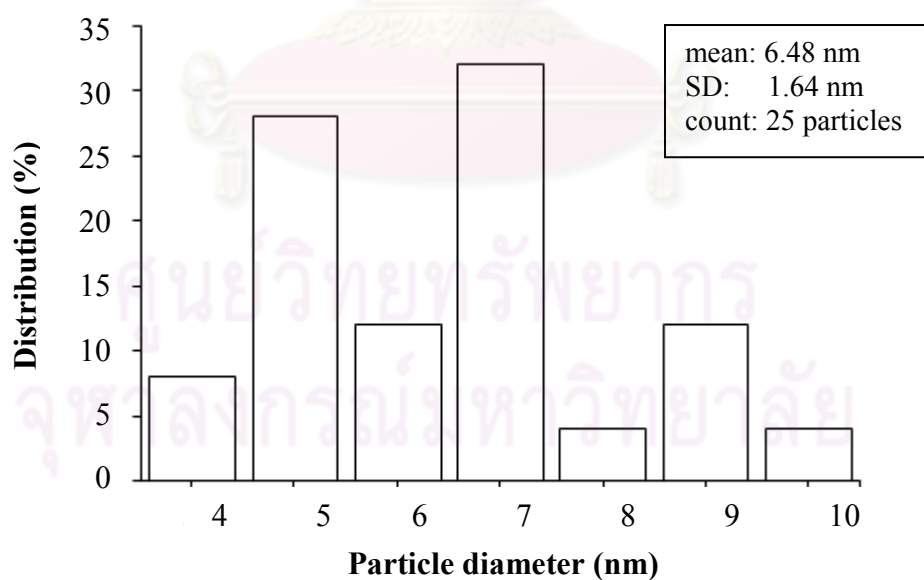


Figure 39 Size distribution of PVP stabilized AuNPs after 1 month storage

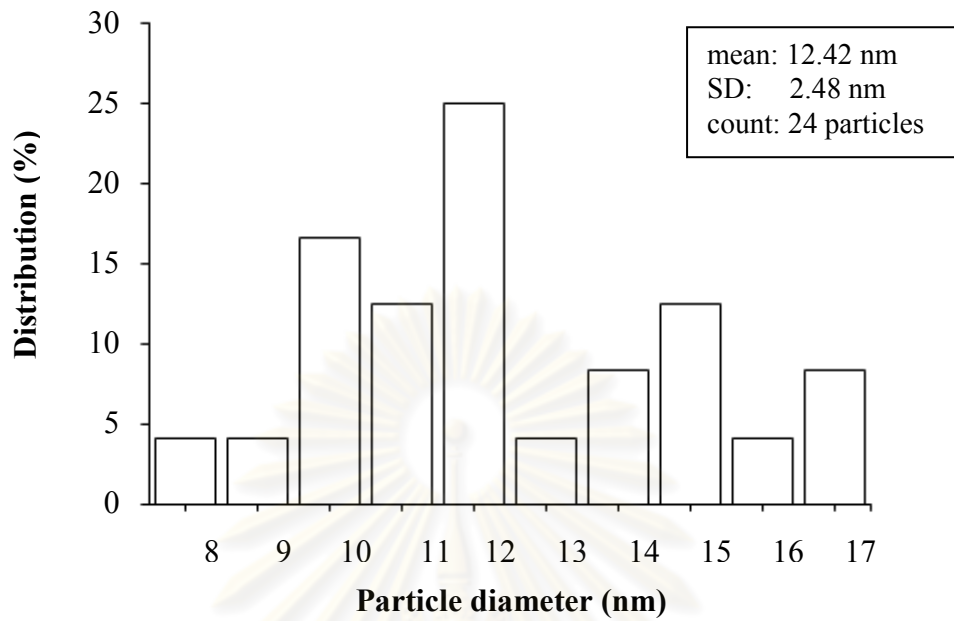


Figure 40 Size distribution of AgNPs after preparation

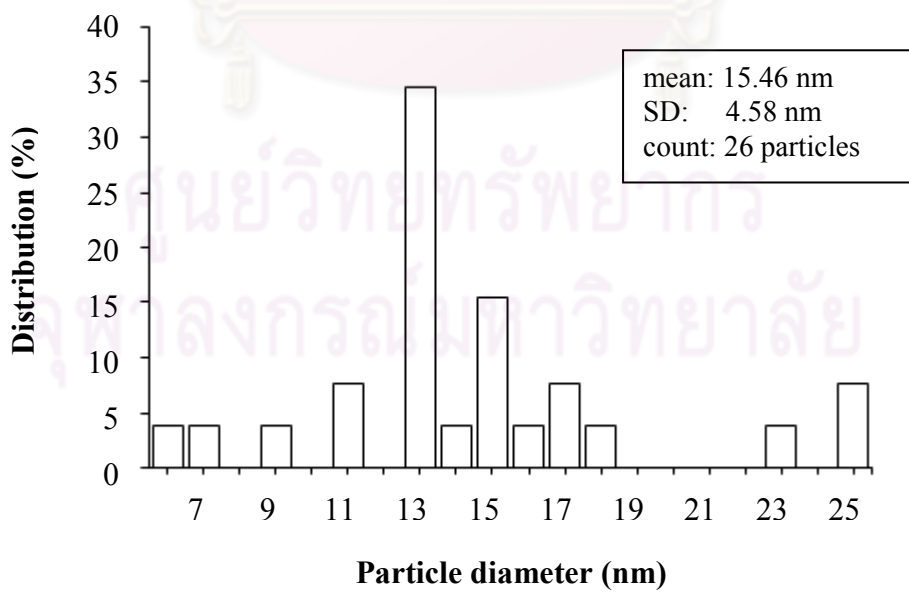


Figure 41 Size distribution of AgNPs after 1 month storage

2.3 Zeta potential measurement

The zeta potential of the particles was measured by using Zetasizer NanoZS in order to detect the surface charge of the nanoparticles. The values of surface potential of AuNPs and AgNPs are given in Table 11. As the results, citrate stabilized AuNPs and AgNPs demonstrated negative charges and the charge slightly decreased after 1 month storage. The charge of PVP stabilized AuNPs was slightly negative and little increased after 1 month storage. PEI stabilized AuNPs presented positive charge and the charge decreased after 1 month storage. The charges of the nanoparticles are related to their stabilizers, surrounding the particles. Sodium citrate and sodium borohydride provide negative charges whereas PEI presents positive charge. PVP is a nonionic stabilizer; however, PVP stabilized AuNPs present slightly negative charge, which could be from a reductant, sodium borohydride. The results from this study were agreement with the study of Goodman *et al.* (2004) and Solomon *et al.* (2007).

Table 11 Zeta potential (mean \pm SD, n=3) of citrate, PEI and PVP stabilized AuNPs and AgNPs after preparation and 1 month storage.

| | Zeta potential (mV) | |
|---------------------------------|---------------------|-----------------------|
| | After preparation | After 1 month storage |
| Citrate stabilized AuNPs | -34.1 \pm 1.3 | -33.1 \pm 3.0 |
| PEI stabilized AuNPs | 28.7 \pm 2.2 | 19.5 \pm 2.4 |
| PVP stabilized AuNPs | -3.3 \pm 0.7 | -4.3 \pm 0.3 |
| AgNPs | -43.6 \pm 0.7 | -33.9 \pm 1.0 |

3. Human cytochrome P450 inhibition of AuNPs and AgNPs

The basic reaction of CYP catalysis is a monooxygenase reaction. Vivid[®] substrates used in this study were EOMCC (ethyloxymethyloxy-3-cyanocoumarin) and BOMCC (7-benzyloxymethyloxy-3-cyanocoumarin). Specific CYP Baculosomes[®] reagent is microsome prepared from insect cells expressing a human P450 isozyme mixed with rabbit NADPH-P450 reductase. The cleavage of CYP Baculosomes[®] reagent and Vivid[®] substrates yields blue fluorescent product (7-hydroxy-3-cyanocoumarin). Citrate, PEI and PVP stabilized AuNPs and AgNPs were tested for inhibitory effect by the decrease in fluorescent products. It is notably that the stabilizer of AgNPs was not varied in this study and only common AgNPs were used, since the main application of AgNPs were for external use which was unnecessary to CYP inhibition test.

3.1 Verification of the Vivid[®] CYP450 inhibition test

The IC₅₀ and 95% confidence interval of the known inhibitors of each CYP isozyme were determined for comparison to the IC₅₀ as reported in the previous studies to verify the method before using the inhibition test for the sample. P450 inhibitors used in the assay included α -naphthoflavone, sulfaphenazole, miconazole and ketoconazole for CYP1A2, CYP2C9, CYP2C19 and CYP3A4, respectively. The IC₅₀ and 95% confidence interval of the particular CYP are presented in Table 12. The percentages of inhibition of each inhibitor are shown in Appendix B.

According to the results (Table 12), IC₅₀ values of sulfaphenazole and ketoconazole on CYP1A2, CYP2C9 and CYP3A4 were 0.11, 0.26 and 0.27 μ M, respectively, were similar to the values from other studies (Marks and Larson, 2009;

Turpeinen *et al.*, 2006; Marques-Soares *et al.*, 2003; Monostory *et al.*, 2004). The IC₅₀ values of CYP2C19 seemed to be different from others. However, the IC₅₀ values among previous reports appeared to be different too. The differences in IC₅₀ among groups of researcher might be due to several experimental factors e.g. type of probe substrate, source of enzyme, instrument, temperature condition, etc. The enzyme in this study was obtained from human CYP expressed in insect cell whereas other studies used human lymphoblast CYP (Kleiner, Reed and DiGiovanni, 2003), human liver tissue (Monostory, *et al.*, 2004; Turpeinen *et al.*, 2006), human CYP expressed in yeast microsome (Marques-Soares, *et al.*, 2003) and cDNA-directed human CYP (Chang, Gonzalez and Waxman, 1994). The probe substrates were differed among studies, which could affect the result of different IC₅₀ values. The probe substrates used in this study were 7-ethyloxymethyloxy-3-cyanocoumarin (EOMCC) for CYP1A2 and CYP2C19 and 7-benzyloxymethyloxy-3-cyanocoumarin (BOMCC) for CYP2C9 and CYP3A4. In contrast, other studies used (S)-mephenytoin 4'-hydroxycoumarin and nifedipine for CYP2C19 and CYP3A4 (Monostory, *et al.*, 2004), resorufin ethyl ether (EROD) for CYP1A2 (Kleiner *et al.*, 2003), 7-methoxy-4-coumarin and omeprazole sulphoxidation for CYP2C9 and CYP3A4 (Turpeinen *et al.*, 2006), progesterone for CYP2C9 (Marques-Soares, *et al.*, 2003).

In the assay, test compounds with IC₅₀ values $\leq 10 \mu\text{M}$ are concerned to be potent inhibitor while test compounds with IC₅₀ value of 10-50 μM are considered to be moderate inhibitor (Zou, Harkey and Henderson, 2002). Therefore, all known inhibitors, used for verification of the Vivid[®] CYP450 inhibition test, acted as potent inhibitors.

Table 12 IC₅₀ and 95% confidence interval of the known inhibitors

| Isozyme | Inhibitor | IC ₅₀ (μM) from other studies | IC ₅₀ (μM) from this study (95% CI) |
|---------|------------------|---|--|
| CYP1A2 | α-Naphthoflavone | 0.03 ^a 0.04 ± 0.02 ^c 0.4 - 0.5 ^f | 0.11 (0.10 to 0.11) |
| CYP2C9 | Sulfaphenazole | 0.31 ^a 0.3 ^b 0.6 ^d | 0.26 (0.08 to 0.78) |
| CYP2C19 | Miconazole | 0.07 ^a 1.78 ± 0.84 ^e | 0.39 (0.26 to 0.57) |
| CYP3A4 | Ketoconazole | 0.13 ^a 0.01 ^b 0.40 ± 0.16 ^e | 0.27 (0.18 to 0.41) |

^a = Marks and Larson, 2009; ^b = Turpeinen *et al.*, 2006; ^c = Kleiner *et al.*, 2003; ^d = Marques-Soares *et al.*, 2003; ^e = Monostory *et al.*, 2004; ^f = Chang *et al.*, 1994.

After test, AuNPs and AgNPs were examined for inhibitory effect on CYP1A2, CYP2C9, CYP2C19 and CYP3A4. The dose-response curves of citrate, PEI and PVP stabilized AuNPs and AgNPs for each CYP are presented in Figures 41-52. IC₅₀ values of citrate, PEI and PVP stabilized AuNPs and AgNPs are shown in Table 15. The % inhibitions of AuNPs and AgNPs on various CYPs are shown in Appendix A.

3.2 CYP inhibition of citrate stabilized AuNPs

Citrate stabilized AuNPs inhibited CYP1A2, CYP2C9, CYP2C19 and CYP3A4 at 9.75 ± 1.45 %, 34.42 ± 4.67 %, 46.01 ± 2.05 % and 31.22 ± 3.55 % at the highest concentration of AuNPs that could be prepared (406 μM). Therefore, their IC₅₀ values were expected to be higher than 406 μM. However, the IC₅₀ values of citrate stabilized AuNPs could not be determined due to inability to synthesis the nanoparticles at the higher concentrations. Compared at the same concentration,

citrate stabilized AuNPs showed the lower CYP inhibitory effect compared to PEI and PVP stabilized AuNPs (Table 13). The inhibitory effect of citrate stabilized AuNPs was highest for CYP2C19 followed by CYP2C9, CYP3A4 and CYP1A2, respectively. In contrast, AgNPs presented more inhibitory effect than the AuNPs for all CYPs at 10 times lower concentration (Table 14).

Table 13 Percentages of inhibition of AuNPs on CYP isozymes at 406 μM (n=4)

| Isozyme | % Inhibition at 406 μM (Mean \pm SD) | | |
|---------|---|----------------------|----------------------|
| | Citrate stabilized AuNPs | PEI stabilized AuNPs | PVP stabilized AuNPs |
| CYP1A2 | 9.75 \pm 1.45 | 95.02 \pm 0.37 | 28.61 \pm 3.83 |
| CYP2C9 | 34.42 \pm 4.67 | 91.17 \pm 1.53 | 59.36 \pm 1.35 |
| CYP2C19 | 46.01 \pm 2.05 | 98.02 \pm 0.05 | 61.25 \pm 2.26 |
| CYP3A4 | 31.22 \pm 3.55 | 86.40 \pm 3.50 | 78.38 \pm 2.64 |

Table 14 Percentages of inhibition of AgNPs on CYP isozymes at 40 μM (n=4)

| Isozyme | % Inhibition of AgNPs at 40 μM (Mean \pm SD) |
|---------|---|
| CYP1A2 | 33.62 \pm 6.00 |
| CYP2C9 | 101.61 \pm 1.47 |
| CYP2C19 | 99.87 \pm 2.09 |
| CYP3A4 | 97.44 \pm 1.12 |

3.3 CYP inhibition of PEI stabilized AuNPs

IC₅₀ values of PEI stabilized AuNPs on CYP1A2, CYP2C9, CYP2C19 and CYP3A4 inhibition were 64.34 \pm 0.05, 4.47 \pm 0.03, 4.84 \pm 0.01 and 16.89 \pm 0.02 μM , respectively. In addition, PEI stabilized AuNPs inhibited CYP1A2, CYP2C9 and

CYP3A4 activities for 95.02%, 91.17% and 86.40% of the control at the concentrations of 406 μM (Table 13). PEI stabilized AuNPs inhibited CYP2C19 activity for 97.28% of the control at the concentration of 203 μM . The curves of %inhibition of CYP activity versus logarithmic concentrations of PEI stabilized AuNPs are shown as Figures 42-45.

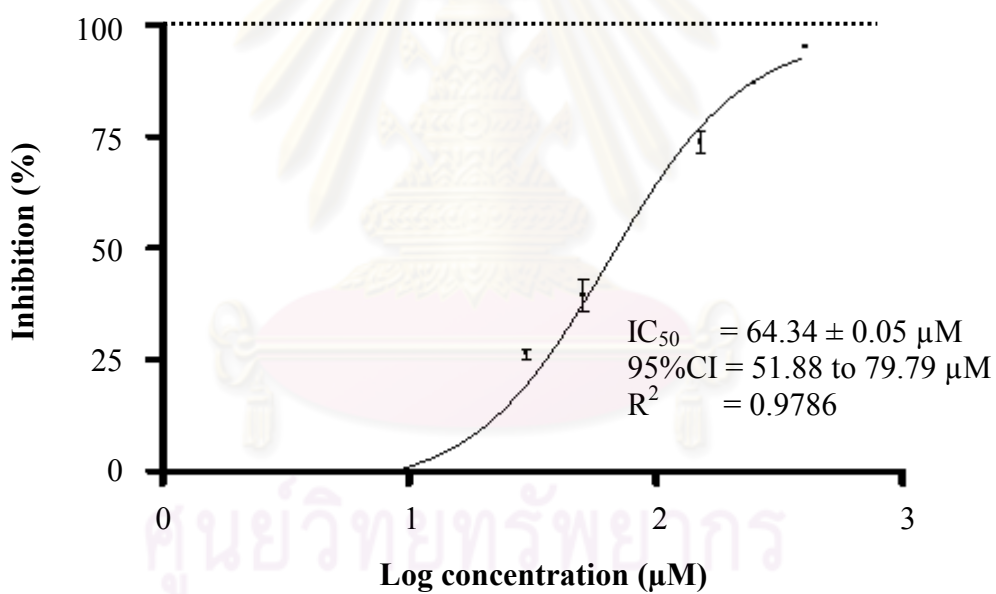


Figure 42 Inhibition curve of PEI stabilized AuNPs on CYP1A2

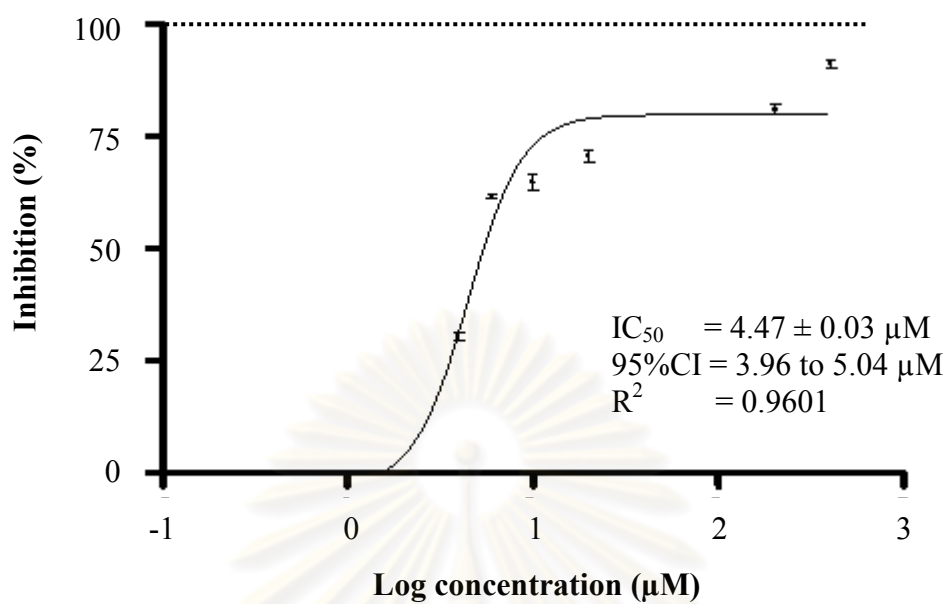


Figure 43 Inhibition curve of PEI stabilized AuNPs on CYP2C9

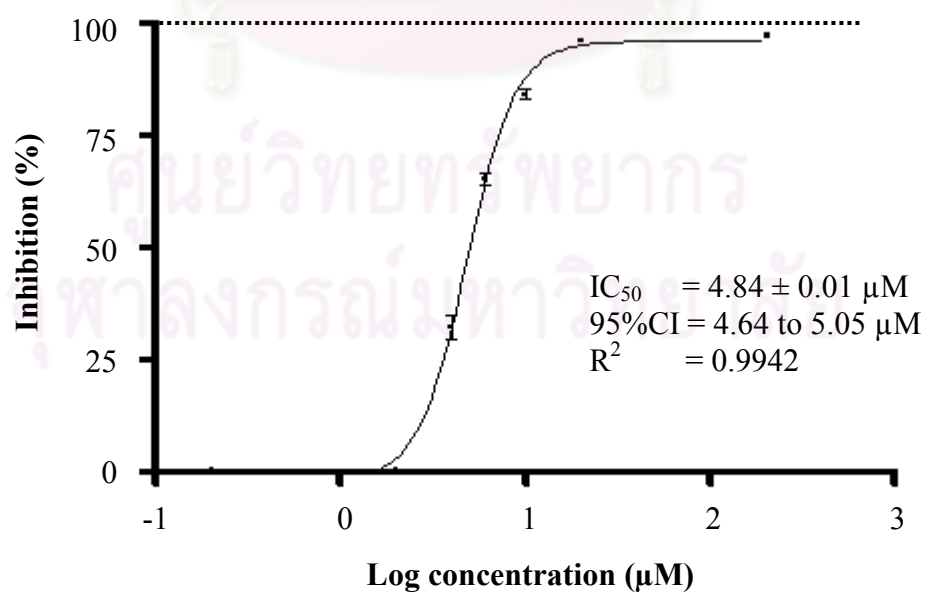


Figure 44 Inhibition curve of PEI stabilized AuNPs on CYP2C19

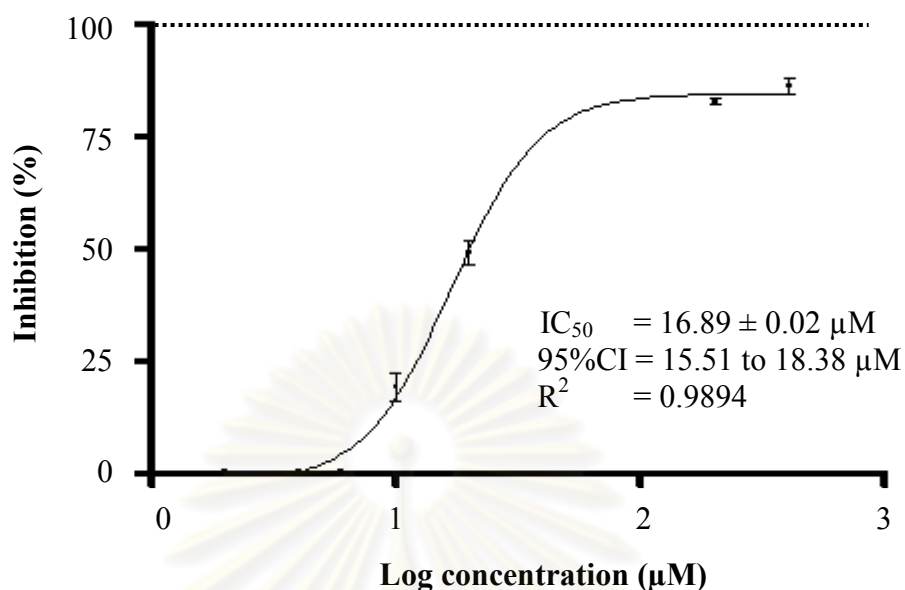


Figure 45 Inhibition curve of PEI stabilized AuNPs on CYP3A4

From the results, PEI stabilized AuNPs exhibited the higher CYP inhibition than citrate and PVP stabilized AuNPs as compared at the same concentration of 406 μM (Table 13). The inhibitory effect of PEI stabilized AuNPs was highest for CYP2C9 followed by CYP2C19, CYP3A4 and CYP1A2, respectively, as compared by the IC_{50} values.

3.4 CYP inhibition of PVP stabilized AuNPs

IC_{50} values of PVP stabilized AuNPs on CYP1A2, CYP2C9, CYP2C19 and CYP3A4 were 449.6 ± 0.02 , 339.3 ± 0.04 , 418.8 ± 0.12 and $233.4 \pm 0.03 \mu M$, respectively. In addition, PVP stabilized AuNPs inhibited CYP1A2, CYP2C9, CYP2C19 and CYP3A4 activities for 84.39%, 85.28%, 97.87% and 99.45% of the control at the concentration of 812 μM . The curves of %inhibition of CYP activity versus logarithmic concentrations of PVP stabilized AuNPs are shown as Figures 46-49.

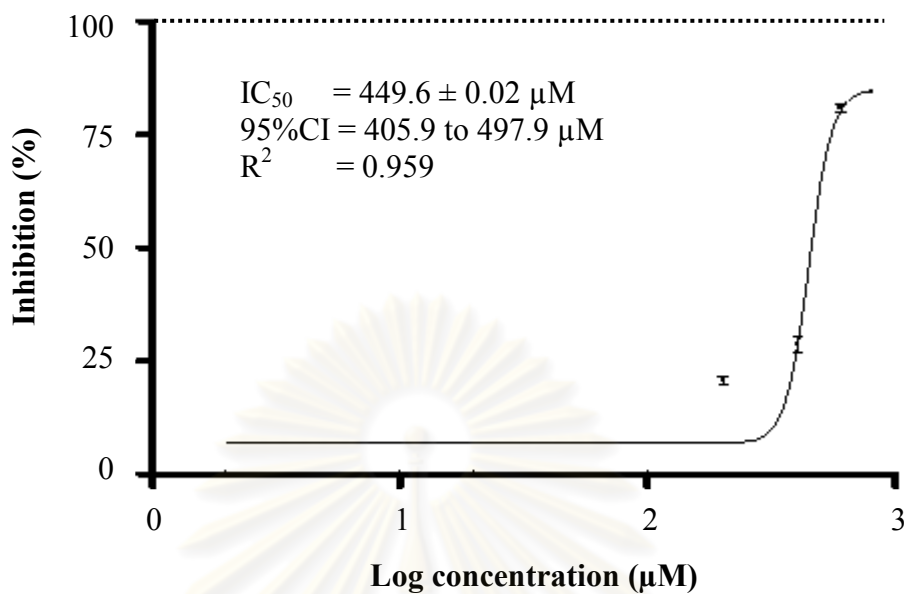


Figure 46 Inhibition curve of PVP stabilized AuNPs on CYP1A2

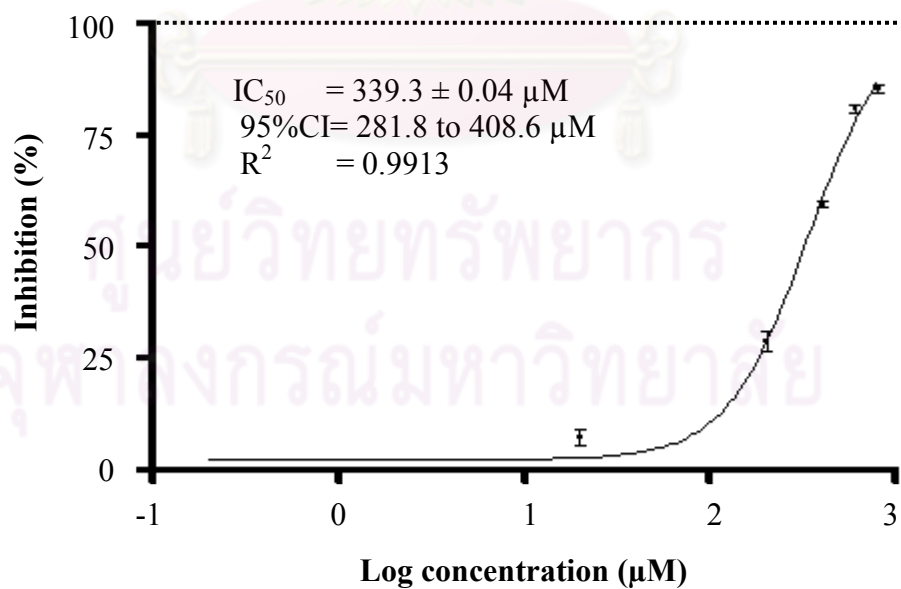


Figure 47 Inhibition curve of PVP stabilized AuNPs on CYP2C9

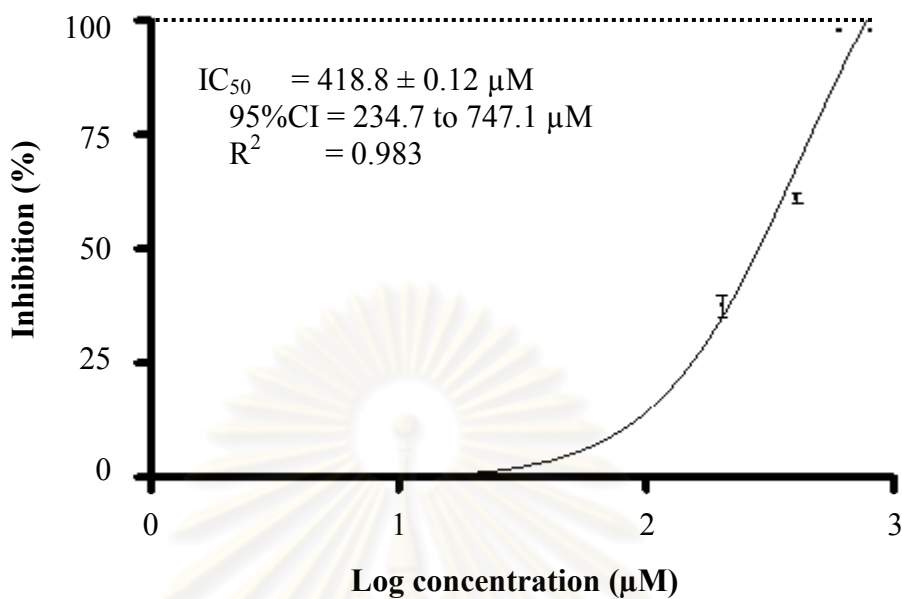


Figure 48 Inhibition curve of PVP stabilized AuNPs on CYP2C19

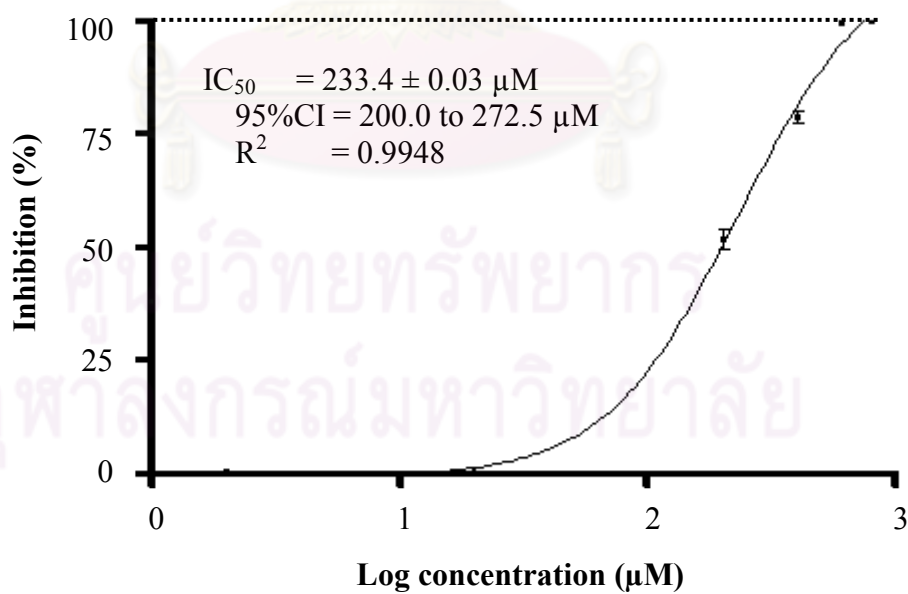


Figure 49 Inhibition curve of PVP stabilized AuNPs on CYP3A4

The result showed that PVP stabilized AuNPs exhibited less inhibitory effect as compared to PEI stabilized AuNPs and AgNPs (Table 15). The inhibition of PVP stabilized AuNPs was highest for CYP3A4 followed by CYP2C9, CYP2C19 and CYP1A2, respectively.

3.5 CYP inhibition of AgNPs

IC_{50} of AgNPs on CYP1A2, CYP2C9, CYP2C19 and CYP3A4 inhibition were 43.51 ± 0.03 , 26.46 ± 0.00 , 14.31 ± 0.01 and 13.52 ± 0.01 μM , respectively (Table 15). In addition, AgNPs inhibited CYP1A2 activity for 95.44% of the control at the concentration of 80 μM (Table 30). AgNPs inhibited CYP2C9, CYP2C19 and CYP3A4 activities for 101.61%, 99.87% and 97.44% of the control at the concentrations of 40 μM (Tables 31-33). The curves of %inhibition of CYP activity versus logarithmic concentrations of PVP stabilized AuNPs are shown as Figures 50-53.

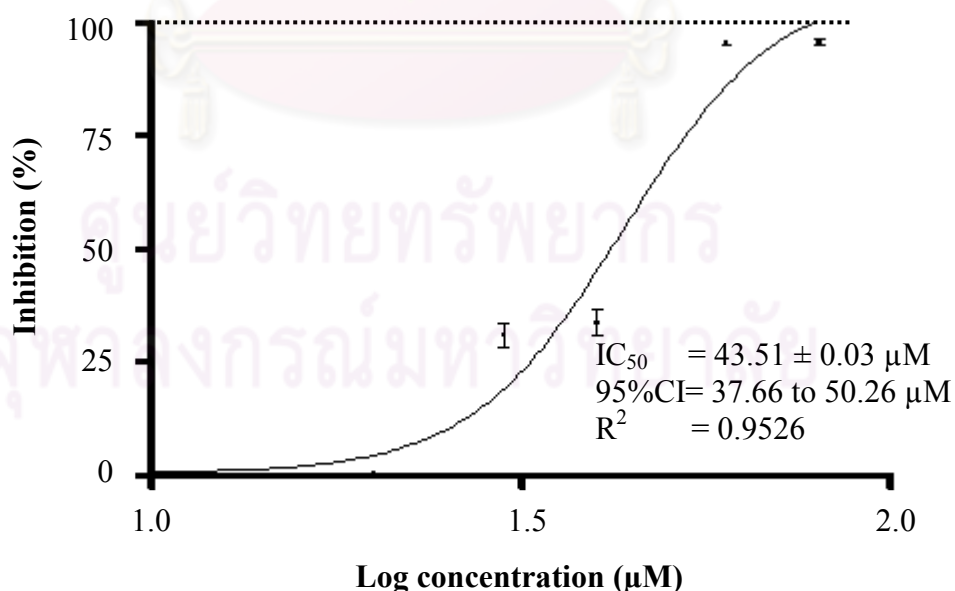


Figure 50 Inhibition curve of AgNPs on CYP1A2

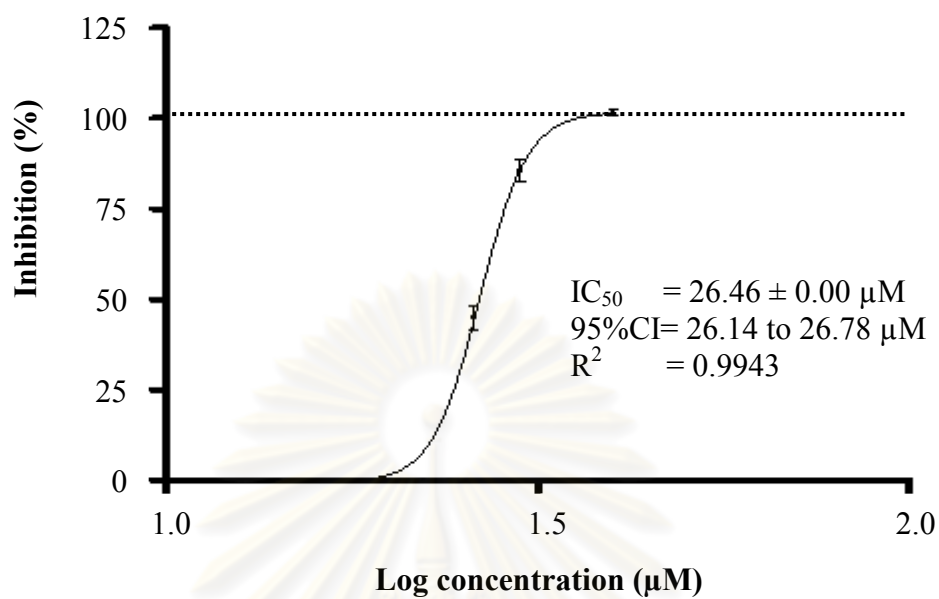


Figure 51 Inhibition curve of AgNPs on CYP2C9

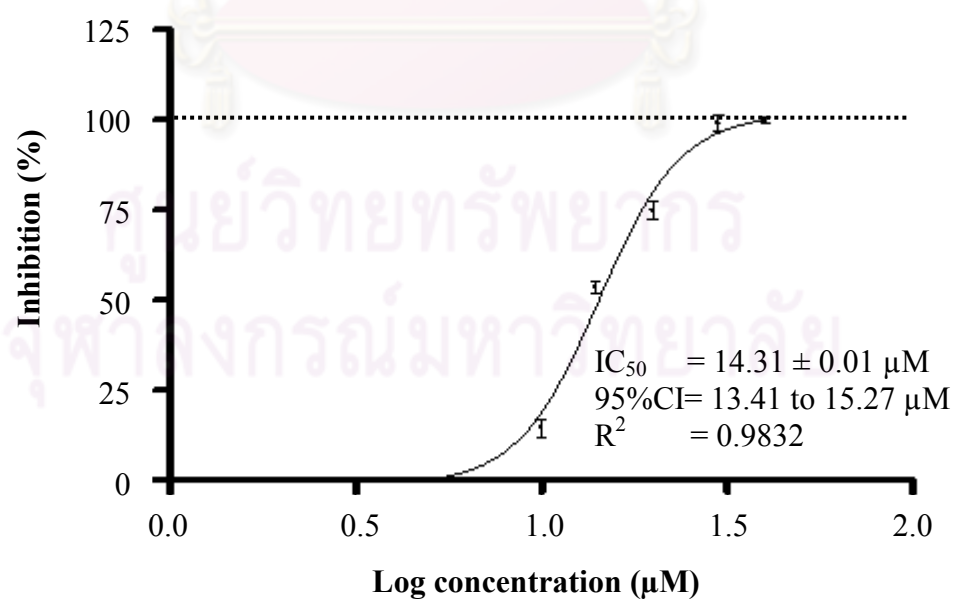


Figure 52 Inhibition curve of AgNPs on CYP2C19

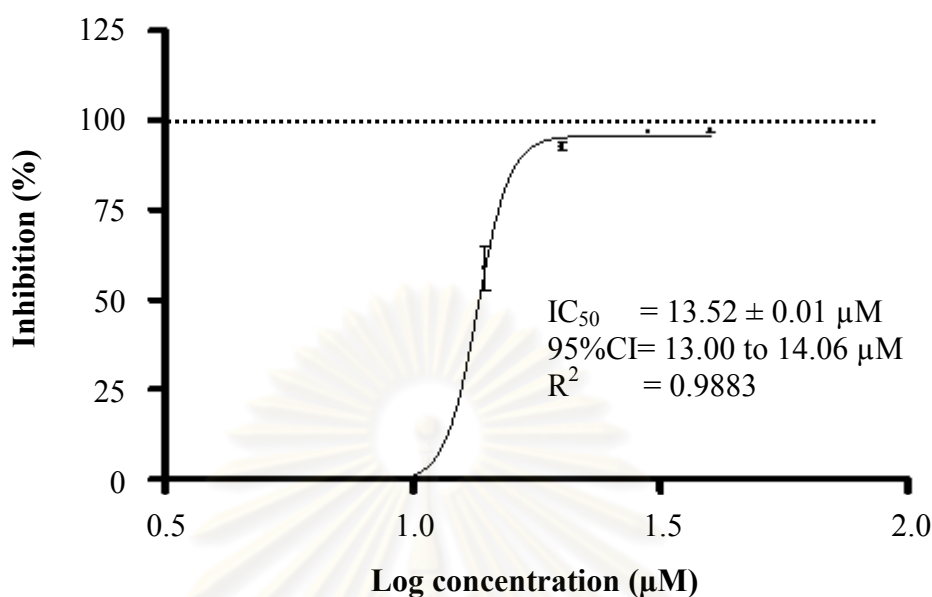


Figure 53 Inhibition curve of AgNPs on CYP3A4

According to the results, AgNPs presented higher CYP inhibition than citrate and PVP stabilized AuNPs (Table 15). AgNPs had more potent inhibitory effect for CYP1A2 and CYP3A4 than AuNPs, but they had less potent inhibitory effect for CYP2C9 and 2C19 compared to PEI stabilized AuNPs. The inhibitory effect of AgNPs was highest for CYP3A4 followed by CYP2C19, CYP2C9 and CYP1A2, respectively. The overall $IC_{50} \pm SD$ ($n=4$) of citrate, PEI and PVP stabilized AuNPs and AgNPs are summarized in Table 15. For statistical analysis, one-way analysis of variance (ANOVA) was carried out to compare the effect of each nanoparticles on different CYPs and different nanoparticles on each CYP isozyme. Then bonferroni post hoc test was used for determining significant different among IC_{50} values. Three kinds of AuNPs stabilizer (citrate, PEI and PVP) were also tested for CYP inhibition to approve that the inhibitory effect of AuNPs were not related to their excess

stabilizers. The concentrations of the stabilizers (16.2 μM , 0.7 μM and 90.1 μM for citrate, PEI and PVP, in orderly), used for the test, were the same as concentration used for AuNPs preparation. The percentage of inhibition of citrate, PEI and PVP at the mentioned concentrations are shown in Table 16. In addition, AuNPs and AgNPs were 2 times repetitively centrifuged (20 minutes, 5000 x g) by 3 kDa ultracentrifugal filters in order to get rid of the excess stabilizer before the enzyme inhibition test. This is to confirm that the inhibition of AuNPs were not associate with the excess stabilizer.

Table 15 IC_{50} values on CYP inhibition of citrate, PEI and PVP stabilized AuNPs and AgNPs (n=4)

| Chemicals | $\text{IC}_{50} \pm \text{SD} (\mu\text{M})$ | | | |
|--------------------------|--|-----------------------|-----------------------|-----------------------|
| | CYP1A2 | CYP2C9 | CYP2C19 | CYP3A4 |
| Citrate stabilized AuNPs | ND | ND | ND | ND |
| PEI stabilized AuNPs | 64.34 ± 0.05^{aA} | 4.47 ± 0.03^{bA} | 4.84 ± 0.01^{cA} | 16.89 ± 0.02^{dA} |
| PVP stabilized AuNPs | 449.6 ± 0.02^{aB} | 339.3 ± 0.04^{bB} | 418.8 ± 0.12^{cB} | 233.4 ± 0.03^{dB} |
| AgNPs | 43.51 ± 0.03^{aC} | 26.46 ± 0.00^{bC} | 14.31 ± 0.01^{cC} | 13.52 ± 0.01^{dC} |

^a, ^b, ^c and ^d Significantly different among IC_{50} of the individual CYP of each nanoparticle, $p < 0.05$

^A, ^B and ^C Significantly different among IC_{50} of the nanoparticles of each CYP isozyme, $p < 0.05$

ND = could not determine

Table 16 Percentage of inhibition of citrate, PEI and PVP solutions (n=2)

| Isozyme | % Inhibition | | |
|---------|--------------|-------|-------|
| | Citrate | PEI | PVP |
| CYP1A2 | 0 | 36.96 | 0 |
| CYP2C9 | 0 | 62.89 | 7.68 |
| CYP2C19 | 0 | 92.34 | 5.73 |
| CYP3A4 | 0 | 51.35 | 58.26 |

CYPs have a significant responsibility for the oxidative metabolism of drugs and other xenobiotics. CYP1A2, CYP2C9, CYP2C19 and CYP3A4 are the common isozymes for drug metabolism in human. The inhibition of CYPs-mediated metabolism is the important mechanism for drug-drug interactions.

According to Zou *et al.* (2002), test compound with IC_{50} value $\leq 10 \mu\text{M}$ are concerned to be potent inhibitor while test compounds with IC_{50} value of 10-50 μM are considered to be moderate inhibitor. If the assumption was applied for comparing concentration of Au in the system studied, PEI stabilized AuNPs present potent inhibitor of CYP2C9 and CYP2C19 and moderate inhibitor of CYP3A4. AgNPs demonstrate moderate inhibitor of CYP1A2, CYP2C9, CYP2C19 and CYP3A4. As the CYP inhibition of AuNPs results, PEI stabilized AuNPs caused the efficient P450 inhibition rather than citrate and PVP stabilized AuNPs. It can be seen that cationic nanoparticles had clearly more potent inhibitory effect than the nonionic and anionic. The negative surface coating might not effectively interact with the cell membrane, contained the overall negative charge of the lipid bilayer (Goodman *et al.*, 2004). Recently, the study reported that the nanoparticles with positive charge exhibited

greater interaction with human breast cancer cells than the nanoparticles with negative charge (Osaka *et al.*, 2009). Miller *et al.* (1998) observed the effect of liposome surface charge on liposomal binding and endocytosis in a human ovarian carcinoma cell line (HeLa) and a murine derived mononuclear macrophage cell line (J774). The positively charged liposomes had a greater endocytosis than either neutral or negatively charged liposomes. Moreover, the size of the nanoparticles had an impact on the interaction of the particles and cell membrane. The relation between size of the particles and percentage of inhibition are exhibited in Table 17. From the study, the smallest particle size (PEI stabilized AuNPs) presented the greatest CYP inhibition followed by PVP and citrate stabilized AuNPs. The earlier study examined the uptake into dendritic cells of model fluorescent polystyrene particles with varied size range and charge. Particles with diameter of 0.5 μm or below presented the greater cell uptake compared to larger particles. However, the particles with positively charged surface better enhanced cell interaction than the particles with negatively charged surface (Foged *et al.*, 2005). Smaller particles were dispersed quickly to almost all tissues while larger particles were not broadly dispersed into tissues (Aillon *et al.*, 2009). Therefore, the results from this study are in agreement with the results found by Foged *et al.* (2005) and Aillon *et al.* (2009).

Table 17 The sizes of AuNPs and percentage of CYP inhibition at 406 μ M

| AuNPs | Size of particle after preparation (nm) (Mean \pm SD, n= 19-27) | % Inhibition at 406 μ M (Mean \pm SD, n=4) | | | |
|--------------------------|---|--|------------------|------------------|------------------|
| | | CYP1A2 | CYP2C9 | CYP2C19 | CYP3A4 |
| Citrate stabilized AuNPs | 8.36 \pm 1.94 | 9.75 \pm 1.45 | 34.42 \pm 4.67 | 46.01 \pm 2.05 | 31.22 \pm 3.55 |
| PEI stabilized AuNPs | 2.67 \pm 1.04 | 95.02 \pm 0.37 | 91.17 \pm 1.53 | 98.02 \pm 0.05 | 86.40 \pm 3.50 |
| PVP stabilized AuNPs | 5.05 \pm 1.51 | 28.61 \pm 3.83 | 59.36 \pm 1.35 | 61.25 \pm 2.26 | 78.38 \pm 2.64 |

It could be seen that CYP inhibitory effect of PEI stabilized AuNPs was associated the combination effect of the smaller size and positively charged properties. PEI stabilized AuNPs have been used for increasing the transfected efficiencies into monkey kidney (COS-7) cells (Thomas and Klibanov, 2003). They could interact with the DNA backbone, inhibiting transcription by T7 RNA polymerase *in vitro* (McIntosh *et al.*, 2001). Because cationic polymer stabilized AuNPs present transfected capabilities, they have been developed for several applications e.g. transfection vectors, DNA-binding agents, protein inhibitor, etc (Goodman *et al.*, 2004). For example, mixed monolayer protected gold clusters (MMPCs) functionalized with quaternary ammonium chains had the ability to transfect mammalian cell cultures, as determined through beta-galactosidase transfer and activity (Sandhu *et al.*, 2002). In addition, anionically functionalized amphiphilic MMPCs were used for the binding and inhibition of chymotrypsin for studying the mechanism of inhibition (Fischer *et al.*, 2002). It can be seen that AuNPs with cationic polymer surface can effectively interact with negative charged cell membrane.

From this study, AgNPs exhibited negatively charged surface because their particles were stabilized by tetrahydridoborate (III) ion (BH_4^-), which was formed from sodium borohydride (NaBH_4). The inhibitory effect of AgNPs is compared to which of citrate stabilized AuNPs due to the close proximal zeta potential values. IC_{50} values of AgNPs on CYP1A2, CYP2C9, CYP2C19 and CYP3A4 were 43.51 ± 0.03 , 26.46 ± 0.00 , 14.31 ± 0.01 and 13.52 ± 0.01 μM , respectively whereas of citrate stabilized AuNPs were expected to be higher than 406 μM . From the results, AgNPs provide the greater inhibitory effect than citrate stabilized AuNPs. Therefore, CYP

inhibition of AgNPs could be from Ag atom. According to the study of Sondi and Salopek-Sondi (2004), both of positively charged Ag ions and negatively charged AgNPs were permeable and accumulated in bacterial membrane, leading to cell death. This study confirmed that the charge of AgNPs is not involved to the transfection of cell membrane. Additionally, the transfected efficiency of AgNPs depends on size of the particle. The smaller size of the nanoparticle the greater potential toxicity was examined in zebrafish embryos (Bar-Ilan *et al.*, 2009). Moreover, there are previous studies reported that AgNPs can interact with other cell membrane. AgNPs interacted with HIV-1 virus by binding to the gp 120 glycoprotein knobs (Elechiguerra *et al.*, 2005). AgNPs could interact with platelet or fibroblast cells (Chung, Chen and Chen, 2008).

In this study, several CYP isozymes were examined owing to the individual different inhibitory effect on different substances. CYP1A2 is significant for the bioactivation of procarcinogens. It metabolizes drugs that resemble aromatic amines, including caffeine, β -naphthylamine (carcinogen), theophylline and tricyclic antidepressants (TCAs). It also oxidizes estrogen and this series of hormones. The increase of this CYP isozyme is related to the risk of breast cancer (Hong *et al.*, 2004) colon cancer (Saebø *et al.*, 2008) and lung cancer (Seow *et al.*, 2001). As the results, PEI and PVP stabilized AuNPs and AgNPs present less inhibitory effect on CYP1A2. This may decrease xenobiotic-induced carcinogenesis. However, this might reduce the biotransformation of drugs, acted as CYP1A2 substrates, causing drug interaction (Coleman, 2005; Manzi and Shannon, 2005).

CYP2C9 metabolizes several common drugs, including phenytoin, warfarin, losartan, tolbutamide, plipizide and non-steroidal anti-inflammatory drugs (e.g.

diclofenac, ibuprofen, etc.). CYP2C19 presents genetic polymorphism. Approximately 3-5% of Caucasians and 20% of Asians and African-Americans are poor metabolizers. Unpredictable drug level could be occurred because of genetic polymorphism. CYP2C19 oxidizes antidepressants (TCAs and SSRIs), anticonvulsants, anxiolytics and benzodiazepines. According to the results, the function of CYP2C is more potent inhibited by PEI stabilized AuNPs. In addition, AgNPs exhibit moderate inhibitory effect (IC_{50} value of 10-50 μ M (Zou *et al.*, 2002)) on CYP2C. This may cause toxicity of drugs that metabolized by CYP2C, especially, drugs with narrow therapeutic window (phenytoin and warfarin) (Goshman *et al.*, 1999). In contrast, the inhibitory effect on CYP2C may be beneficial in term of toxicity protection from xenobiotic-bioactivation.

CYP3A4 are responsible for the metabolism of more than 150 drugs, including antiarrhythmics, calcium antagonists, psychotropics, opioid analgesics, antihistamines benzodiazepines, antimicrobial agents, antiretroviral agents, antiulcer agents, anticonvulsants and immunosuppressants. In addition, about 70% of CYP3A4 appears in the gut to metabolize substrates before reaching to the liver, resulting in the decrease of bioavailability. From the result, PEI stabilized AuNPs and AgNPs exhibited the moderate inhibitory effect on CYP3A4. Also, PVP stabilized AuNPs had less inhibitory effect. The concomitant administration of the drugs with PEI AuNPs and AgNPs should be concerned in term of drug interaction resulting in serious medical consequences (Coleman, 2005; Gibson and Skett, 1996; Goshman *et al.*, 1999).

The results obtained from CYP inhibition provides the suggestion on the consideration of drug to be delivered by AuNPs and AgNPs. Due to the lack of drug

interaction, the nanoparticles exhibited no CYP inhibitory effect could be used for drug delivery. The CYP inhibition potency seemed to depend upon the charge and size of the Nanoparticles. According to the study results, citrate and PVP stabilized AuNPs can be used for further developed for delivery of drug metabolized by CYP1A2, CYP2C9, CYP2A19 and CYP3A4. PEI stabilized AuNPs potentially inhibit the metabolism of co-administered medication which passes CYPs as primary route of elimination according to positive charged surface and very small particle size. Also, AgNPs exhibited potent CYP inhibitory effect may possibly cause drug interaction. The study the mechanism of CYP inhibition and the effect *in vivo* should be further investigated.



ศูนย์วิทยทรัพยากร
จุฬาลงกรณ์มหาวิทยาลัย

CHAPTER V

CONCLUSION

AuNPs are recently interested for medical applications such as drug and gene delivery, diagnosis and therapy. This is because AuNPs show physical properties, including unique optical properties and high surface areas. In general, colloidal solutions of spherical AuNPs are red with SPR band centered approximately at 520 nm. This band is dependent on size, shape and inter-particle distance of the particles. AgNPs present antimicrobial activity which would be employed for varied fields of application e.g. external use, medical devices, etc. Typically, colloidal solutions of spherical AgNPs are yellow with SPR band centered approximately at 400 nm. As AuNPs and AgNPs are widely used for different applications, the effect of them on biotransformation enzymes is determined in order to gain the information regarding less therapeutic effect or toxicity during co-administration. Citrate, PEI and PVP stabilized AuNPs and AgNPs were synthesized for investigating the inhibitory effect on CYP isozymes for phase I drug metabolisms, CYP1A2, CYP2C9, CYP2C19 and CYP3A4.

The citrate, PEI and PVP stabilized AuNPs (1,015 μM) and AgNPs (500 μM) were prepared by using various molar ratios of stabilizer solution to Au or Ag solution. According to the result of citrate stabilized AuNPs, the concentration ratio of trisodium citrate to hydrogen tetrachloroaurate of 16 : 1 was found to be suitable for preparing the stable AuNPs. The PEI stabilized AuNPs could be prepared using the concentration ratio of polyethyleneimine to hydrogen tetrachloroaurate of higher than 0.7 : 1. The concentration ratio of polyvinylpyrrolidone to hydrogen

tetrachloroaurate of higher than 90 : 1 was recommended for preparing the PVP stabilized AuNPs. Additionally, the concentration of sodium borohydride was twice which of silver nitrate for the suitable condition for AgNP preparation.

The average particle diameters of citrate, PEI and PVP stabilized AuNPs and AgNPs for freshly prepared systems were 8.36 ± 1.94 , 2.67 ± 1.04 , 5.05 ± 1.51 and 12.42 ± 2.48 nm, respectively. The particle sizes of AuNPs and AgNPs seemed to slightly increase after 1 month storage. From the results of zeta potential measurement, citrate stabilized AuNPs and AgNPs presented negative charges, which were slightly decreased after storage for a month. The charge of PVP stabilized AuNPs was slightly negative and little increased after 1 month storage. PEI stabilized AuNPs presented positive charges which were decreased after storage time.

From the result of CYP inhibition, PEI stabilized AuNPs demonstrated potent inhibitory effect on CYP2C9 and CYP2C19 with IC_{50} values of 4.47 ± 0.03 and 4.84 ± 0.01 μ M and moderate inhibition on CYP3A4 with IC_{50} value of 16.89 ± 0.02 μ M. In contrast, they had mild inhibition for CYP1A2 with IC_{50} value of 64.34 ± 0.05 μ M. PVP stabilized AuNPs exhibited less CYP inhibitory effect. They had the greatest inhibition on CYP3A4 followed by CYP2C9, CYP2C19 and CYP1A2, in orderly, with IC_{50} values of 233.4 ± 0.03 , 339.3 ± 0.04 , 418.8 ± 0.12 and 449.6 ± 0.02 μ M. AgNPs showed the moderate CYP inhibition. The inhibitory effect of AgNPs was highest for CYP3A4 ($IC_{50} = 13.52 \pm 0.01$ μ M) followed by CYP2C19 ($IC_{50} = 14.31 \pm 0.01$ μ M), CYP2C9 ($IC_{50} = 26.46 \pm 0.00$ μ M) and CYP1A2 ($IC_{50} = 43.51 \pm 0.03$ μ M), respectively. For citrate stabilized AuNPs the IC_{50} values were expected to be higher than 406 μ M. From the results, CYP inhibitory effect of the nanoparticles corresponds to their charges and particle sizes. PEI stabilized AuNPs exhibited the

highest CYP inhibition compared to AuNPs with other stabilizers. It was possibly due to their smaller size and positively charged particle. Although AgNPs showed the negatively charged particles, they inhibited the CYP activities more strongly than the negatively charged AuNPs stabilized by citrate. The inhibitory effect of AgNPs was considered to be from Ag atom.

The overall of the study concluded that PEI stabilized AuNPs and AgNPs probably would promote drug interaction involved in phase I metabolism during concomitant administration. Nevertheless, citrate and PVP stabilized AuNPs were considered to possibly cause low occurrence of drug interaction. The mechanism of CYP inhibition and *in vivo* study should be investigated for further use of nanoparticles.



ศูนย์วิทยทรัพยากร
จุฬาลงกรณ์มหาวิทยาลัย

REFERENCES

- Aillon, K.L., Xie, Y., El-Gendy, N., Berkland, C.J. and Forrest, M.L., 2009. Effects of nanomaterial physicochemical properties on *in vivo* toxicity. Adv. Drug Deliv. Rev. 61: 457-466.
- Baptista, P., Pereira, E., Eaton, P., Doria, G., Miranda, A., Gomes, I., Quaresma, P. and Franco, R. 2007. Gold nanoparticles for the development of clinical diagnosis methods. Anal. Bioanal. Chem. 391: 943-950.
- Bar-Ilan, O., Albrecht, R.M., Fako, V.E. and Furgeson, D.Y. 2009. Toxicity assessments of multisized gold and silver nanoparticles in zebrafish embryos. Small. 16: 1897-1910.
- Bhattacharya, R., Patra, C.R., Verma, R., Kumar, S., Greipp, P.R. and Mukherjee, P. 2007. Gold nanoparticles inhibit the proliferation of multiple myeloma cells. Adv. Mater. 19: 711-716.
- Bhattacharya, R. and Mukherjee, P. 2008. Biological properties of “naked” metal nanoparticles. Adv. Drug Deliv. Rev. 60: 1289–1306.
- Brust, M., Bethell, D., Kiely, C.J., and Schiffrin, D.J. 1998. Self-assembly gold nanoparticle thin films with nonmetallic optical and electronic properties. Langmuir. 14: 5425-5429.
- Chang, T.K., Gonzalez, F.J. and Waxman, D.J. 1994. Evaluation of tricetyloleandomycin, alpha-naphthoflavone and diethyldithiocarbamate as selective chemical probes for inhibition of human cytochromes P450. Arch. Biochem. Biophys. 311:437-442.

- Chung, Y.C., Chen, T.H. and Chen, C.J. 2008. The surface modification of silver nanoparticles by phosphoryl disulfides for improved biocompatibility and intracellular uptake. Biomater. 29: 1807-1816.
- Coleman, M.D., 2005. Human drug metabolism. John Wiley and Sons, Birmingham.
- Daniel, M.C. and Astruc, D. 2004. Gold nanoparticles: assembly, supramolecular chemistry, quantum-size-related properties, and applications toward biology, catalysis, and nanotechnology. Chem. Rev. 104: 293-346.
- Elechiguerra, J.L., Burt, J.L., Morones. J.R., Camacho-Bragado, A., Gao, X., Lara, H.H. and Yacaman, M.J. 2005. Interaction of silver nanoparticles with HIV-1. J. Nanobiotechnol. 3:6.
- Fischer, N.O., McIntosh, C.M., Simard, J.M. and Rotello, V.M. 2002. Inhibition of chymotrypsin through surface binding using nanoparticle-based receptors. Proc. Natl. Acad. Sci. 295: 5018-5023.
- Foged, C., Brodin, B., Frokjaer, S. and Sundblad, A. 2005. Particle size and surface charge affect particle uptake by human dendritic cells in an *in vitro* model. Int. J. Pharm. 298: 315-322.
- Ghosh, P., Han, G., De, M., Kim, C.K. and Rotello, V.M. 2008. Gold nanoparticles in delivery applications. Adv. Drug Deliv. Rev. 60: 1307-1315.
- Gibson, G.G. and Skett, P. 1996. Introduction to drug metabolism. New York: Chapman and Hall.
- Gibson, J.D., Khanal, B.P. and Zubarev, E.R. 2007. Paclitaxel-functionalized gold nanoparticles. J. Am. Chem. Soc. 129: 11653-11661.
- Glue, P. and Clement, R.P. 1997. Cytochrome P450 enzymes and drug metabolism- Basic concepts and methods of assessment. Cell. Mol. Neurobiol. 19: 309-323.

- Goodman, C.M., McCusker, C.D., Yilmaz, T. and Rotello, V.M. 2004. Toxicity of gold nanoparticles functionalized with cationic and anionic side chains. Bioconjugate Chem. 15: 897-900.
- Goshman, L., Fish, J. and Roller, K. 1999. Clinically significant cytochrom P450 drug interactions. J. Pharm. Soc. Wisconsin. May/June: 23-38.
- Haiss, W., Thanh, N.T.K., Aveyard, J. and Fernig, D.G. 2007. Determination of size and concentration of gold nanoparticles from UV-Vis spectra. Anal. Chem. 79: 4215-4221.
- Han, G., Ghosh, P., De, M. and Rotello, V.M. 2007. Drug and gene delivery using gold nanoparticles. J. Nanobiotechnol. 3: 40-45.
- Hasler, J.A., Estabrook, R., Murray, M., Pikuleva, I., Waterman, M., Capdevila, J., Holla, V., Helvig, C., Falck, J.R., Farrell, G., Kaminsky, L.S., Spivack, S.D., Boitier, E. and Beaune, P. 1999. Human cytochromes P450. Mol. Asp. Med. 20: 1-137.
- Hong, C.C., Tang, B.K., Hammond, G.L., Tritchler, D., Yaffe, M., Boyd, N.F. 2004. Cytochrome P450 1A2 (CYP1A2) activity and risk factors for breast cancer: a cross-sectional study. Breast Cancer Res. 6: R352-R365.
- Invitrogen Corporation, Vivid[®] CYP450 screening kits protocol [online]. 2008. Available from: <http://www.invitrogen.com/content/sfs/panvera/L0504.pdf> [2008, December 27]
- Jensen, T.R., Malinsky, M.D., Haynes, C.L. and Van Duyne, R.P. 2000. Nanosphere lithography: Tunable localized surface Plasmon resonance spectra of silver nanoparticles. J. Phys. Chem. B. 104: 10549-10556.

- Kim, S.M., Kim, G.S. and Lee, S.Y. 2008. Effects of PVP and KCl concentrations on the synthesis of gold nanoparticles using a solution plasma processing. Mater. Lett. 62: 4354-4356.
- Kim, J.S., Kuk, E., Yu, K.N., Kim, J.H., Park, S.J., Lee, H.J., Kim, S.H., Park, Y.K., Park, Y.H., Hwang, C.Y., Kim, Y.K., Lee, Y.S., Jeong, D.H. and Cho, M.H. 2007. Antimicrobial effects of silver nanoparticles. J. Nanomed. 3: 95-101.
- Kimling, J., Maier, M., Okenve, B., Kotaidis, V., Ballot, H. and Plech, A. 2006. Turkevich method for gold nanoparticle synthesis revisited. J. Phys. Chem. B. 110: 15700-15707.
- Kiss, I., Orsós, Z., Gombos, K., Bogner, B., Csejtei, A., Tibold, A., Varga, Z., Pázsit, E., Magda, I., Zölyomi, A. and Ember, I. 2007. Association between allelic polymorphisms of metabolizing enzymes (CYP 1A1, CYP 1A2, CYP 2E1, mEH) and occurrence of colorectal cancer in Hungary. Anticancer Res. 27: 2931-2937.
- Kleiner, H.E., Reed, M.J. and DiGiovanni, J. 2003. Naturally occurring coumarins inhibit human cytochromes P450 and block benzo[a]pyrene and 7, 12-dimethylbenz[a]anthracene DNA adduct formation in MCF-7 cells. Chem. Res. Toxicol. 16: 415-422.
- Lee, S. and Pérez-Luna, V.H. 2005. Dextran-gold nanoparticle hybrid material for biomolecule immobilization and detection. Anal. Chem. 77: 22: 7204-7211.
- Lin, J.H. and Lu, A.Y.H. 1998. Inhibition and induction of cytochrome P450 and the clinical implications. Clin. Pharmacokinet. 35: 301-390.

- Liu, H., Zhou, Q., Liang, Y., Yin, G. and Xu, Z. 2006. Synthesis of nearly monodisperse gold nanoparticles by a sodium diphenylamine sulfonate reduction process. J. Mater. Sci. 41: 3657-3662.
- Lynch, T. and Price, A. 2007. The effect of cytochrome P450 metabolism on drug response, interactions, and adverse effects. Am. Fam. Physician. 76: 391-396.
- Manzi, S.F. and Shannon, M. 2005. Drug interactions – A review. Clin. Ped. Emerg. Med. 6: 93-102.
- Marks, B.D. and Larson, B.R. Miniaturization and automation of cytochrome P450 inhibition assays [online]. 2009. Available from: <http://www.invitrogen.com/site/us/en/home/Products-and-Services/Applications/Drug-Discovery/DD-Misc/Drug-Discovery-Posters.html> [2009, March 2]
- Marques-Soares, C., Dijols, S., Macherey, A.C., Wester, M.R., Johnson, E.F., Dansette, P.M. and Mansuy, D. 2003. Sulfaphenazole derivatives as tools for comparing cytochrome P450 2C5 and human cytochrome P450 2Cs: identification of a new high affinity substrate common to those enzymes. Biochem. 42: 6363-6369.
- McIntosh, C.M., Esposito, E.A., Boal, A.K., Simard, J.M. and Martin, C.T. Rotello, V.M. 2001. Inhibition of DNA transcription using cationic mixed monolayer protected gold clusters. J. Am. Chem. Soc. 123: 7626-7629.
- Miller, C.R., Bondurant, B., McLean, S.D., McGovern, K.A. and O'Brien, D.F. 1998. Liposome-cell interactions *in vitro*: effect of liposome surface charge on the

binding and endocytosis of conventional and sterically stabilized liposomes.

Biochem. 37: 12875-12883.

Monostory, K., Hazai, E. and Vereczkey, L. 2004. Inhibition of cytochrome P450 enzymes participating in p-nitrophenol hydroxylation by drugs known as CYP2E1 inhibitors. Chem. Biol. Interact. 147: 331-340.

Mukherjee, P., Bhattacharya, R., Wang, P., Wang, L., Basu, S., Nagy, J.A., Atala, A., Mukhopadhyay, D. and Soker, S. 2005. Antiangiogenic properties of gold nanoparticles. Clin. Cancer Res. 11: 9: 3530-3534.

Nakamoto, M., Kashiwagi, Y. and Yamamoto, M. 2005. Synthesis and size regulation of gold nanoparticles by controlled thermolysis of ammonium gold (I) thiolate in the absence or presence of amines. Inorg. Chem. Acta. 358: 4229-4236.

Navarro, E., Piccapietra, F., Wagner, B., Marconi, F., Kaegi, R., Odzak, N., Sigg, L. and Behra, R. 2008. Toxicity of silver nanoparticles to *Chlamydomonas reinhardtii*. Environ. Sci. Technol. 42: 8959-8964.

Note, C., Kosmella, S. and Koetz, J. 2006. Poly(ethyleneimine) as reducing and stabilizing agent for the formation of gold nanoparticles in w/o microemulsions. Colloid Surf. A. 290: 150-156.

Osaka, T., Nakanishi, T., Shanmugam, S., Takahama, S. and Zhang, H. 2009. Effect of surface charge of magnetite nanoparticles on their internalization into breast cancer and umbilical vein endothelial cells. Colloids Surf. B. 71: 325-330.

Pelkonen, O., Kapitulnik, J., Gundert-Remy, U., Boobis, A.R. and Stockis, A. 2008. Local kinetics and dynamics of xenobiotics. Crit. Rev. Toxicol. 38 : 697-720.

- Pardiñas-Blanco, I., Hoppe, C.E., López-Quintela, M.A. and Rivas, J. 2007. Control on the dispersion of gold nanoparticles in an epoxy network. J. Non-Crystalline Solids. 353: 826-828.
- Pong, B.K., Elim, H.I., Chong, J.X., Ji, W., Trout, B.L. and Lee, J.Y. 2007. New insights on the nanoparticle growth mechanism in the citrate reduction of gold (III) salt: Formation of the Au nanowire intermediate and its nonlinear optical properties. J. Phys. Chem. 111: 6281-6287.
- Rai, M., Yadav, A. and Gade, A. 2008. Silver nanoparticles as a new generation of antimicrobials. Biotechnol. Adv. 27: 76-83.
- Saebø, M., Skjelbred, C.F., Brekke Li, K., Bowitz Lothe, I.M., Hagen, P.C., Johnsen, E., Tveit, K.M. and Kure, E.H. 2008. CYP1A2 164 A- → C polymorphism, cigarette smoking, consumption of well-done red meat and risk of developing colorectal adenomas and carcinomas. Anticancer Res. 28: 2289-2295.
- Sandhu, K.K., McIntosh, C.M., Simard, J.M., Smith, S.W. and Rotello, V.M. 2002. Gold nanoparticle-mediated transfection of mammalian cells. Bioconjug. Chem. 13: 3-6.
- Seow, A., Zhao, B., Lee, E.J., Poh, W.T., The, M., Eng, P., Wang, Y.T., Tan, W.C. and Lee, H.P. 2001. Cytochrome P450 1A2 (CYP1A2) activity and lung cancer risk: a preliminary study among Chinese women in Singapore. Carcinogenesis. 22: 673-677.
- Shimada, T., Yamazaki, H., Mimura, M., Inui, Y., Guengerich, F.P. 1994. Interindividual variations in human liver cytochrome P-450 enzymes involved in the oxidation of drugs, carcinogens and toxic chemicals: studies with liver

- microsomes of 30 Japanese and 30 Caucasians. J. Pharmacol. Exp. Ther. 270: 414–423.
- Sjöblom, J., 2006. Emulsions and emulsion stability. Taylor and Francis, New York.
- Singh, M., Singh, S., Prasad, S. and Gambhir, I.S. 2008. Nanotechnology in medicine and antibacterial effect of silver nanoparticles. Dig. J. Nanomater. Biostruct. 3: 115-122.
- Solomon, S.D., Bahadory, M., Jeyarajasingam, A.V., Rutkowsky, S.A. and Boritz, C. 2007. Synthesis and study of silver nanoparticles. J. Chem. Educ. 84: 2: 322-325.
- Sondi, I. and Salopek-Sondi, B. 2004. Silver nanoparticles as antimicrobial agent: a case study on *E. coli* as a model for Gram-negative bacteria. J. Colloid Interface Sci. 275: 177-182.
- Song, K.C., Lee, S.M., Park, T.S. and Lee, B.S. 2009. Preparation of colloidal silver nanoparticles by chemical reduction method. Korean J. Chem. Eng. 26: 153-155.
- Sun, X.P., Zhang, Z.L., Zhang, B.L., Dong, X.D., Dong, S.J. and Wang, E.K. 2003. Preparation of gold nanoparticles protected with polyelectrolyte. Chinese Chem. Lett. 14: 866-869.
- Thomas, M. and Klibanov, A.M. 2003. Conjugation to gold nanoparticles enhances polyethylenimine's transfer of plasmid DNA into mammalian cells. Proc. Natl. Acad. Sci. 100: 9138-9143.

- Turpeinen, M., Korhonen, L.E., Tolonen, A., Unsitalo, J., Juvonen, R., Raunio, H. and Pelkonen, O. 2006. Cytochrome P450 (CYP) inhibition screening: Comparison of three tests. Eur. J. Pharm. Sci. 29: 130-138.
- Wang, S.T., Yan, J.C. and Chen, L. 2005. Formation of gold nanoparticles and self-assembly into dimer and trimer aggregates. Mater. Lett. 59: 1383-1386.
- Yonzon, C.R., Zhang, X. and Van Duyne, R.P. 2003. Localized surface Plasmon resonance immunoassay and verification using surface-enhanced raman spectroscopy. Proc. SPIE. 5224: 78–85.
- Zhou, J., Ralston, J., Sedev, R. and Beattie, D.A. 2009. Functionalized gold nanoparticles: Synthesis, structure and colloid stability. J. Colloid Interface Sci. 331: 251-262.
- Zou, L., Harkey, M.R. and Henderson, G.L. 2002. Effects of herbal components on cDNA-expressed cytochrome P450 enzyme catalytic activity. Life Sci. 71: 1579-1589.



APPENDICES

ศูนย์วิทยทรัพยากร
จุฬาลงกรณ์มหาวิทยาลัย

APPENDIX A

PERCENTAGE OF INHIBITION ON VARIOUS CYPs OF

AuNPs AND AgNPs

Table 18 Percentage of inhibition of citrate stabilized AuNPs on CYP1A2 activity (n=4)

| Concentration of citrate stabilized AuNPs in the reaction mixture (μM) | % Inhibition | | | | |
|---|--------------|------|------|-------|-----------------|
| | 1 | 2 | 3 | 4 | Mean \pm S.D. |
| 203 | 0 | 0 | 0 | 0 | 0 |
| 406 | 11.49 | 8.01 | 9.41 | 10.09 | 9.75 \pm 1.45 |

Table 19 Percentage of inhibition of citrate stabilized AuNPs on CYP2C9 activity (n=4)

| Concentration of citrate stabilized AuNPs in the reaction mixture (μM) | % Inhibition | | | | |
|---|--------------|-------|-------|-------|------------------|
| | 1 | 2 | 3 | 4 | Mean \pm S.D. |
| 203 | 0 | 0 | 0 | 0 | 0 |
| 406 | 39.21 | 29.70 | 31.22 | 37.56 | 34.42 \pm 4.67 |

Table 20 Percentage of inhibition of citrate stabilized AuNPs on CYP2C19 activity (n=4)

| Concentration of citrate stabilized AuNPs in the reaction mixture (μM) | % Inhibition | | | | |
|---|--------------|-------|-------|-------|------------------|
| | 1 | 2 | 3 | 4 | Mean \pm S.D. |
| 20 | -2.74 | 0.54 | 0 | 0 | -0.55 \pm 1.48 |
| 203 | 38.12 | 37.16 | 32.95 | 38.49 | 36.68 \pm 2.55 |
| 406 | 44.20 | 44.81 | 46.22 | 48.81 | 46.01 \pm 2.05 |

Table 21 Percentage of inhibition of citrate stabilized AuNPs on CYP3A4 activity (n=4)

| Concentration of citrate stabilized AuNPs in the reaction mixture (μM) | % Inhibition | | | | |
|---|--------------|-------|-------|-------|------------------|
| | 1 | 2 | 3 | 4 | Mean \pm S.D. |
| 203 | 0 | 0 | 0 | 0 | 0 |
| 406 | 33.36 | 31.81 | 26.03 | 33.67 | 31.22 \pm 3.55 |

Table 22 Percentage of inhibition of PEI stabilized AuNPs on CYP1A2 activity (n=4)

| Concentration of PEI stabilized AuNPs in the reaction mixture (μM) | % Inhibition | | | | |
|---|--------------|-------|-------|-------|------------------|
| | 1 | 2 | 3 | 4 | Mean \pm S.D. |
| 2 | 0 | 0 | 0 | 0 | 0 |
| 10 | 0 | 0 | 0 | 0 | 0 |
| 20 | 0 | 0 | 0 | 0 | 0 |
| 30 | 28.56 | 23.76 | 27.85 | 25.19 | 26.34 \pm 2.25 |
| 51 | 42.57 | 47.90 | 37.02 | 30.73 | 39.56 \pm 7.37 |
| 152 | 74.49 | 80.24 | 73.20 | 67.26 | 73.80 \pm 5.33 |
| 254 | 87.74 | 86.73 | 86.61 | 87.35 | 87.11 \pm 0.53 |
| 406 | 95.51 | 95.51 | 94.78 | 95.02 | 95.02 \pm 0.37 |

Table 23 Percentage of inhibition of PEI stabilized AuNPs on CYP2C9 activity (n=4)

| Concentration of PEI stabilized AuNPs in the reaction mixture (μM) | % Inhibition | | | | |
|---|--------------|-------|-------|-------|------------------|
| | 1 | 2 | 3 | 4 | Mean \pm S.D. |
| 0.2 | 0 | 0 | 0 | 0 | 0 |
| 2 | 0 | 0 | 0 | 0 | 0 |
| 4 | 28.79 | 29.10 | 32.71 | 31.26 | 30.47 \pm 1.86 |
| 6 | 60.71 | 62.71 | 62.85 | 61.18 | 61.86 \pm 1.08 |
| 10 | 61.46 | 62.67 | 68.13 | 67.01 | 64.82 \pm 3.25 |
| 20 | 68.31 | 69.31 | 70.67 | 74.05 | 70.59 \pm 2.50 |
| 203 | 78.65 | 79.45 | 82.44 | 83.50 | 81.01 \pm 2.33 |
| 406 | 92.28 | 92.24 | 91.14 | 89.01 | 91.17 \pm 1.53 |

Table 24 Percentage of inhibition of PEI stabilized AuNPs on CYP2C19 activity (n=4)

| Concentration of PEI stabilized AuNPs in the reaction mixture (μM) | % Inhibition | | | | |
|---|--------------|-------|-------|-------|------------------|
| | 1 | 2 | 3 | 4 | Mean \pm S.D. |
| 0.2 | 0 | 0 | 0 | 0 | 0 |
| 2 | 0 | 0 | 0 | 0 | 0 |
| 4 | 35.52 | 37.3 | 30.49 | 25.12 | 32.11 \pm 5.48 |
| 6 | 63.8 | 63.41 | 69.56 | 63.75 | 65.13 \pm 2.96 |
| 10 | 81.39 | 83.93 | 85.18 | 86.05 | 84.14 \pm 2.03 |
| 20 | 95.66 | 95.32 | 96.76 | 96.76 | 96.13 \pm 0.75 |
| 203 | 97.58 | 97.52 | 97.00 | 97.00 | 97.28 \pm 0.32 |
| 406 | 98.04 | 97.96 | 98.01 | 98.07 | 98.02 \pm 0.05 |

Table 25 Percentage of inhibition of PEI stabilized AuNPs on CYP3A4 activity (n=4)

| Concentration of PEI stabilized AuNPs in the reaction mixture (μM) | % Inhibition | | | | |
|---|--------------|-------|-------|-------|------------------|
| | 1 | 2 | 3 | 4 | Mean \pm S.D. |
| 2 | 0 | 0 | 0 | 0 | 0 |
| 4 | 0 | 0 | 0 | 0 | 0 |
| 6 | 0 | 0 | 0 | 0 | 0 |
| 10 | 17.63 | 27.26 | 11.92 | 19.66 | 19.12 \pm 6.34 |
| 20 | 54.94 | 50.81 | 41.93 | 49.09 | 49.19 \pm 5.43 |
| 203 | 84.06 | 83.44 | 80.69 | 82.97 | 82.79 \pm 1.47 |
| 406 | 88.95 | 88.68 | 81.39 | 86.59 | 86.40 \pm 3.50 |

Table 26 Percentage of inhibition of PVP stabilized AuNPs on CYP1A2 activity (n=4)

| Concentration of PVP stabilized AuNPs in the reaction mixture (μM) | % Inhibition | | | | |
|---|--------------|-------|-------|-------|------------------|
| | 1 | 2 | 3 | 4 | Mean \pm S.D. |
| 2 | 0 | 0 | 0 | 0 | 0 |
| 20 | 0 | 0 | 0 | 0 | 0 |
| 203 | 18.95 | 19.62 | 23.34 | 20.25 | 20.54 \pm 1.94 |
| 406 | 26.79 | 24.07 | 31.88 | 31.68 | 28.61 \pm 3.83 |
| 609 | 81.38 | 80.76 | 78.46 | 82.83 | 80.86 \pm 1.82 |
| 812 | 84.21 | 84.39 | 84.84 | 84.12 | 84.39 \pm 0.32 |

Table 27 Percentage of inhibition of PVP stabilized AuNPs on CYP2C9 activity (n=4)

| Concentration of PVP stabilized AuNPs in the reaction mixture (μM) | % Inhibition | | | | |
|---|--------------|-------|-------|-------|------------------|
| | 1 | 2 | 3 | 4 | Mean \pm S.D. |
| 0.2 | 0 | 0 | 0 | 0 | 0 |
| 2 | 0 | 0 | 0 | 0 | 0 |
| 20 | 10.49 | 5.31 | 3.19 | 9.55 | 7.14 \pm 3.46 |
| 203 | 27.55 | 23.08 | 31.14 | 33.52 | 28.82 \pm 4.55 |
| 406 | 57.52 | 59.66 | 60.76 | 59.48 | 59.36 \pm 1.35 |
| 609 | 78.95 | 80.71 | 83.05 | 80.89 | 80.90 \pm 1.68 |
| 812 | 85.42 | 84.58 | 87.91 | 83.20 | 85.28 \pm 1.98 |

ศูนย์วิทยาศาสตร์
จุฬาลงกรณ์มหาวิทยาลัย

Table 28 Percentage of inhibition of PVP stabilized AuNPs on CYP2C19 activity (n=4)

| Concentration of PVP stabilized AuNPs in the reaction mixture (μM) | % Inhibition | | | | |
|---|--------------|-------|-------|-------|------------------|
| | 1 | 2 | 3 | 4 | Mean \pm S.D. |
| 2 | 0 | 0 | 0 | 0 | 0 |
| 20 | 0 | 0 | 0 | 0 | 0 |
| 203 | 31.25 | 37.03 | 40.38 | 41.41 | 37.52 \pm 4.58 |
| 406 | 58.12 | 61.81 | 63.53 | 61.53 | 61.25 \pm 2.26 |
| 609 | 97.52 | 98.28 | 97.48 | 97.41 | 97.67 \pm 0.41 |
| 812 | 97.77 | 98.23 | 97.87 | 97.61 | 97.87 \pm 0.26 |

Table 29 Percentage of inhibition of PVP stabilized AuNPs on CYP3A4 activity (n=4)

| Concentration of PVP stabilized AuNPs in the reaction mixture (μM) | % Inhibition | | | | |
|---|--------------|-------|-------|-------|------------------|
| | 1 | 2 | 3 | 4 | Mean \pm S.D. |
| 2 | 0 | 0 | 0 | 0 | 0 |
| 20 | 0 | 0 | 0 | 0 | 0 |
| 203 | 53.95 | 56.10 | 47.40 | 48.51 | 51.49 \pm 4.20 |
| 406 | 78.31 | 82.12 | 76.31 | 76.77 | 78.38 \pm 2.64 |
| 609 | 99.19 | 99.17 | 99.21 | 99.26 | 99.21 \pm 0.04 |
| 812 | 99.48 | 99.38 | 99.56 | 99.39 | 99.45 \pm 0.08 |

Table 30 Percentage of inhibition of AgNPs on CYP1A2 activity (n=4)

| Concentration of AgNPs in the reaction mixture (μM) | % Inhibition | | | | |
|--|--------------|-------|-------|-------|------------------|
| | 1 | 2 | 3 | 4 | Mean \pm S.D. |
| 10 | 0 | 0 | 0 | 0 | 0 |
| 20 | 0 | 0 | 0 | 0 | 0 |
| 30 | 28.63 | 35.68 | 24.68 | 34.82 | 30.95 \pm 5.23 |
| 40 | 30.48 | 42.60 | 30.15 | 31.26 | 33.62 \pm 6.00 |
| 60 | 94.14 | 96.32 | 95.71 | 95.17 | 95.34 \pm 0.92 |
| 80 | 94.40 | 95.16 | 94.82 | 97.38 | 95.44 \pm 1.33 |

Table 31 Percentage of inhibition of AgNPs on CYP2C9 activity (n=4)

| Concentration of AgNPs in the reaction mixture (μM) | % Inhibition | | | | |
|--|--------------|--------|--------|--------|-------------------|
| | 1 | 2 | 3 | 4 | Mean \pm S.D. |
| 10 | 0 | 0 | 0 | 0 | 0 |
| 14 | 0 | 0 | 0 | 0 | 0 |
| 20 | 0 | 0 | 0 | 0 | 0 |
| 26 | 44.42 | 37.64 | 52.98 | 44.34 | 44.85 \pm 6.29 |
| 30 | 77.87 | 83.77 | 89.72 | 90.63 | 85.50 \pm 5.93 |
| 40 | 100.01 | 101.79 | 103.51 | 101.12 | 101.61 \pm 1.47 |

Table 32 Percentage of inhibition of AgNPs on CYP2C19 activity (n=4)

| Concentration of AgNPs in the reaction mixture (μM) | % Inhibition | | | | |
|--|--------------|--------|-------|--------|------------------|
| | 1 | 2 | 3 | 4 | Mean \pm S.D. |
| 2 | 0 | 0 | 0 | 0 | 0 |
| 10 | 16.25 | 20.47 | 12.43 | 8.44 | 14.40 \pm 5.15 |
| 14 | 51.97 | 58.49 | 51.52 | 52.37 | 53.59 \pm 3.29 |
| 20 | 71.36 | 79.65 | 78.18 | 69.57 | 74.69 \pm 4.97 |
| 30 | 92.94 | 101.03 | 98.12 | 103.50 | 98.90 \pm 4.54 |
| 40 | 97.42 | 102.38 | 99.23 | 100.46 | 99.87 \pm 2.09 |

Table 33 Percentage of inhibition of AgNPs on CYP3A4 activity (n=4)

| Concentration of AgNPs in the reaction mixture (μM) | % Inhibition | | | | |
|--|--------------|-------|-------|-------|-------------------|
| | 1 | 2 | 3 | 4 | Mean \pm S.D. |
| 2 | 0 | 0 | 0 | 0 | 0 |
| 10 | 0 | 0 | 0 | 0 | 0 |
| 14 | 41.17 | 68.71 | 65.39 | 58.95 | 58.56 \pm 12.28 |
| 20 | 95.85 | 91.09 | 92.04 | 91.22 | 92.55 \pm 2.24 |
| 30 | 97.00 | 96.47 | 96.82 | 96.29 | 96.65 \pm 0.32 |
| 40 | 98.36 | 98.36 | 96.09 | 96.93 | 97.44 \pm 1.12 |

APPENDIX B

VERIFICATION OF THE VIVID[®] CYP450 INHIBITION TEST**Table 34** Inhibitory effect of α -naphthoflavone on CYP1A2 activity (n=2)

| Concentration of α -naphthoflavone in the reaction mixture (μ M) | % Inhibition | | |
|--|--------------|--------|--------|
| | 1 | 2 | Mean |
| 0.001 | 0 | 0 | 0 |
| 0.010 | 0 | 0 | 0 |
| 0.025 | 0 | 0 | 0 |
| 0.050 | 2.28 | 9.06 | 5.67 |
| 0.100 | 40.24 | 48.95 | 44.60 |
| 0.250 | 100.32 | 97.71 | 99.01 |
| 1.000 | 100.61 | 104.37 | 102.49 |

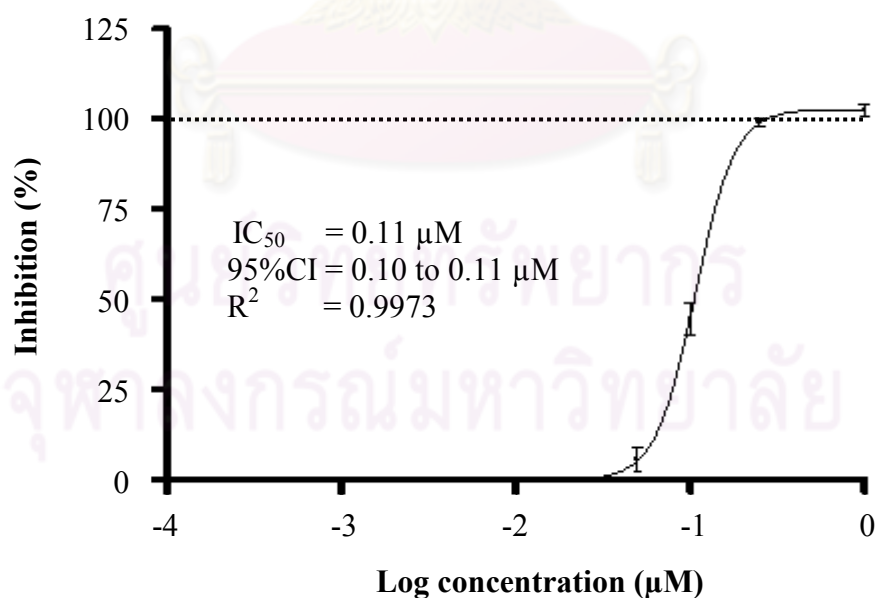
**Figure 54** Inhibition curve of α -naphthoflavone on CYP1A2

Table 35 Inhibitory effect of sulfaphenazole on CYP2C9 activity (n=2)

| Concentration of sulfaphenazole in the reaction mixture (μM) | % Inhibition | | |
|---|--------------|-------|-------|
| | 1 | 2 | Mean |
| 0.001 | 23.46 | 19.74 | 21.60 |
| 0.010 | 25.72 | 24.04 | 24.88 |
| 0.050 | 48.56 | 50.84 | 49.70 |
| 0.250 | 52.28 | 58.11 | 55.19 |
| 0.500 | 74.23 | 72.92 | 73.58 |
| 2.000 | 89.08 | 91.41 | 90.25 |
| 10.000 | 102.92 | 91.63 | 97.27 |

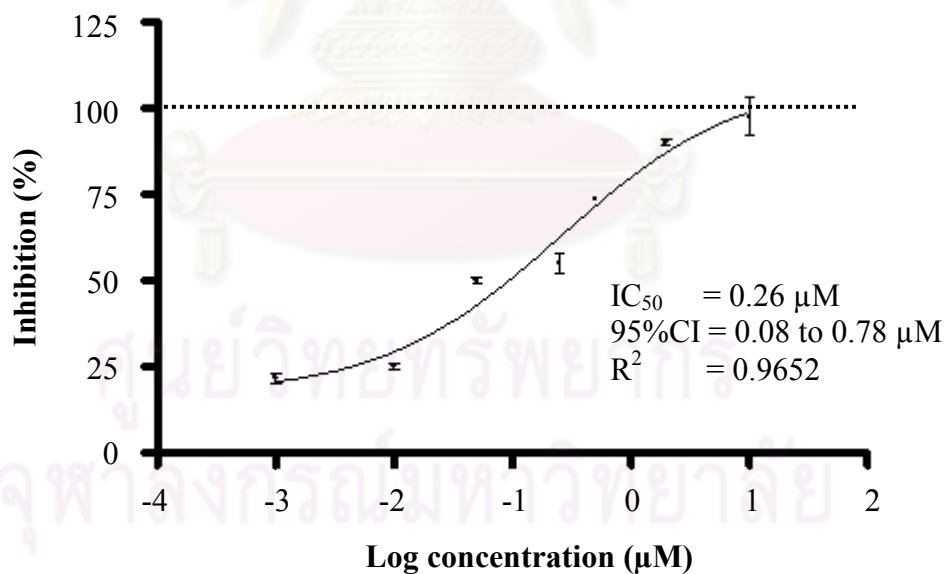
**Figure 55** Inhibition curve of sulfaphenazole on CYP2C9

Table 36 Inhibitory effect of miconazole on CYP2C19 activity (n=2)

| Concentration of miconazole in the reaction mixture (μM) | % Inhibition | | |
|---|--------------|-------|-------|
| | 1 | 2 | Mean |
| 0.005 | 0 | 0 | 0 |
| 0.010 | 0 | 0 | 0 |
| 0.025 | 0 | 0 | 0 |
| 0.050 | 6.41 | 0.11 | 3.26 |
| 0.100 | 3.77 | 19.39 | 11.58 |
| 0.250 | 23.64 | 43.48 | 33.56 |
| 0.500 | 66.31 | 80.16 | 73.23 |
| 1.000 | 98.48 | 99.12 | 98.80 |

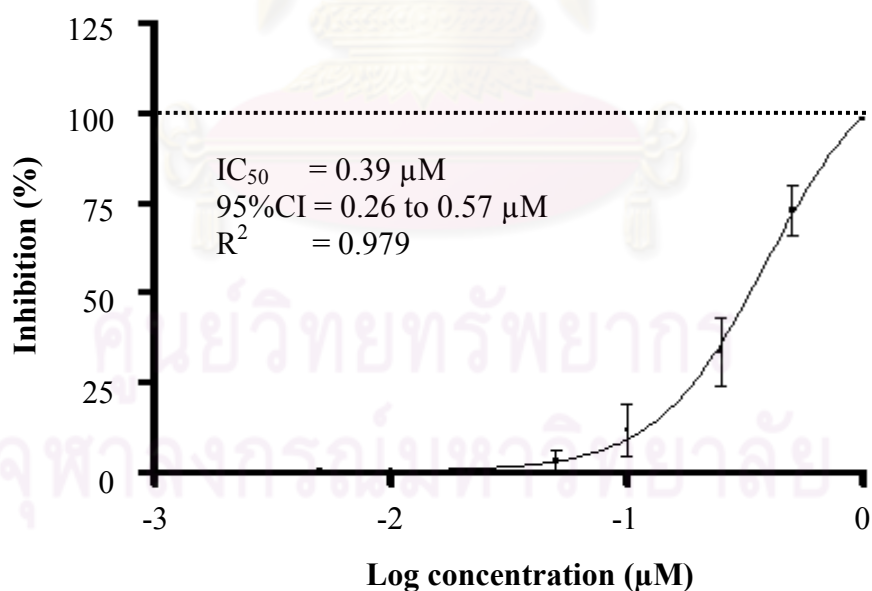
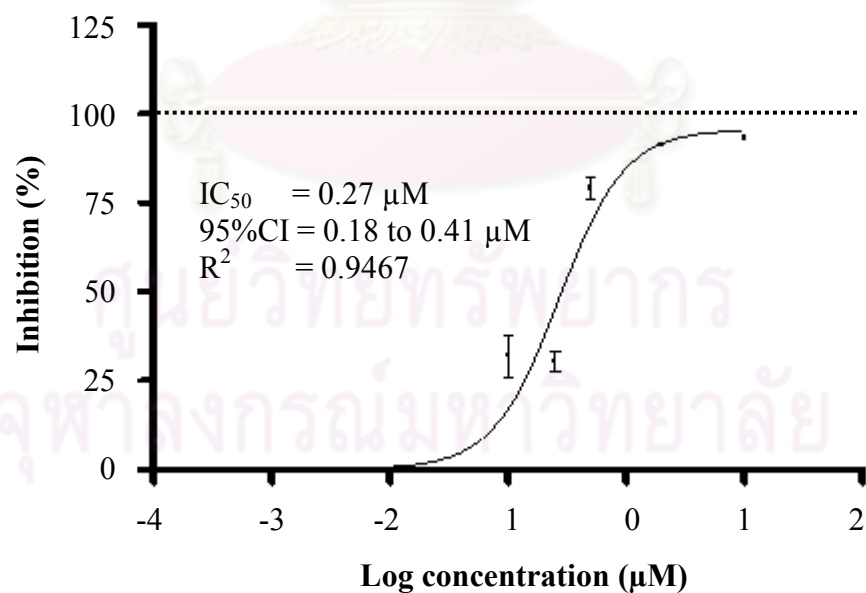
**Figure 56** Inhibition curve of miconazole on CYP2C19

Table 37 Inhibitory effect of ketoconazole on CYP3A4 activity (n=2)

| Concentration of ketoconazole in the reaction mixture (μM) | % Inhibition | | |
|---|--------------|-------|-------|
| | 1 | 2 | Mean |
| 0.001 | 0 | 0 | 0 |
| 0.010 | 0 | 0 | 0 |
| 0.050 | 0 | 0 | 0 |
| 0.100 | 26.11 | 37.91 | 32.01 |
| 0.250 | 27.69 | 33.14 | 30.42 |
| 0.500 | 82.17 | 76.04 | 79.11 |
| 2.000 | 91.03 | 91.85 | 91.44 |
| 10.000 | 92.74 | 93.84 | 93.29 |

**Figure 57** Inhibition curve of ketoconazole on CYP3A4

APPENDIX C

VIVID® CYP450 SCREENING KITS PROTOCOL



ศูนย์วิทยุทรัพยากร
จุฬาลงกรณ์มหาวิทยาลัย



Vivid[®] CYP450 Screening Kits Protocol

Cat. no. P2556, P2557, P2558, P2559, P2560, P2561, P2562, P2563, P2564, P2568, P2569, P2570, P2571, P2572, P3019, P3020 and P3021

INTRO-011.0-0008

TABLE OF CONTENTS

| | | |
|------|--|----|
| 1.0 | INTRODUCTION | 1 |
| 2.0 | MATERIALS SUPPLIED | 2 |
| 2.1 | Materials Required but not Supplied | 3 |
| 3.0 | STORAGE AND STABILITY | 3 |
| 4.0 | ASSAY THEORY | 4 |
| 5.0 | VIVID [®] CYP450 HIGH-THROUGHPUT SCREENING ASSAY PROTOCOL | 5 |
| 5.1 | Assay Procedure | 5 |
| 6.0 | SUGGESTED PROTOCOL FOR THE ANALYSIS OF RESULTS | 10 |
| 6.1 | Kinetic Assay Mode | 10 |
| 6.2 | Endpoint Assay Mode | 10 |
| 7.0 | SUGGESTED CYP450 INHIBITORS (STOP REAGENT) | 10 |
| 8.0 | SOLVENT TOLERANCES | 11 |
| 9.0 | REFERENCES | 12 |
| 10.0 | PURCHASER NOTIFICATION | 12 |

1.0 INTRODUCTION

Vivid[®] CYP450 Screening Kits enable rapid measurement of interactions between drug candidates and cytochrome P450 enzymes using a simple "mix-and-read" fluorescent assay that is designed for high-throughput screening in multiwell plates. These kits will allow investigators to rapidly identify compound CYP450 interactions, eliminating unsuitable compounds early in the drug discovery process. Vivid[®] CYP450 Screening Kits can also be used to generate predictive structure activity relationship models to guide medicinal chemists in their design of compounds.

Test compounds are analyzed by their capacity to inhibit the production of a fluorescent signal in reactions using recombinant CYP450 isozymes and specific Vivid[®] CYP450 Substrates. The availability of more than one structurally unrelated fluorescent Vivid[®] CYP450 Substrate for CYP3A4, CYP3A5, CYP2C9, CYP2D6 and CYP2D6 reduces the potential for false negatives (and false positives) that could result from substrate-dependent interactions.

ศูนย์วิทยทรัพยากร
จุฬาลงกรณ์มหาวิทยาลัย

2.0 MATERIALS SUPPLIED

| ViroP™ CYP450 Screening Kit | Description | Cat. no. | Quantity | Storage |
|---|----------------------------------|----------|----------|------------------------|
| ViroP™ CYP1A2 Kit (P347) | ViroP™ CYP450 Reaction Buffer I | P340 | 75 µl | RT |
| | ViroP™ CYP450 Reaction Buffer II | P342 | 0.5 µmol | 4°C |
| | Yield™ LBALC Substrate | 1254 | 0.1 mg | -20°C, light protected |
| ViroP™ CYP2A6 Kit (P349) | ViroP™ CYP450 Reaction Buffer I | P340 | 75 µl | RT |
| | ViroP™ CYP450 Reaction Buffer II | P342 | 0.5 µmol | 4°C |
| | Yield™ LBALC Substrate | 1254 | 0.1 mg | -20°C, light protected |
| ViroP™ CYP2B6 Kit (P348) | ViroP™ CYP450 Reaction Buffer I | P340 | 75 µl | RT |
| | ViroP™ CYP450 Reaction Buffer II | P342 | 0.5 µmol | 4°C |
| | Yield™ LBALC Substrate | 1254 | 0.1 mg | -20°C, light protected |
| ViroP™ CYP2C8 Kit (P349) | ViroP™ CYP450 Reaction Buffer I | P340 | 75 µl | RT |
| | ViroP™ CYP450 Reaction Buffer II | P342 | 0.5 µmol | 4°C |
| | Yield™ LBALC Substrate | 1254 | 0.1 mg | -20°C, light protected |
| ViroP™ CYP2C9 Kit (P349) | ViroP™ CYP450 Reaction Buffer I | P340 | 75 µl | RT |
| | ViroP™ CYP450 Reaction Buffer II | P342 | 0.5 µmol | 4°C |
| | Yield™ LBALC Substrate | 1254 | 0.1 mg | -20°C, light protected |
| ViroP™ CYP2C19 Kit (P348) | ViroP™ CYP450 Reaction Buffer I | P340 | 75 µl | RT |
| | ViroP™ CYP450 Reaction Buffer II | P342 | 0.5 µmol | 4°C |
| | Yield™ LBALC Substrate | 1254 | 0.1 mg | -20°C, light protected |
| ViroP™ CYP2D6 Kit (P347) | ViroP™ CYP450 Reaction Buffer I | P340 | 75 µl | RT |
| | ViroP™ CYP450 Reaction Buffer II | P342 | 0.5 µmol | 4°C |
| | Yield™ LBALC Substrate | 1254 | 0.1 mg | -20°C, light protected |
| ViroP™ CYP2D6 C ₂ Kit (P347) | ViroP™ CYP450 Reaction Buffer I | P340 | 75 µl | RT |
| | ViroP™ CYP450 Reaction Buffer II | P342 | 0.5 µmol | 4°C |
| | Yield™ LBALC Substrate | 1254 | 0.1 mg | -20°C, light protected |
| ViroP™ CYP2E1 Kit (P348) | ViroP™ CYP450 Reaction Buffer I | P340 | 75 µl | RT |
| | ViroP™ CYP450 Reaction Buffer II | P342 | 0.5 µmol | 4°C |
| | Yield™ LBALC Substrate | 1254 | 0.1 mg | -20°C, light protected |
| ViroP™ CYP2A4 Kit (P349) | ViroP™ CYP450 Reaction Buffer I | P340 | 75 µl | RT |
| | ViroP™ CYP450 Reaction Buffer II | P342 | 0.5 µmol | 4°C |
| | Yield™ LBALC Substrate | 1254 | 0.1 mg | -20°C, light protected |
| ViroP™ CYP2A6 C ₂ Kit (P348) | ViroP™ CYP450 Reaction Buffer I | P340 | 75 µl | RT |
| | ViroP™ CYP450 Reaction Buffer II | P342 | 0.5 µmol | 4°C |
| | Yield™ LBALC Substrate | 1254 | 0.1 mg | -20°C, light protected |
| ViroP™ CYP2A6 C ₂ Kit (P347) | ViroP™ CYP450 Reaction Buffer I | P340 | 75 µl | RT |
| | ViroP™ CYP450 Reaction Buffer II | P342 | 0.5 µmol | 4°C |
| | Yield™ LBALC Substrate | 1254 | 0.1 mg | -20°C, light protected |
| ViroP™ CYP2A6 Kit (P349) | ViroP™ CYP450 Reaction Buffer I | P340 | 75 µl | RT |
| | ViroP™ CYP450 Reaction Buffer II | P342 | 0.5 µmol | 4°C |
| | Yield™ LBALC Substrate | 1254 | 0.1 mg | -20°C, light protected |
| ViroP™ CYP2A6 C ₂ Kit (P348) | ViroP™ CYP450 Reaction Buffer I | P340 | 75 µl | RT |
| | ViroP™ CYP450 Reaction Buffer II | P342 | 0.5 µmol | 4°C |
| | Yield™ LBALC Substrate | 1254 | 0.1 mg | -20°C, light protected |
| ViroP™ CYP2A6 C ₂ Kit (P347) | ViroP™ CYP450 Reaction Buffer I | P340 | 75 µl | RT |
| | ViroP™ CYP450 Reaction Buffer II | P342 | 0.5 µmol | 4°C |
| | Yield™ LBALC Substrate | 1254 | 0.1 mg | -20°C, light protected |
| ViroP™ CYP2A6 C ₂ Kit (P347) | ViroP™ CYP450 Reaction Buffer I | P340 | 75 µl | RT |
| | ViroP™ CYP450 Reaction Buffer II | P342 | 0.5 µmol | 4°C |
| | Yield™ LBALC Substrate | 1254 | 0.1 mg | -20°C, light protected |
| ViroP™ CYP2A6 C ₂ Kit (P348) | ViroP™ CYP450 Reaction Buffer I | P340 | 75 µl | RT |
| | ViroP™ CYP450 Reaction Buffer II | P342 | 0.5 µmol | 4°C |
| | Yield™ LBALC Substrate | 1254 | 0.1 mg | -20°C, light protected |
| ViroP™ CYP2A6 C ₂ Kit (P347) | ViroP™ CYP450 Reaction Buffer I | P340 | 75 µl | RT |
| | ViroP™ CYP450 Reaction Buffer II | P342 | 0.5 µmol | 4°C |
| | Yield™ LBALC Substrate | 1254 | 0.1 mg | -20°C, light protected |
| ViroP™ CYP2A6 C ₂ Kit (P348) | ViroP™ CYP450 Reaction Buffer I | P340 | 75 µl | RT |
| | ViroP™ CYP450 Reaction Buffer II | P342 | 0.5 µmol | 4°C |
| | Yield™ LBALC Substrate | 1254 | 0.1 mg | -20°C, light protected |
| ViroP™ CYP2A6 C ₂ Kit (P347) | ViroP™ CYP450 Reaction Buffer I | P340 | 75 µl | RT |
| | ViroP™ CYP450 Reaction Buffer II | P342 | 0.5 µmol | 4°C |
| | Yield™ LBALC Substrate | 1254 | 0.1 mg | -20°C, light protected |

All kits are supplied with 100 µl of each component. ViroP™ CYP450 Reaction Buffer I (100 µl), ViroP™ CYP450 Reaction Buffer II (100 µl), and Yield™ LBALC Substrate (100 µl) are supplied in 1.5 ml microcentrifuge tubes. ViroP™ CYP450 Reaction Buffer I (100 µl), ViroP™ CYP450 Reaction Buffer II (100 µl), and Yield™ LBALC Substrate (100 µl) are supplied in 1.5 ml microcentrifuge tubes. ViroP™ CYP450 Reaction Buffer I (100 µl), ViroP™ CYP450 Reaction Buffer II (100 µl), and Yield™ LBALC Substrate (100 µl) are supplied in 1.5 ml microcentrifuge tubes. ViroP™ CYP450 Reaction Buffer I (100 µl), ViroP™ CYP450 Reaction Buffer II (100 µl), and Yield™ LBALC Substrate (100 µl) are supplied in 1.5 ml microcentrifuge tubes.

- The Yield™ CYP450 Reaction Buffer I (100 µl) is supplied in a 1.5 ml microcentrifuge tube.
- The Yield™ CYP450 Reaction Buffer II (100 µl) is supplied in a 1.5 ml microcentrifuge tube.
- The Yield™ Substrate and Standard are supplied as described in the accompanying assay protocols.

2.1 Materials Required but not Supplied

- Multiwell black plates suitable for fluorescence measurements (Note: black-walled, clear bottom plates are needed for bottom read fluorescent microplate readers). Invitrogen recommends using Corning 9605 non-treated plates
- Fluorescence plate reader with filters as described in Table 6
- Pipetting device
- Reagent reservoir(s)
- Acetonitrile, anhydrous
- DMSO, reagent grade
- Deionized water
- Stop Reagent (CYP450 isozyme specific inhibitor) if performing an endpoint assay or in kinetic mode for the positive control of inhibition. For more information on inhibitors, see Section 7.0.

3.0 STORAGE AND STABILITY

Vivid® CYP450 Substrates and Fluorescent Standards are stable for at least six months when stored desiccated and protected from light at -20°C. For short term storage, acetonitrile or DMSO based stock solutions should be stored in a desiccator at 4°C. Long term storage requires that organic solutions be kept desiccated at -20°C. DMSO solutions are hygroscopic, and cold vials should be warmed to ambient temperature before opening. After opening, they should be capped promptly to avoid reagent dilution by absorbed moisture. The CYP450 BACULOVIRUSES® Reagent should be stored at -80°C. No significant decrease in activity (see enclosed Certificate of Analysis) was observed after 5 freeze/thaw cycles except for CYP2D6 which showed a 5% decrease. The Regeneration System should be stored at -80°C. Upon first thaw, aliquot into single use vials as the reagent should not be subjected to additional freeze/thaw cycles. The NADP+ should be stored at -80°C and is stable for at least 10 freeze/thaw cycles. Store protected from light. The Vivid® CYP450 Reaction Buffer (2X) can be stored at 4°C or room temperature.

ศูนย์วิทยทรัพยากร
จุฬาลงกรณ์มหาวิทยาลัย

4.0 ASSAY THEORY

Vivid[®] CYP450 Screening Kits are designed to assess metabolism and inhibition of the predominant human P450 isozymes involved in hepatic drug metabolism: CYP1A2, CYP2B6, CYP2C9, CYP2C19, CYP2D6, CYP2E1, CYP3A4 and CYP3A5. The kits employ Vivid[®] CYP450 Substrates and CYP450 BACULOSOMES[®] Reagents. The CYP450 BACULOSOMES[®] Reagents are microsomes prepared from insect cells expressing a human P450 isozyme and rabbit NADPH P450 reductase (CYP2E1) also contains human cytochrome *b₅*. CYP450 BACULOSOMES[®] Reagents offer a distinct advantage over human liver microsomes in that only one CYP450 enzyme is expressed, thereby preventing metabolism by other CYP450s. The Vivid[®] substrates are metabolized by a specific CYP450 enzyme into products that are highly fluorescent in aqueous solutions. Figure 1 schematically depicts the metabolism of a Vivid[®] CYP450 Substrate into a fluorescent metabolite. Note that the Vivid[®] Substrates have two potential sites for metabolism (indicated by arrows in Figure 1) and that oxidation at either site releases the highly fluorescent metabolite.

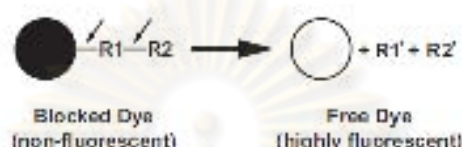


Figure 1. Schematic of the metabolism of the "blocked" dye substrate into a fluorescent metabolite.

The fluorescent metabolites are emitted in the visible light spectrum, which minimizes interference caused by the background fluorescence of UV-sensitive compounds and NADPH. The excellent reaction kinetics and optical properties of the Vivid[®] substrates allow their use at concentrations at or below their K_m value in a reaction with P450 isozymes, assuring detection of even weak CYP450 inhibitors and providing the convenience of room temperature or 37°C incubations. The Vivid[®] CYP450 Assay may be run in a kinetic or endpoint mode (which is illustrated in Figure 2).

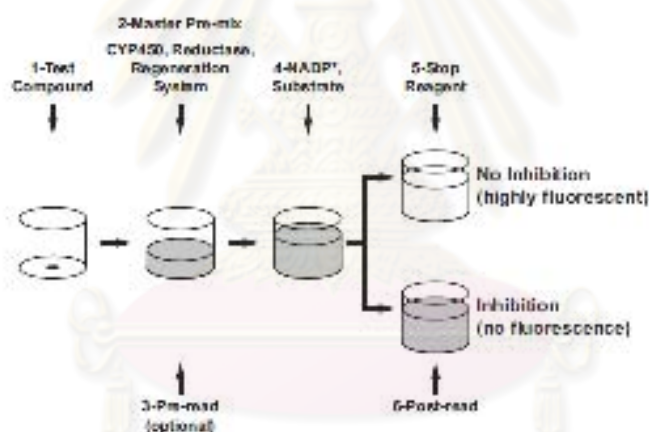


Figure 2. A schematic representation of an endpoint Vivid[®] CYP450 Assay.

In end point (Section 5.1.9.2) mode, the test compounds (Step 1) are first combined with the Master Pre mix (Step 2), consisting of CYP450 BACULOSOMES[®] Reagents and the Regeneration System (consisting of glucose-6-phosphate and glucose-6-phosphate dehydrogenase). The Regeneration System converts NADP⁺ into NADPH, which is required to start the CYP450 reaction. After a brief pre incubation, the background fluorescence of the test compound and Master Pre mix is measured (Step 3, pre-read). The enzymatic reaction is initiated by the addition of a mix of NADP⁺ and the appropriate Vivid[®] Substrate (Step 4) and plate is incubated for the desired reaction time. After the addition of a Stop Reagent (Step 5), the fluorescence is measured in Step 6.

In kinetic mode (Section 5.1.9.3), the fluorescence is measured continuously starting after Step 4 (and eliminating Steps 5 and 6). Standard curves, constructed from the supplied Fluorescent Standard, can be used to calculate reaction rates from the observed fluorescence intensities in both assay formats. Assay parameters for isozymes CYP1A2, CYP2B6, CYP2C9, CYP2C19, CYP2D6, CYP2E1, CYP3A4 and CYP3A5 are listed in Tables 4 and 5.

6.0 VIVID® CYP450 HIGH-THROUGHPUT SCREENING ASSAY PROTOCOL

Each complete reaction must contain CYP450 BACULOSOMES® Reagent, Vivid® CYP450 Substrate, NADPH and Regeneration System, all in the appropriate Vivid® CYP450 Reaction Buffer (supplied with each kit as a 2X solution). There are two possible modes for this assay: kinetic and endpoint. The method you choose will depend on your analytical needs and the equipment available. The kinetic mode is useful for analyses of one multiwell plate at a time and does not require the addition of the stop reagent. In endpoint mode, after an appropriate incubation time, the reaction is stopped by the addition of the CYP450 isozyme-specific inhibitor. Running in endpoint mode allows the reaction to be performed in several multiwell plates simultaneously.

Note: The following protocol is configured for use with one 96-well plate and 100 µl reactions. However, the protocol can be modified to accommodate several different plate formats by adjusting the calculations for the number of wells (and volume per well) in your experiment. See Erbeskosy et al. (2005) (see Section 9.0 for a complete list of references) for use of Vivid® kits in 1536-well plate formats. Each kit supplies enough reagents for at least 200 x 100 µl reactions.

6.1 Assay Procedure

6.1.1 Thaw Reagents

1. Thaw the P450 BACULOSOMES®, Regeneration System, and NADPH on ice until ready to use. Do not vortex P450 BACULOSOMES® or Regeneration System.
2. Suggested assay conditions for screening with Vivid® kits are described in Table 1.

Table 1. Assay Conditions

| Condition | Purpose | Dispensing |
|--------------------------------|--|--|
| Test Compound | Screen for inhibition by compound of interest | 40 µl 25X test compound 50 µl Master Pre-Mix 10 µl Vivid Substrate and NADPH |
| Positive Inhibition Control | Inhibit the reaction with a known P450 inhibitor | 40 µl 25X positive inhibition control (see Section 7.0) 50 µl Master Pre-Mix 10 µl Vivid Substrate and NADPH |
| Solvent Control (No inhibitor) | Account for possible solvent inhibition caused by transcription or heat components originally dissolved in an organic solvent such as DMSO | 40 µl 25X solvent control 50 µl Master Pre-Mix 10 µl Vivid Substrate and NADPH |
| Background | Enables subtraction of background fluorescence during data analysis | 40 µl 25X solvent control 50 µl Vivid® CYP450 Reaction Buffer 10 µl Vivid Substrate and NADPH |

ศูนย์วิทยทรัพยากร
จุฬาลงกรณ์มหาวิทยาลัย

5.1.2 Reconstitution of Vivid[®] Substrate and Fluorescent Standard

1. Reconstitute the Vivid[®] Standard using anhydrous acetonitrile and Fluorescent Standard using DMSO (see Tables 2 and 3).
2. Keep these solutions at room temperature for immediate use, or store at -20°C.

Table 2. Reconstitution of the Vivid[®] CYP450 substrates

| Assay Type | Vivid [®] CYP450 Substrate | Molecular weight | mg per tube | µmol per tube | µl acetonitrile added per tube | [stock solution] (nM) | [working concentration] (µM) |
|------------|--------------------------------------|------------------|-------------|---------------|--------------------------------|-----------------------|------------------------------|
| 1A2 | Vivid [®] DUBOL | 262 | 0.1 | 0.41 | 2.5 | 2 | 2 |
| 2B6 | Vivid [®] BOMBY | 303 | 0.1 | 0.33 | 100 | 2 | 2 |
| | Vivid [®] BUMBIC | 262 | 0.1 | 0.28 | 100 | 2 | 2 |
| | Vivid [®] BUNOL | 303 | 0.1 | 0.32 | 100 | 2 | 10 |
| 2C9 | Vivid [®] BOMF | 325 | 0.1 | 0.32 | 110 | 2 | 2 |
| | Vivid [®] COMF ¹ | 324 | 0.1 | 0.36 | 100 | 2 | 2 |
| 2C19 | Vivid [®] DUBOL | 262 | 0.1 | 0.41 | 2.5 | 2 | 10 |
| | Vivid [®] DUBOL | 262 | 0.1 | 0.41 | 2.5 | 2 | 10 |
| 2J6 | Vivid [®] MOMB | 325 | 0.1 | 0.36 | 100 | 2 | 2 |
| | Vivid [®] BOMBY | 303 | 0.1 | 0.31 | 205 | 2 | 10 |
| 3A4 | Vivid [®] BUNOL | 303 | 0.1 | 0.32 | 100 | 2 | 10 |
| | Vivid [®] BOMBY | 303 | 0.1 | 0.36 | 100 | 2 | 2 |
| | Vivid [®] DBUM | 172.6 | 0.1 | 0.17 | 85 | 2 | 2 |
| | Vivid [®] BUMB | 222 | 0.1 | 0.30 | 100 | 2 | 2 |
| 3A5 | Vivid [®] BUNOL | 303 | 0.1 | 0.32 | 100 | 2 | 10 |
| | Vivid [®] BUMBIC | 262 | 0.1 | 0.28 | 100 | 2 | 2 |
| | Vivid [®] DBUM | 172.6 | 0.1 | 0.17 | 85 | 2 | 2 |

¹ Dissolve in DMSO for 1-5 minutes and vortex as recommended.

Table 3. Reconstitution of the Fluorescent Standard. Use the blank cells in the table for your calculations. The value [X] is the amount of Assay Standard listed on the tube label.

| Assay Standard | µmol per tube [X] | Reconstitution Solvent | µl Reconstitution Solvent added per tube [X x 10000] | [Fluorescent Standard after Reconstitution, µM] |
|----------------------|-------------------|------------------------|--|---|
| Example Red Standard | 0.11 | DMSO | 100 µl | 100 |
| Green Standard | | DMSO | | 100 |
| Blue Standard | | DMSO | | 100 |
| Cyan Standard | | DMSO | | 100 |

6.1.3 Prepare Standard Curve (Optional)

1. With room temperature water, dilute enough Reaction Buffer (2X) to prepare enough 1X Reaction Buffer for your standard curves. In a 96-well plate, one standard curve can be run in 8 wells using 1 µl of Reaction Buffer. We recommend that at least six points (in addition to the blank) be used for the standard curve and that it be performed in duplicate.
2. To the first well of the column add 195 µl 1X Reaction Buffer.
3. Add 100 µl of 1X Reaction Buffer to each of the remaining wells in the columns.
4. Add 5 µl of Fluorescent Standard (Table 3) to the first well containing 195 µl of buffer to achieve a starting concentration of 2.5 µM. Mix well.
5. Transfer 100 µl from this well into the next well containing 100 µl 1X Reaction Buffer and mix by pipetting. This is a two-fold dilution.
6. Repeat this dilution step, leaving the last well as an assay blank containing 1X Reaction Buffer only and no standard. The resulting Fluorescent Standard concentrations are 2.5 µM, 1.25 µM, 625 nM, 312.5 nM, 156.25 nM, 78.125 nM, 39.063 nM and 0 nM.

Note: These are suggested initial concentrations for the standard curve. More or less may be appropriate depending on your experimental needs.

Note: The assay can be performed simply using fluorescence values instead of converting to concentration of product formed.

5.1.4 Prepare Test Compounds, Positive Inhibition Control, and Solvent Control

1. Prepare 2.5X Test Compounds by dilution into deionized water. (For IC₅₀ determination, a serial dilution of the test compound is required.)
2. Prepare a 2.5X solution of a known P450 inhibitor in deionized water for positive control of inhibition (optional).
Note: We recommend use of the inhibitors listed in Section 7.0.
3. Prepare a solution of the solvent used to dissolve the test compounds and known P450 inhibitor at 2.5X final concentration.
Note: See Section 8.0 for information about particular solvents and tolerances.

6.1.5 Dispense Test Compounds, Positive Inhibition Control, and Solvent Control

1. Add 40 µl of the 2.5X solutions prepared in Section 5.1.4 to desired wells of the plate.
2. We recommend at least three replicates for the Positive Inhibition Control and Solvent Control.

6.1.6 Prepare and Dispense Master Pre-Mix

1. Prepare the Master Pre-Mix by diluting P450 BACULOSOMES[®] Reagent and Reconstitution System in Vial® CYP450 Reaction Buffer (2X) on ice (see Table 4). Mix by inversion.
2. Dispense 50 µl of Master Pre-Mix to each well. Mix.
Note: To account for background fluorescence in the absence of CYP450 activity, dispense 50 µl of Vial® CYP450 Reaction Buffer without P450 BACULOSOMES[®] to desired wells of the plate.

Table 4. Master Pre-mix (pre-mix of CYP450 BACULOSOMES[®] Reagents and Reconstitution System). Keep on ice until ready to use.

| Incubation Type | Vial® CYP450 Reaction Buffer | µl of Vial® CYP450 Reaction Buffer (2X) added | µl of Reconstitution System (100X) added | µl of CYP450 BACULOSOMES [®] added | Concentration of CYP450 in Master Pre-mix (P ₄₅₀), nM | Screening concentration of CYP450, nM ^a |
|-----------------|------------------------------|---|--|---|---|--|
| 1A7 | Vial® P450C7 | 450 (1.0 µl × 45) | 100 | 50 | 10 | 5 |
| | Vial® BURUL | 450 (1.0 µl × 45) | 100 | 100 | 20 | 10 |
| 7E6 | Vial® P450C7 | 450 (1.0 µl × 45) | 100 | 50 | 4 | 2 |
| | Vial® P450C7 | 450 (1.0 µl × 45) | 100 | 100 | 50 | 10 |
| 2A7 | Vial® BURU | 450 (1.0 µl × 45) | 100 | 100 | 20 | 10 |
| | Vial® CORU | 450 (1.0 µl × 45) | 100 | 100 | 20 | 10 |
| 7C19 | Vial® P450C7 | 450 (1.0 µl × 45) | 100 | 50 | 10 | 5 |
| | Vial® P450C7 | 450 (1.0 µl × 45) | 100 | 100 | 50 | 10 |
| 7N6 | Vial® BURU | 450 (1.0 µl × 45) | 100 | 200 | 40 | 20 |
| | Vial® P450C7 | 450 (1.0 µl × 45) | 100 | 50 | 10 | 5 |
| 7E1 | Vial® P450C7 | 450 (1.0 µl × 45) | 100 | 50 | 10 | 5 |
| | Vial® BURU | 450 (1.0 µl × 45) | 100 | 50 | 10 | 5 |
| 3A4 | Vial® DROM | 450 (1.0 µl × 45) | 100 | 50 | 10 | 5 |
| | Vial® DROM | 450 (1.0 µl × 45) | 100 | 50 | 10 | 5 |
| | Vial® BURU | 450 (1.0 µl × 45) | 100 | 50 | 10 | 5 |
| | Vial® DROM | 450 (1.0 µl × 45) | 100 | 50 | 10 | 5 |
| 3A5 | Vial® P450C7 | 450 (1.0 µl × 45) | 100 | 50 | 10 | 5 |
| | Vial® DROM | 450 (1.0 µl × 45) | 100 | 50 | 10 | 5 |

^a For your first experiment, we suggest these concentrations of the CYP450 enzyme. Based on your results, you may find more or less enzyme is necessary.

6.1.7 Pre-Incubate

1. Incubate the plate for 20 minutes at room temperature to allow the compounds to interact with the CYP450 in the absence of enzyme turnover.
2. During this pre incubation, prepare the pre mixture of Vivid[®] Substrate and NADP⁺ (see Table 5).
3. You may also wish to include a prescreen at this point to determine if your compounds are fluorescent.

| Assay Type | Vivid [®] Control Reagent | µl of Vivid [®] CYP450 Reaction Mixture (20) added | µl of Reconstituted Substrate/Co-factor (Reaction 2.1.2) | µl of NADP ⁺ (1000) added | Final % ACS from substrate |
|------------|------------------------------------|---|--|--------------------------------------|----------------------------|
| 1A2 | Vivid [®] DIBOLC | 85 (Substr 1) | 15 | 100 | 0.15 |
| | Vivid [®] BUBOLC | 85 (Substr 1) | 25 | 100 | 0.25 |
| | Vivid [®] BUBOLC | 90 (Substr 1) | 10 | 20 | 0.10 |
| 2C9 | Vivid [®] DIBOCT | 80 (Substr 2) | 20 | 100 | 0.20 |
| | Vivid [®] DIBOCT | 80 (Substr 2) | 10 | 100 | 0.10 |
| | Vivid [®] DIBOCT | 80 (Substr 2) | 10 | 100 | 0.10 |
| 2C19 | Vivid [®] DIBOLC | 80 (Substr 2) | 20 | 100 | 0.20 |
| | Vivid [®] DIBOCT | 80 (Substr 2) | 20 | 100 | 0.20 |
| | Vivid [®] DIBOCT | 80 (Substr 2) | 20 | 100 | 0.20 |
| 2C8 | Vivid [®] DIBOCT | 80 (Substr 2) | 20 | 100 | 0.20 |
| | Vivid [®] DIBOCT | 80 (Substr 2) | 20 | 100 | 0.20 |
| | Vivid [®] DIBOCT | 80 (Substr 2) | 20 | 100 | 0.20 |
| 2C17 | Vivid [®] DIBOLC | 80 (Substr 2) | 20 | 100 | 0.20 |
| | Vivid [®] BUBOLC | 80 (Substr 2) | 20 | 100 | 0.20 |
| | Vivid [®] BUBOLC | 80 (Substr 2) | 20 | 100 | 0.20 |
| 3A4 | Vivid [®] DIBOLC | 80 (Substr 2) | 20 | 100 | 0.20 |
| | Vivid [®] BUBOLC | 80 (Substr 2) | 20 | 100 | 0.20 |
| | Vivid [®] BUBOLC | 80 (Substr 2) | 20 | 100 | 0.20 |
| 3A5 | Vivid [®] DIBOLC | 80 (Substr 2) | 20 | 100 | 0.20 |
| | Vivid [®] BUBOLC | 80 (Substr 2) | 20 | 100 | 0.20 |
| | Vivid [®] BUBOLC | 80 (Substr 2) | 20 | 100 | 0.20 |

5.1.8 Start Reaction

1. Start the reaction by adding 10 µl per well of the Vivid[®] Substrate and NADP⁺ mixture prepared in Step 5.1.7 and mix.

5.1.9 Measure Fluorescence

1. **Kinetic Assay Mode (recommended):** Immediately (less than 2 minutes) transfer the plate into the fluorescence plate reader and monitor fluorescence over time at excitation and emission wavelengths listed in Table 6.
2. **Endpoint Assay Mode:** Incubate the plate for the desired amount of time, then add 10 µl of recommended stop reagent (see Section 7.0) to each well to quench the reaction. Measure fluorescence in the fluorescence plate reader at excitation and emission wavelengths listed in Table 6.
Note: Appropriate reaction times will vary by kit and experimental conditions. We recommend that you determine the linear activity range for the assay under the conditions you wish to use. Typically, such reaction times will fall within 5 to 60 minutes.
3. Proceed to Section 6.0 for data analysis.

| | | Vivid [®] Fluorescent Standard | | | | | | | |
|---------------------------|---------------------|---|------------|-------------|------------|-------------|------------|-------------|------------|
| | | Red | | Blue | | Green | | Cyan | |
| Fluorescence Plate Reader | Excitation/Emission | center (nm) | band width | center (nm) | band width | center (nm) | band width | center (nm) | band width |
| with standard optics | excitation | 570 | – | 439 | – | 487 | – | 490 | – |
| | emission | 585 | – | 490 | – | 500 | – | 500 | – |
| with filter | excitation | 570 | 25 | 435 | 20 | 485 | 20 | 495 | 20 |
| | emission | 605 | 25 | 490 | 40 | 500 | 25 | 490 | 40 |
| | excitation | 500 | 25 | 435 | 20 | 485 | 20 | 485 | 40 |
| with dichroic mirror | excitation | 485 | 25 | 490 | 40 | 500 | 25 | 490 | 40 |
| | dichroic | 555 | – | 475 | – | 505 | – | 505 | – |

Red Standard is sodium salt of resorufin. Blue Standard is 3-cyano-7-hydroxycoumarin. Cyan Standard is 7-hydroxy-4-trifluoromethylcoumarin. We recommend exciting this dye off peak at 400 nm (its excitation maximum is 386 nm) to minimize background from NADPH fluorescence. Green Standard is fluorescein.

For optimal signal to noise, filters must be blocked to OD of 6 outside their transparency range (UV and red blockage) and be free of pinholes. Filters may be purchased from:

Chroma Technology Corp.
72 Colton Mill Hill, Unit A 9
Brattleboro, VT 05301
Phone: (800) 824-7662 or (802) 257-1800
Fax: (802) 257-9400
www.chroma.com

6.0 SUGGESTED PROTOCOL FOR THE ANALYSIS OF RESULTS

6.1 Kinetic Assay Mode

- Obtain reaction rates by calculating the change in fluorescence per unit time.
- Calculate the percent inhibition due to presence of test compound or positive inhibition control using the equation:

$$\% \text{ Inhibition} = \left(1 - \frac{\text{rate in presence of test compound or positive inhibition control}}{\text{rate in absence of test compound or positive inhibition control}} \right) \times 100\%$$

6.2 Endpoint Assay Mode

- Subtract background fluorescence.
- Calculate percent inhibition due to presence of test compound or positive inhibition using the following equation:

$$\% \text{ Inhibition} = \left(1 - \frac{\text{RFU in presence of test compound or positive inhibition control}}{\text{RFU in absence of test compound or positive inhibition control}} \right) \times 100\%$$

Optional: Both types of data analysis above can be performed using a standard curve as described in Section 5.1.3 in order to calculate reaction rates as nmol product formed per unit time.

ศูนย์วิทยาศาสตร์
จุฬาลงกรณ์มหาวิทยาลัย

7.0 SUGGESTED CYP450 INHIBITORS (STOP REAGENT)

| Enzyme | Inhibitor (Stop Reagent) | Sigma Aldrich Cat. no. | Suggested Final Concentration** |
|---------|--------------------------|------------------------|---------------------------------|
| CYP1A2 | <i>m</i> -naphthoflavone | N7707 | 5 μ M |
| CYP2C6 | nicotinic acid | M7515 | 50 μ M |
| CYP2C7 | sulfaphenazole | 50768 | 10 μ M |
| CYP2C19 | nicotinic acid | M7515 | 50 μ M |
| CYP2D6 | quinidine | Q3625 | 1 μ M |
| CYP2E1 | diethylthiocarbamate | 77660 | 100 μ M |
| CYP3A4 | ketocazole | K1003 | 10 μ M |
| CYP3A5 | ketocazole | K1003 | 50 μ M |

** To stop the reaction, the suggested final inhibitor concentrations in the assay to produce inhibition of 90% or better is indicated in the above table. For an endpoint assay the volume of the added stop reagent should not exceed 10% of the final reaction volume (e.g., 10 μ l will be added per 100 μ l reaction volume. This 10% increase in the volume of an endpoint reaction does not have a significant effect on the reaction (or the calculations).

8.0 SOLVENT TOLERANCES

CYP450 activity can be inhibited by solvents commonly used to dissolve test compounds. While we always recommend including a solvent control in your experimental design, the following sample data is intended as a guide for the selection and use of organic solvents. Table values are percent inhibition at the indicated solvent concentration. Values preceded by a (*) indicate an increase in activity. Dashed lines indicate inhibition not detected. Note that lower concentrations are listed for 2D6 Blue, this enzyme is particularly sensitive to the presence of organic solvents.

| Wvid [®] Kit | Solvent concentration (%) | DMSO (% Inhibition) | Acetonitrile (% Inhibition) | Methanol (% Inhibition) | Ethanol (% Inhibition) |
|-----------------------|---------------------------|---------------------|-----------------------------|-------------------------|------------------------|
| 1A2 Blue | 0.1 | 2 | — | — | — |
| | 0.1 | — | — | — | — |
| | 1 | 15 | 2 | 20 | 27 |
| | 0.01 | — | — | — | — |
| 2B6 Blue | 0.1 | — | — | — | — |
| | 0.1 | — | — | — | — |
| | 1 | — | — | — | — |
| | 0.01 | — | — | — | — |
| 2C9 Blue | 0.1 | — | — | — | — |
| | 0.1 | — | — | — | — |
| | 1 | 35 | 4 | 45 | 61 |
| | 0.01 | — | — | — | — |
| 2C9 Red | 0.1 | — | — | — | — |
| | 0.1 | — | — | — | — |
| | 1 | 51 | 5 | 45 | 65 |
| | 0.01 | — | — | — | — |
| 2C19 Blue | 0.1 | 20 | — | 21 | 26 |
| | 0.1 | — | — | — | — |
| | 1 | 34 | — | 19 | 35 |
| | 0.01 | — | — | — | — |
| 2D6 Blue | 0.1 | 21 | — | 20 | 27 |
| | 0.1 | — | — | — | — |
| | 1 | 35 | — | 19 | 35 |
| | 0.01 | — | — | — | — |
| 2E1 Blue | 0.1 | — | — | 4 | 5 |
| | 0.1 | 35 | 3 | 26 | 34 |
| | 0.1 | 35 | 16 | 7 | 25 |
| | 0.01 | 23 | 7 | 8 | 25 |
| 3A4 Blue | 0.1 | 22 | — | 4 | 12 |
| | 0.1 | — | — | — | — |
| | 1 | 64 | 4 | 20 | 31 |
| | 0.01 | 24 | — | — | — |
| 3A4 Cyan | 0.1 | — | — | — | — |
| | 0.1 | — | — | — | — |
| | 1 | 7 | — | — | — |
| | 0.01 | 12 | — | — | — |
| 3A4 Green | 0.1 | 9 | — | — | — |
| | 0.1 | — | — | — | — |
| | 1 | 44 | — | 6 | 5 |
| | 0.01 | 15 | — | — | — |
| 3A4 Red | 0.1 | — | — | — | — |
| | 0.1 | — | — | — | — |
| | 1 | 35 | 2 | 20 | 25 |
| | 0.01 | — | — | — | — |
| 3A5 Blue | 0.1 | 25 | — | 21 | 2 |
| | 0.1 | — | — | — | — |
| | 1 | 35 | 5 | 21 | 30 |
| | 0.01 | — | — | — | — |
| 3A5 Cyan | 0.1 | 31 | — | 3 | 5 |
| | 0.1 | — | — | — | — |
| | 1 | 31 | — | 2 | 6 |
| | 0.01 | — | — | — | — |
| 3A5 Green | 0.1 | 17 | — | — | — |
| | 0.1 | — | — | — | — |
| | 1 | — | — | — | — |
| | 0.01 | — | — | — | — |

9.0 REFERENCES

- Cohen, L.J., et al. (2003) *In vitro* drug interactions of cytochrome P450: an evaluation of fluorogenic to conventional substrates. *Drug Metab. Dispos.* 31:1003-15.
- Marks, B.D., et al. (2002) A high throughput screening assay to screen for CYP2E1 metabolism and inhibition using a fluorogenic Vival® P450 substrate. *Assay Drug Dev. Technol.* 1:77-81.
- Marks, B.D., et al. (2003) High throughput screening assays for CYP2B6 metabolism and inhibition using fluorogenic Vival® substrates. *AAPS PharmSci.* 3:F18.
- Marks, B.D., et al. (2004) High-throughput screening assays for the assessment of CYP2C9*1, CYP2C9*2, and CYP2C9*3 metabolism using fluorogenic Vival® substrates. *J. Biomol. Screen.* 9:439-49.
- Trubeskey, O.V., et al. (2005) Highly miniaturized formats for *in vitro* drug metabolism assays using Vival® fluorescent substrates and recombinant human cytochrome P450 enzymes. *J. Biomol. Screen.* 10:66-66.
- For structures of the Vival Substrates and poster presentations containing additional details and applications of Vival CYP450 Screening Kits, please visit us online at: www.invitrogen.com/drugdiscovery.



ศูนย์วิทยทรัพยากร
จุฬาลงกรณ์มหาวิทยาลัย

10.0 PURCHASER NOTIFICATION

Limited Use Label License No. 162: Cytochrome P450 enzymes, assays and substrates

This product is the subject of one or more of US Patent 5,891,696, 6,343,492, and 6,420,130. The purchase of this product conveys to the buyer the non-transferable right to use the purchased amount of the product and components of the product in research conducted by the buyer (whether the buyer is an academic or for-profit entity). The buyer cannot sell or otherwise transfer (a) this product (b) its components or (c) materials made using this product or its components to a third party or otherwise use this product or its components or materials made using the product or its components for Commercial Purposes. The buyer may transfer information or materials made through use of this product to a scientific collaborator, provided that such transfer is not for any Commercial Purpose, and that such collaborator agrees in writing (a) to not transfer such materials to any third party, and (b) to use such transferred materials and/or information solely for research and not for Commercial Purposes. Commercial Purposes means any activity by a party for consideration and may include, but is not limited to: (1) use of the product or its components in manufacturing; (2) use of the product or its components to provide a service, information, or data; (3) use of the product or its components for therapeutic, diagnostic or prophylactic purposes; or (4) resale of the product or its components, whether or not such product or its components are resold for use in research. Invitrogen Corporation will not assert a claim against the buyer of infringement of the above patent claiming this product based upon the manufacture, use or sale of a therapeutic, clinical diagnostic, vaccine or prophylactic product developed in research by the buyer in which this product or its components was employed, provided that neither this product nor any of its components was used in the manufacture of such product. If the purchaser is not willing to accept the limitations of this limited use license, Invitrogen is willing to accept return of the product with a full refund. For information on purchasing a license to this product for purposes other than research, contact Licensing Department, Invitrogen Corporation, 1600 Faraday Avenue, Carlsbad, California, 92008. Tel: (760) 603-7200. Fax: (760) 602-6500.

ศูนย์วิทยทรัพยากร
จุฬาลงกรณ์มหาวิทยาลัย

BIOLIF CCKM007[®] is a registered trademark of Invitrogen Corporation.

Vival[®] is a registered trademark of Invitrogen Corporation.

© 2003 Invitrogen Corporation. All rights reserved. Reproduction forbidden without permission.

BIOGRAPHY

Miss Patthanan Hongpiticharoen was born on October 22, 1983 in Bangkok, Thailand. She was graduated with a Bachelor Degree of Pharmaceutical Sciences in 2006 from the Faculty of Pharmacy, Srinakharinwirot University, Thailand.



ศูนย์วิทยทรัพยากร
จุฬาลงกรณ์มหาวิทยาลัย